UNIVERSITY OF GHANA, LEGON

COLLEGE OF BASIC AND APPLIED SCIENCE

EVALUATION OF ATMOSPHERIC POLLUTANTS USING SATELLITE DERIVED AND LOW-COST SENSOR DATA OVER ACCRA, GHANA

By

JAMES NIMO (10432954)

THIS THESIS IS SUBMITTED TO THE UNIVERSITY OF GHANA, LEGON IN PARTIAL FULFILLMENT OF THE REQUIREMENT FOR THE AWARD OF MPHIL IN PHYSICS DEGREE

August, 2022

DECLARATION

I hereby declare that this submission is my own work and that, to the best of my knowledge, it contains no material previously published by another person nor materials which has been accepted for the award of any other degree of the University, except where due acknowledgement has been made in the text.

11th October, 2023

…….. …….

(10432954) JAMES NIMO DATE

STUDENT

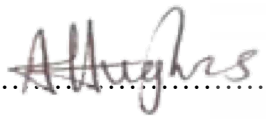

21st October 2023

…….. ……..

DR. ALLISON FELIX HUGHES DATE

(SUPERVISOR)

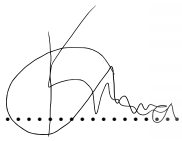

23/10/2023

…….. …… ……

PROF. NANA AMA BROWNE KLUTSE DATE

(CO-SUPERVISOR)

ACKNOWLEDGEMENTS

This thesis would not exist without a great number of people. I extend a most sincere and heartfelt thank you:

To my supervisor and co-supervisor, Dr. Allison Felix Hughes and Prof. Nana Ama Browne Klutse, for agreeing to take responsibility to supervise my work and above all, offered so much love, support, encouragement and advice that was so spot on.

To the African Institute of Mathematical Sciences (AIMS) – Canada Masters by Research Scholarship, Kigali, Rwanda for sponsoring my studies at the Department of Physics, University of Ghana, Legon, Ghana.

To the HOD of the Physics Department, Dr. Martin Egblewogbe for his assistance during my period of study.

To my wife for her constant love, prayers, support, patience and advice.

To my elder brother Mr. Asamoah Mireku for his constant call, encouragement and advice.

To all the technicians of the Department of Physics, University of Ghana for their help in one way or the other.

DEDICATION

This thesis is dedicated to the Almighty God who gave me the strength throughout the whole period of study. I also dedicate this thesis to my wife, Mrs. Jessica Nimo and Dr. Azoda Koffi, a Senior Lecturer at the Department of Physics, University of Ghana.

ABSTRACT

It is well established that high pollution concentrations negatively impact the climate and public health. According to the WHO, poor air quality is responsible for approximately 7 million deaths worldwide each year. With rising urban emissions and population growth, the situation is similar in sub-Saharan Africa, where poor air quality is increasing alarmingly. Therefore, regular monitoring is needed to assess the levels of pollutants at both local and regional scales. However, there needs to be more monitoring in sub-Saharan Africa since purchasing, installing, and maintaining many high-grade air quality monitoring sensors is expensive. Hence, the gap in studies focusing on associations between particulates with aerodynamic diameter less than 2.5 microns ($PM_{2.5}$) and gas pollutants like nitrogen dioxide (NO_2) and ozone (O_3) in sub-Saharan African cities. Furthermore, this study seeks to bridge this gap by utilizing data from five Clarity Node-S $PM_{2.5}$ sensors, total column particulates or Aerosol Optical Depth (AOD), NO_2 and O_3 data from satellites, and data from five different Ghana Environmental Protection Agency (GEPA) air quality traffic sites in the Greater Accra Metropolitan Area (GAMA). The AOD, NO_2 and O_3 data were retrieved from Moderate Resolution Imaging Spectro-Radiometer (MODIS) Terra and Ozone Monitoring Instrument (OMI). The long-term trends over the 5 stations on $(25 \times 25)\ km^2$ grid for OMI and $(50 \times 50)\ km^2$ grid for MODIS Terra AOD from 2012 to 2021 were assessed using Mann-Kendall sequential test while the Pearson correlation coefficient was used to find correlations between the pollutants. In addition, characterization of $PM_{2.5}$, AOD, NO_2, and O_3 levels in the GAMA was evaluated. Overall, there was an increasing trend in NO_2 (with $p < 0.05$) over 4 stations, no trend in O_3 (with $p > 0.05$) and a decreasing trend in AOD (with $p < 0.01$). Coefficients of determination between $PM_{2.5}$ data and MODIS Terra AOD on $(50 \times 50)\ km^2$ grid across the stations were ($R^2 = 0.72$, 0.72, 0.67, 0.58 and 0.57) respectively. Coefficients of determination between total column NO_2 and O_3 were ($R^2 = 0.83 \pm$

0.030, $p < 0.01$), AOD and O_3 ($R^2 = 0.43 \pm 0.003$, $p < 0.01$) and, NO_2 and AOD ($R^2 = 0.21 \pm 0.010$, $p > 0.01$). $PM_{2.5}$, AOD and NO_2 levels were generally high during the dry season while high concentrations of O_3 were observed in the wet season across the stations. Moreover, the $PM_{2.5}$ daily mean level of 32.8 μgm^{-3} for 25 months between 2018 and 2021 was more than twice World Health Organization (WHO) recommended daily mean level of 15 μgm^{-3}. A high correlation coefficient was observed between total column NO_2 and O_3. Low correlation coefficients between AOD, NO_2 and O_3 may reveal different emission sources from open burning, street cooking, traffic, and industrial activities in the GAMA. High population growth coupled with increasing traffic, biomass burning, and climate change in growing sub-Saharan African cities requires urgent policy measures and regulations as ground air quality monitoring sensors are limited.

TABLE OF CONTENT

LIST OF FIGURES

LIST OF TABLES

CHAPTER ONE

INTRODUCTION

1.1 Background of the Study

Poor air quality has become a growing concern particularly in low-income countries of sub-Saharan Africa. According to (Fisher et al., 2021), over one million people die prematurely in Africa as a result of long-term exposure to poor air quality.

Poor air quality is usually a constituent of pollutants emissions such as carbon monoxide (CO), sulphur dioxide (SO_2), ozone (O_3) and particulates with aerodynamic diameter less than 2.5 microns ($PM_{2.5}$) exceeding recommended levels in ambient air. These constituents - CO_2, CO, O_3, SO_2 and $PM_{2.5}$ from sources such as agricultural and waste burning, transportation and residential cooking are linked to adverse environmental health impacts such as stroke, cardiovascular and respiratory diseases such as lung cancer, obstructive pulmonary disease and myocardial infarction (Abera et al., 2020; Cohen et al., 2017; Rao et al., 2013). According to the State of Global Air Report (2018) published by the Health Effects Institute (HEI), in 2016, poor air quality contributed about 4.1 million deaths from heart disease, stroke, lung cancer, chronic lung disease as well as respiratory infections. High levels of PM2.5 exposure during pregnancy can lead to preterm birth, low birth weight and reduced cognitive function in children (Johnson et al., 2021). While cities in high-income countries such as the US, Europe and parts of China with a number of air quality monitoring stations have observed much improvement in air quality, many cities in Africa have seen poor air quality levels worsening over time (World Health Organization et al., 2020).

Poor air quality occurs when the concentrations of pollutants in ambient air exceeds recommended values. According to (World Bank, 2015), outdoor poor air quality due to particulates smaller than 2.5 microns occurs when outdoor concentration exceeds recommended daily mean levels of 25 $\mu g/m^3$.

Particulate matter is tiny particles suspended in the atmosphere that range in size between nanometres (nm) to micrometres (µm). Particulates smaller than 2.5 microns harm human health due to their ease of penetration through the lungs and skin. Particulate matter is produced through natural and anthropogenic processes. Natural processes that produce aerosols include re-suspended Harmattan dust and sea spray usually from the desert and the sea respectively. Anthropogenic activities such as biomass burning and deforestation also release aerosols into the atmosphere. A common source of PM2.5 is smoke, usually from agricultural biomass burning as a result of clearing the land for farming. Smoke is typically dominant, especially from wildfires in most European and Asian countries (Hens et al., n.d.; Shaheen et al., 2017; Weber et al., 2016).

Witte et al. (2011) obseved the adverse effect of wildfires based on the levels of particulate matter over western Russia and parts of Eastern Europe. The researchers also revealed consistent heat over those regions during the summer due to wildfires. Further, Chem et al. (2018) observed escalated levels of particulate matter concentrations over most sub-Saharan African countries like Ghana and Togo as a consequence of anthropogenic activities mainly from the burning of biomass due to agricultural practices during the raining seasons.

Another source of particulate matter pollution is mineral dust. Mineral dust is usually common in the Saharan regions as result of Saharan desert. Mineral dust can also originate from re-suspended dust due to bare lands (Emetere & Akinyemi, 2015). Mineral dust is dominant over the Saharan regions and part of Asian countries (Fairlie et al., 2016). Mineral dust is one of the common particulate matter source and

is coarse in nature with a size of ranging several micrometres in diameter (Schroedter-Homscheidt et al., 2013). Again, about several billions of mineral dust are emitted annually with its effects on climate and population health (Cheng, 2010; Hao & Qu, 2017). For example, dust storms from the Saharan desert fertilizes the Amazon basin and affects the formation of hurricanes in the Atlantic (Hao & Qu, 2017).

Several authors including Eck et al. (1999), Fawole et al. (2016), Kahn and Gaitley (2015) and Madhavan et al. (2017) revealed that the increasing rate of mineral dust from the Saharan and Asian regions causes an escalation in the global concentrations of particulate matter. Sub-Saharan Africa countries such as Ghana, Togo, Benin and Nigeria are mostly affected by mineral dust storms originated from the Saharan desert (Akinyoola et al., 2018; Nwofor, 2010; Ofosu et al., 2012, 2013). Ofosu et al. (2013) revealed the influence of Saharan dust storms on poor air quality over the northern part of Ghana especially in the Navrongo metropolis.

Sea spray is another dominant source which has huge impact on the concentration of particulate matter over the Mediterranean regions and Oceanic environment (Fawole et al., 2016; Lynch, 2018; Schaap et al., 2009). The component of sea spray is usually is made of sea salt, but also consists of organic carbon, or even bacteria, phytoplankton, and organic matter. The influence of sea spray which originates mainly from the Mediterranean Sea, has huge impact on particulate matter concentrations over the southern regions of most West African countries including Benin, Togo, Ghana and Nigeria (Abam, 2015; Dionisio et al., 2010; Ofosu et al., 2012; Onyeuwaoma et al., 2015). Dionisio et al. (2010) and Abam (2015) revealed the influence of sea spray originated from the Mediterranean sea on particulate matter concentrations over the southern part of Ghana and Nigeria respectively.

Moreover, the concentration of particulate matter and their transport around the world over a certain period of time depends also on the impact of the climatic conditions at that period. For example, Harmattan is a

dry and dusty West African wind which blows south from the Sahara into the Gulf of Guinea between the end of November and the middle of March (Alpert et al., 2012; Ikoku & College, 2016; Mao et al., 2014a). During the Harmattan season as the wind blows hard, it usually transport sand and dust through to North America. Ofosu et al., (2012) confirmed concentrations of fine dust particulates over most southern metropolis in the Greater Accra Region of Ghana during the dry seasons.

Particulates of a certain size usually $PM_{2.5}$ at ground level have an adverse effect on human health. Particulate matter with aerodynamic diameter smaller than 10 but greater than 2.5 microns is mainly coarse particles and is difficult to penetrate the human body. These are generated through natural process such as dust storms and sea salt. Fine particulate matter, with aerodynamic diameters less than 2.5 microns ($PM_{2.5}$), is a mass concentration near the surface, and the most consistent predictor of mortality from cardiovascular, respiratory and other diseases in recent studies of long-term exposure (Chu et al., 2003; Weber et al., 2016; World Bank, 2015). $PM_{2.5}$ is mainly generated through anthropogenic processes such as smoke, vehicular emissions, and fumes from industries, among others, which are harmful to human health. The impact of aerosols on human health has adverse effects ranging from respiratory diseases to lung cancer. Aerosols affect more people than any other pollutant. The major components of ambient particulate matter are sulphate, nitrates, ammonia, sodium chloride, black carbon, mineral dust and water that can penetrate the lung barrier and enter the blood system.

Chronic exposure to particulates contributes to the risk of developing cardiovascular, lung cancer and respiratory diseases especially in sensitive groups such as children and older adults. An assessment by the International Agency for Research on Cancer (IARC) of WHO in 2013, concluded that ambient particulate matter pollution is carcinogenic to humans, with the ambient particulate matter component most closely linked with increased cancer incidence, especially lung cancer. The effects of particulate matter on human

health occur at levels of exposure currently being experienced by many people both in urban and rural areas and in developed and developing countries.

Aerosols can affect visibility depending on the levels of their concentrations in the atmosphere. The exposures in many fast-developing cities today are often far higher than in developed cities of comparable size. In some West African countries, the heavy amount of dust in the air can severely limit visibility and block the sun several days, comparable to heavy fog (*WHO Releases Country Estimates on Air Pollution Exposure and Health Impact*, n.d.).

Furthermore, particulates or aerosols can reduce incoming solar radiation with wavelengths between 0.4 and 1.0 micrometre (μm), where the radiation is scattered or reflected (Cheng, 2010; Gupta & Christopher, 2009b). Aerosols in the atmosphere reflect solar radiation differently depending on their size distribution. Aerosols much smaller than the wavelength of visible light have little influence. Very large particles (unless they are coloured and absorb light) also have minimal impact. The size of the particles determines whether shorter –wave radiation is reflected more effectively than the long-wave infrared radiation (Kahn & Gaitley, 2015). Aerosols also affect outgoing terrestrial radiation. Aerosols in the size range of 0.1 to 2.0 μm do not intercept the outgoing infrared radiation of the earth. However, if the aerosols consist of liquid droplets, strong back reflection of infrared radiation occurs. This results in the absorption of the radiation by aerosols, causing heating effect in the atmosphere.

Meteorological parameters such as wind speed, temperature and humidity can also affect the concentrations of aerosols in the atmosphere. Gupta & Christopher (2009b) conducted a study to determine the impact of meteorological parameters on the concentration of particulate matter over the United States. The study revealed that in well-mixed boundary layer regimes, there is a strong correlation

between particulates as well as meteorological parameters such as temperature, humidity and wind speed, during the summer.

Aerosols have a positive effect on the formation of clouds depending on the levels of concentrations in the atmosphere and other favourable meteorological conditions. If no aerosols are present, large super-saturation (relative humidity over 100%) can be observed without the formation of droplets. Cloud formation is enhanced if particles (less than $200cm^{-3}$) are available as cloud condensation nuclei (Vermote et al., 2016). However, excessive concentration of aerosols lead to the formation of small water droplets which trap the outgoing terrestrial radiation to produce heating effect in the atmosphere (Chow et al., 2006). Hence, excessive aerosols in the atmosphere contribute to global warming (Weber et al., 2016).

There are different methods of monitoring aerosols. The concentration of aerosols in the atmosphere can be monitored by using in situ or conventional methods, modelling and remote sensing techniques. Examples of conventional methods include the receptor models which are used for point source detection and other ground-based air quality monitoring instruments mounted at ground stations. Remote sensing techniques include satellite derived aerosol optical depth (AOD) and modelling which incorporate information such as population data and topography (Donkelaar et al., 2010; Gupta & Christopher, 2009a; Ite et al., 2017; Sulprizio, 2015)

Receptor models are tools used for identifying sources of particulate matter (Ede & Edokpa, 2017; Nwachukwu et al., 2012; Ofosu et al., 2013; World Bank, 2015). The receptor models utilise the characteristics of pollutants collected at its locations to identify the sources. Receptor models such as Positive Matrix Factorization (PMF) and Principal Component Analysis (PCA) are used to develop mitigating strategies for particulate matter pollution.

Most researchers in sub-Saharan Africa use receptor models in monitoring particulate matter concentrations. For example Nwachukwu et al. 2012 and Ofosu et al. 2013 used receptor models in monitoring particulate matter. In using PCA models, (Oluyemi & Asubiojo, 2001) identified the sources of PM_{10} sampled at three sampling points in Lagos. The study identified sources such as sulphate, soil and vehicular emission. Furthermore, Ofosu et al. (2013 used positive matrix factorization to analyse the seasonal patterns (non-Harmattan and Harmattan) of $PM_{2.5}$ and carbon levels and their possible sources over Navrongo, in the northern part of Ghana. Their results revealed that about 16% of biomass combustion was the most important source next to soil dust over Navrongo during the study period.

In sub-Saharan Africa, ground-based monitoring stations have been the basis for most studies of the health effects of ambient particulate matter and air quality management, particularly in most West African countries such as Nigeria and Ghana. For example, Ede & Edokpa (2017) assessed the spatial and seasonal $PM_{2.5}$ levels using 14 ground-based air monitoring sensors in Port Harcourt. Dionisio et al. (2010) also assessed the space-time variability of $PM_{2.5}$ in four neighbourhoods in Greater Accra Metropolitan Area (GAMA), Ghana, using integrated and continuous rooftop monitors. The study revealed that the $PM_{2.5}$ levels over four selected neighbourhoods in the GAMA was higher than the WHO Air Quality guidelines.

The University of Bath together with World Health Organization have developed a model called the Data Integrating Model for Air Quality (DIMAQ). The model incorporates information such as population data, topography and land use, and satellite data to estimate ambient particulate matter concentrations around the globe with their associated measures of uncertainties ('WHO | WHO Global Urban Ambient Air Pollution Database (Update 2016)', 2017). From the DIMAQ model, WHO ranked Aba, Kaduna, Onitsha and Umuahia to be among the worst 20 cities around the world for particulate matter pollution (*WHO Releases Country Estimates on Air Pollution Exposure and Health Impact*, n.d.).

There are three major satellite remote sensing techniques used in monitoring air quality in cities and urban areas, namely:

1. Land use and land cover change analysis (where changes in urbanization can be used to infer particulate matter concentrations);
2. Visual inspection of satellite imagery (observations of satellite images such as smoke from wildfires to observe particulate matter concentrations);
3. Measurement of aerosol optical depth from satellite sensors.

Various authors have utilized satellite remote sensing techniques to monitor aerosols in different parts of the world. For example, Donkelaar et al. (2010) estimated ground level PM levels using AOD from the Multi-angle Imaging Spectro-radiometer and Moderate Resolution Imaging Spectro-radiometer satellite instruments. The study concluded that AOD provided estimated global trends of particulate matter ($PM_{2.5}$) concentrations. In another study by Mao et al. (2014a), the variations of AOD were mapped using MODIS instrument aboard Terra and Aqua satellites. The study observed high levels of particulates generally distributed in middle and low-income countries. Gupta & Christopher (2009b) assessed particulate matter levels over different locations across the global urban areas spread across 26 locations in high, middle and low-income countries. The study revealed increasing trends of particulate matter concentrations over Delhi, Hong Kong and Sydney respectively, during the study period. Nwofor (2010) analysed NASA Aerosol Robotic Network Aerosol Optical Depth dataset at Ilorin with the aim of deducing trends in dust aerosol loading for period of 10 years. Akinyoola et al. (2018) used the Ozone Monitoring Instrument (OMI) and MODIS to assess space-time variations of aerosols in Nigeria. The study observed that aerosols found in the shoreline of the country were predominantly rich in sulphate due to anthropogenic activities.

Therefore, remote sensing techniques such as satellite retrieval of AOD is viable method for monitoring aerosols and air quality management. This method has the capacity to provide a consistent view of ambient particulate matter levels in large rural and suburban areas and many rapidly developing urban areas of low-income countries such as Ghana, where there is a dearth of ground-based air quality monitoring stations.

1.2 Statement of Research Problem

Particulates, also known as aerosols, and short-lived climate forcers such as NO_2 and O_3 are important species in the atmosphere; that have a significant impact on climate by changing the energy budget of the Earth system due to their ability to form other chemical species in the atmosphere through radiative forcing.

Aerosols pollute the atmosphere and have an adverse effect on human health. For example, poor air quality made up of particulates with aerodynamic diameter less than 2.5 micrometers and other gas pollutants including nitrogen dioxide and ozone is a major environmental risk factor for respiratory diseases. Exposure to $PM_{2.5}$, nitrogen dioxide (NO_2) and surface ozone (O_3) can affect children, old people and pregnant women. Furthermore, and as I have already mentioned, continuous exposure during pregnancy can lead to preterm birth, low birth weight and reduced cognitive function in children (Johnson et al., 2022). Due to the lack of continuous (long-term) ground air quality monitoring stations in sub-Saharan Africa, it is challenging to quantify the region's poor air quality levels so that governmental agencies can formulate policies and control measures (Ardon-Dryer et al., 2019; Miech et al., 2021). Studies have shown that only two countries under the Economic Community of West African States (ECOWAS) monitor particulates pollution (Mir Alvarez et al., 2020). Poor air quality has become a global public health concern especially in densely populated areas in the past few decades (Horwood et al., 2007).

Several national environmental agencies across sub-Saharan Africa monitor particulate matter concentrations at a number of sites which do not constitute populated regions. Also, point measurement collected at monitoring sites cannot serve as a representative of regional concentrations (Vermote et al., 2016). Thus, regional variability is difficult to assess from point measurement alone (Fawole et al., 2016). However, in recent studies (Donkelaar et al., 2010; Gupta & Christopher, 2009b) have shown that poor air quality can be monitored using remote sensing techniques such as utilizing satellite retrieval total column dataset to quantify particulate matter exposure levels.

Ghana is part of the Economic Community of West African States located on the Gulf of Guinea with average temperatures ranging between 25ºC and 30ºC and two distinguished raining seasons - April to June and September to November. From February to December, Ghana experiences large amount of dust along the Intertropical Convergence Zone (ITCZ) found in the southwest of Ghana - with two distinguished dry seasons in the southern part of Ghana – July to August as minor dry season and December to February as major dry season. This occurs when the north-easterly winds also called the Harmattan winds transport dust from the Saharan regions - thus, influencing particulate matter concentrations to surge. For example, Alli et al. (2021) observed that $PM_{2.5}$ concentrations during the Harmattan season skyrocketed from 56 to 71 $\mu g/m^3$ during a city measurement campaign in the Greater Accra Metropolitan Area (GAMA). The Ghana Environmental Protection Agency also estimates that about 2,800 deaths occur annually in the GAMA due to poor air quality. Therefore, there is the need to continuously monitor these harmful pollutants to have an in-depth understanding of their patterns and trends. However, studies conducted in this region are not long-term due to the high cost of funding to extend research more than one year.

The Greater Accra region being the capital city of Ghana, is the hub for huge economic activities and might be imperative to study regional distribution of these pollutants (particulates, NO_2 and O_3). Utilizing satellite retrieval total column data will enable governmental agencies and policy makers understand the long-term trends of these pollutants over the GAMA. This will also enable studies on regional climate variability influenced by short-lived climate forcers (NO_2 and O_3) because of the radiative forcing they generate in the atmosphere.

Therefore, the focus of this study is to address this data gap in sub-Saharan Africa by using satellite total column dataset usually called aerosol optical depth for particulates, total column ozone (O_3) and nitrogen dioxide (NO_2) (for the gas pollutants) over Ghana. This would serve as a surrogate for the scarcity of ground air quality sensors in Ghana for continuous and long term monitoring of poor air quality.

1.3 Objectives of the Study

The overall objective of this study is to:

- investigate in detail the spatio-temporal variations of both ground particulates (PM2.5) and satellite retrieved total column particulates, nitrogen dioxide (NO_2) and ozone (O_3) for the period of 3 years from 2019 to 2021 over 5 Ghana EPA sites (Amasaman, Kaneshie, Tetteh Quarshie, Achimota and Jamestown) in the Greater Accra region, Ghana.

The specific objectives are to:

- Map monthly spatial distribution of AOD (Aerosol Optical Depth), total column ozone (O_3) and nitrogen dioxide (NO_2) over Ghana using OMI (on Aura satellite) and MODIS (NASA Aqua and Terra satellites) during the study period.

- Analyse daily and monthly temporal variations of $PM_{2.5}$, NO_2, O_3 and validate the MODIS total column particulates with the 5 Ghana EPA air quality stations (figure 3.2) dataset for the study period.
- Assess long-term trends using satellite derived total column AOD, NO_2 and O_3 for 10 years from 2012 to 2021 over the 5 Ghana EPA sites using the Mann-Kendall test.

1.4 Limitations of the Research

The climatic condition in Ghana is tropical with two main seasons – the rainy and dry seasons. This poses challenges for satellites sensors such as MODIS and Aura to capture total column particulates and gas pollutants during the wet seasons since cloud cover usually affects them. Thus, there is some data gaps in the total column retrievals mostly in the northern and southern parts of Ghana during the study.

Furthermore, this study is limited by the spatial resolution of the satellite sensors (MODIS – 1 degree and OMI – 0.25 degree) as they could not capture the spatial content of the Ghana EPA air quality stations in detail. For example, the MODIS gridded 1 degree spatial resolution captured the 5 Ghana EPA stations (Amasaman, Jamestown, Kaneshie, Tetteh Quarshie and Achimota) as 1 location. Furthermore, the OMI total column NO_2 and O_3 values were not validated with ground data at the time of this study since the ground monitoring data was insufficient.

CHAPTER TWO

LITERATURE REVIEW

2.1 Fundamentals of Particle Pollution

Particle pollution is when solid, liquid or gaseous particulates found in the atmosphere exceed recommended levels (Chow et al., 2006; Chu et al., 2003). Particle pollution consists of larger particles often called coarse particles and smaller particles called fine particles. Particle pollution is made of 4 major chemical components including carbon, sulfate and nitrate compounds as well as crustal materials such as soil and ash (Nwachukwu et al., 2012; Rowland, 2011; Sifakis, 1992).

In addition, particle pollution can be categorized as primary which consist of particles emitted into the atmosphere and secondary consisting of particles formed indirectly from fuel combustion and other sources (Arku et al., 2008a; Lim et al., 2007). Primary particle pollution is made up of soot (black carbon) emitted from forest fires, agricultural waste and crustal materials from unpaved roads and particularly construction sites. Furthermore, in the atmosphere, particle pollution can also form from gases in the presence water vapor and sunlight.

2.2 Particulate Matter

Particulate Matter (PM) or particulate consists of a mixture of coarse and fine particles of different sizes in the atmosphere. Particulates especially of size smaller than 2.5 microns can remain in the air for a while where the levels of these particles can be analysed. Researchers around the world are usually interested in particulates of particular size at ground level. Particulate types include PM_1, $PM_{2.5}$ and PM_{10}. PM_1 are

aerosol particles with aerodynamic diameters smaller than 1 microgram per meter cubic (1μg/m^3) while $PM_{2.5}$ particles range between 1 and 2.5 μg/m^3 and PM_{10} refers to particles with diameter greater than 10 μg/m^3 respectively (World Bank, 2015).

Air pollution by particulate matter may originate from anthropogenic or natural processes (Rowland, 2011). A high percentage of human-induced aerosols are also generated from the smoke resulting from tropical forest. Another major atmospheric aerosol is sulphate aerosols created by the burning of coal and oil.

Particulate matter concentration in the atmosphere has grown rapidly since the start of industrial revolution (Lim et al., 2007). At current production levels, it is noted that sulphate aerosols of anthropogenic origins outweighs those generated through natural processes from forest fires, sea salt, eruptions of volcanoes, and soil particles.

Fuel combustion by motor vehicles, coal and oil are considered to be sources of the worst form of pollution caused by particulate matter with varying adverse implications on human health (World Bank, 2015). The quality of air is affected by coal power plants because they emit harmful pollutants like carbon monoxide, carbon dioxide, sulphur dioxide and oxide of nitrogen compounds into the atmosphere (Onyeuwaoma et al., 2015). Further, power plants containing crude oil and natural gas also emit compounds such as thorium, uranium, carbon and sulphur in large volume (Ede & Edokpa, 2017). Therefore, due to the emission of these pollutants into the atmosphere, many researchers have documented the harmful effects on population health by triggering many illness where some lead to death (Akuro Adoki, 2012).

Many authors have studied the effects of PM emissions on human life expectancy. A study by (Horwood et al., 2007) showed poor quality decreased life expectancy in countries Europe and Asia. The study

observed that for countries like China and India, there were about 3.5 and 2.5 years estimated life expectancy decreased with increasing infant mortality ratios during the study period.

The adverse effects of particulate matter pollution on human health are immense and vary depending on the source of the particulate matter which differs around the world. For example, a study by Chu et al. (2003), showed that in West African alone, air pollution from anthropogenic emissions, have impacted the quality of air significantly and population health. Their study indicated that anthropogenic activities such as fossil fuel burning and biomass burning pollute the quality of air significantly with the release of harmful pollutants. Their study further observed the negative impact of industrial activities on air quality as they contribute to the release of harmful pollutants into the atmosphere which affect the environment and population health. Moreover, long exposure to these pollutants especially the gaseous pollutants like carbon monoxide affects respiratory health and results in organ failure (Heilman et al., 2014). Carbon monoxide is far more dangerous to population health than carbon dioxide. Exposure to carbon monoxide for a long time can lead to inflammation, cytotoxicity, and cell death (http://www.lung.org/our-initiatives/healthy-air/outdoor/air-pollution/air-quality-index.html).

There has been an increasing rate of death caused by particulate matter pollution. A study by Misra et al. (2015) revealed that over 7,500 deaths each year are attributable to fine particle pollution from power plants in the United States. Particulate matter pollution caused about 3% of mortality from cardiopulmonary disease where about 5% of the mortality was as result of cancer of the trachea, bronchus and lung, and about 1% of mortality from acute respiratory infections in children under 5 years worldwide (Hu, 2009; Sulprizio, 2015; Yakubu, 2017).

Particulate matter pollution has been shown to have negative effect on the environment. For example, greenhouse gases like carbon monoxide, carbon dioxide and some hydrocarbons, are known to raise global

temperatures due the energy of the sun which has been trapped in the atmosphere. Thus, changing weather patterns like temperature, rainfall, and humidity (*WHO Air Quality Guidelines for Particulate Matter, Ozone, Nitrogen Dioxide and Sulfur Dioxide*, 2005). Excess energy from the sun trapped in the atmosphere has significantly affected global temperatures leading to global warming. Also, sulphur dioxide and nitrogen dioxide can cause acid rain when emitted into the atmosphere.

2.2.1 Transportation of Particulate Matter

Transportation of fine and coarse particles in the atmosphere behaves in diverse ways. Particulates with size larger than 2.5 microns are normally found relatively close to their emission sources, while fine particles can be transported long distances by the wind and other weather parameters. As a result, these fine particles can be found in the atmosphere kilometres from their source of origin (Heilman et al., 2014; Stein et al., 2015).

Long-term and short-term transport of aerosols as well as their lifetime, depend mainly on the size of particulates and boundary layer height of the atmosphere (Colarco et al., 2004; Heilman et al., 2014; Kahn et al., 2008; Stein et al., 2015; Witte et al., 2011). For fine particulate matter in ambient air, the lifetime is usually for a few days. The lifetime increases to weeks to several months for particles released into the troposphere. Moreover, fine particulates such as volcanic sulphate in the stratosphere can last for several years.

The paucity of the lifespan of fine particulate near the surface limits their movement. Hence, they are not usually transported far from the source of origin. Higher levels of organic carbon, for example, black carbon and nitrate are commonly found in East Asia, North America and Europe. Organic carbon is also the most prolific source of industrial emissions.

Long-range transport of particulates, for example dust storms originating from the Saharan desert crosses the Atlantic to Central and South America. Also, transportation of mineral dust and industrial aerosols cross the Pacific from China to North America. An example of vertical transportation of aerosols is the release of sulphur dioxide (SO_2) beyond the troposphere as result of volcanic eruptions such as the 1991 Mt. Pinatubo eruption. SO_2 is a type of particulates that is converted to sulphate aerosols and can remain in the in troposphere or stratosphere for several years.

Many authors including Colarco et al. (2004), Heilman et al. (2014), Kahn et al. (2008) and Madhavan et al. (2017) have monitored the transportation of particulate matter, particularly from biomass burning, wildfires emissions, and dust storms in many regions across the globe. For example, Colarco et al. (2004) investigated transportation of smoke from wildfires over Canada. It was shown that smoke and pollutants from Canadian forest fires are sometimes transported over the United States at low altitudes behind advancing cold fronts. In addition, trajectory and three-dimensional model calculations confirmed the origin of the smoke, its transport at high altitudes, and the mechanism for bringing the pollutants to the surface over Canada. Witte et al. (2011) investigated the transportation of particulate matter from wildfires during a continuous heat wave in most parts of Eastern Europe and western Russia. The study showed that coarse particles were normally found relatively closer to the source of emission, while fine particles were transported long distances to other regions within Eastern Europe.

Some authors have also investigated the origin and the transportation of particulate matter in West Africa. Chem et al. (2018) observed the escalated levels of particulate matter concentrations over most West African countries including Ghana, Togo, Benin and Nigeria, as a consequence of anthropogenic activities mainly from biomass burning due to agricultural practices during the raining seasons. For example, Dionisio et al. (2010) and Abam (2015) observed the transportation of sea spray originating mainly from the Mediterranean sea over the southern part of Ghana. Akinyoola et al. (2018) did a 5-day back trajectory

analysis over 12 selected stations across Nigeria. Their study revealed that air masses reaching the northern and southern parts of Nigeria from 500 – 2000 m above ground level, originated majorly from the Saharan desert and the Mediterranean Sea respectively. Their study further indicated that air masses at 3000 m and above, over the northern and southern parts of Nigeria, are mainly due to heavy biomass burning from the Saharan regions and Niger Delta respectively.

2.2.2 Radiative Transfer in the Atmosphere

Radiative transfer is a phenomenon occurring in the atmosphere describing the transfer or propagation of electromagnetic waves. Atmospheric aerosols or particulates are able to interact with solar radiation by as result of scattering and absorption.

Scattering can be defined as the process whereby radiation from the sun are dispersed or scattered due to atmospheric particulates while absorption is a phenomenon which occurs when solar radiation are absorbed rather than being scattered by atmospheric particulates. Thus, atmospheric particulates can attenuate solar radiation through absorption and scattering and other atmospheric processes such as reflection at a particular wavelength - usually at the visible range (0.4 to 0.7μm). Hence, satellite sensor can estimate atmospheric particle optical properties by quantifying the attenuated solar radiation using the visible range.

The attenuated radiation or photon as (Z_λ) along a specified path (dl) is represented for both scattering and absorption as:

Absorption:

$$\frac{dZ_\lambda^a}{dl} = -\alpha_\lambda^a Z_\lambda \quad ----------(1)$$

Scattering:

$$\frac{dZ_\lambda^s}{dl} = -\alpha_\lambda^s Z_\lambda \quad ----------(2)$$

Where α_λ^a and α_λ^s represent total absorption and total scattering coefficients respectively at wavelength λ.

The extinction coefficient can be derived as:

$$\frac{dZ_\lambda^a}{dl} + \frac{dZ_\lambda^s}{dl} = -\alpha_\lambda^a Z_\lambda - \alpha_\lambda^s Z_\lambda \quad ----------(3)$$

$$\frac{dZ_\lambda}{dl} = -\epsilon_\lambda Z_\lambda \quad ----------(4)$$

The extinction coefficient is derived from a phenomenon known as extinction which occurs when the total attenuated radiation along a specified path is induced by atmospheric processes – scattering and absorption due to cloud, atmospheric particulates and atmospheric gases interactions.

Atmospheric optical depth (τ_λ^{atm}) usually called normal optical depth can be defined as the measure of how clear or transparent the atmosphere is at a wavelength (λ).

τ_λ^{atm} can be calculated as:

$$\tau_\lambda^{atm} = \int_0^{s^{TOA}} \epsilon_\lambda l(dl) = \int_0^{z^{TOA}} \epsilon_\lambda z(dz) ----------(5)$$

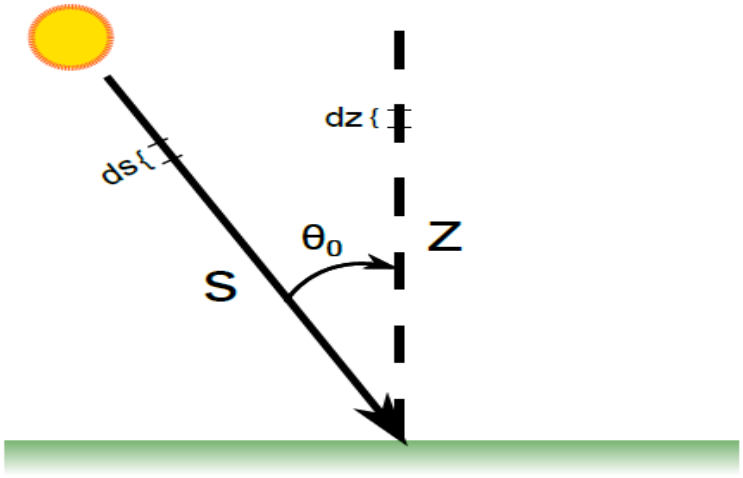

Figure 2.1 (Strandgren et al., 2014)

From the figure 2.1, equation (5) becomes:

$$\tau_\lambda^{atm} = \int_0^{s^{TOA}} \epsilon_\lambda l(dl) = \int_0^{z^{TOA}} \epsilon_\lambda z(dz) = \int_0^{z^{TOA}} \epsilon_\lambda cos(\theta_0) ds \quad ------- (6)$$

Equation (6) can be written as:

$$\tau_\lambda^{atm} = \int_0^{z^{TOA}} \epsilon_\lambda^{clouds} cos(\theta_0) ds + \int_0^{z^{TOA}} \epsilon_\lambda^{gases} cos(\theta_0) ds + \int_0^{z^{TOA}} \epsilon_\lambda^{molecules} cos(\theta_0) ds + \int_0^{z^{TOA}} \epsilon_\lambda^{aerosols} cos(\theta_0) ds \quad --(7)$$

Thus, Aerosol Optical Depth (AOD) can be derived as:

$$\tau_\lambda^{aerosols} = \int_0^{z^{TOA}} \epsilon_\lambda^{aerosols} cos(\theta_0) ds = \int_0^{z^{TOA}} \epsilon_\lambda cos(\theta_0) ds - \left\{ \int_0^{z^{TOA}} \epsilon_\lambda^{clouds} cos(\theta_0) ds + \int_0^{z^{TOA}} \epsilon_\lambda^{molecules} cos(\theta_0) ds + \int_0^{z^{TOA}} \epsilon_\lambda^{gases} cos(\theta_0) ds \right\} --$$

$$----------(8)$$

This implies that:

$$\tau_\lambda^{aerosols} = \tau_\lambda^{atm} - \{\tau_\lambda^{clouds} + \tau_\lambda^{molecules} + \tau_\lambda^{gases}\} ---------(9)$$

Hence, to obtain the AOD – contribution from clouds, gases and molecules interactions must be derived and subtracted from the atmospheric optical depth (Levy et al., 2013).

2.2.3 Satellite Retrieval Total Column and Particulates Less Than 2.5 Microns

Total column data usually called aerosol optical depth differs from ground particulates in terms of particle sizes and the location in the atmosphere. However, many authors including Gupta & Christopher (2009b) and Mao et al. (2014b), who derived particulate matter less than 2.5 microns from a global total column aerosol optical depth over many regions around the world, have established a linear relationship between aerosol optical depth (AOD) and particulate matter less than 2.5 microns. For example, Mao et al. (2014a) derived estimations of $PM_{2.5}$ from AOD obtained from MODIS instrument located on both Terra and Aqua satellites. Their study observed high levels of particulates mainly in middle and low-income countries like African and Asian countries. Another study by (Fawole et al., 2016) analysed Aerosol Robotic Network (AERONET), Aerosol Optical Depth (AOD) data at Ilorin, Nigeria, with the aim of deducing trends of particulate matter dust storms for a period of 10 years.

The Aerosol Optical Depth (AOD) is the extent to which particulates avoid transmission of light rays by scattering or absorption from the ground to the satellite sensor through the vertical column of the atmosphere. AOD is a unitless quantity and depends on particle size, composition, water update (hygroscopic nature of particles) and vertical distribution in the atmosphere. These parameters normally affect the retrievals of aerosol optical depth values from satellites which involves assumptions (end-user algorithms).

Aerosol optical depth which is measured by satellite sensors can also be estimated from measurements of $PM_{2.5}$ obtained from sun photometers which are normally located at the ground level. Estimates of $PM_{2.5}$

can also be derived from AOD values obtained by satellite sensors. Therefore, measurement of aerosol optical depth values can be used to quantify their concentrations in the atmosphere.

2.3 Methods of Monitoring Poor Air Quality

There are different ways of monitoring particulate matter. The concentration of aerosols in the atmosphere can be monitored by using ground-based instruments, remote sensing techniques and modelling which incorporate information such as population data and topography (Donkelaar et al., 2010; Gupta & Christopher, 2009a; Ite et al., 2017; Sulprizio, 2015).

2.3.1 Monitoring Poor Air Quality Using Ground-Based Instruments

High-income countries around the world such as United States of America, Germany and Russia operate extensive network of ground-based air quality monitoring stations in urban areas, which provide continuous daily measurement of ambient particulate matter levels. Emeis and Karlsruhe (2004) used ground instrument for a year study over Germany. The study observed that particulate matter pollution is rising in most urban areas in Germany.

Ground-based instrument has been used to monitor particulate matter in other parts of the world. For example, Welton et al. (2016) also conducted a study in Canary Island of Tenerife. The study revealed that PM concentration in Tenerife was influenced by dust storm from the Saharan desert. Furthermore, Nemuc et al. (2007) conducted a research on particulate matter pollution in Magurele-Bucharest, Romania. The study revealed the seasonal variations of particulate matter resulting from different aerosol sources such as biomass burning and mineral dust. The study also observed the transport of dust storm and biomass burning from sub-Saharan countries, when a 5-day back trajectories analysis was conducted over Romania.

In Africa, ground-based air quality monitoring stations have been the basis for most studies of the adverse health effects of pollutants and control of the quality of air, particularly in most sub-Saharan African countries. Metropolis et al. (2014) examined the spatial and seasonal concentrations of ambient particulate matter pollutants and their health implications using 14 ground-based air monitoring instruments in Port Harcourt, Nigeria. Dionisio et al. (2010) evaluated the spatiotemporal variability of ambient air pollution in four selected neighbourhoods in Accra, Ghana, using integrated and continuous rooftop monitors. The study observed that levels of the PM smaller than 2.5 microns was higher than the WHO Air Quality Guidelines. In another study, Rooney et al., (2012) observed particulate matter pollution in Accra, Ghana, using ground-based air quality monitoring instrument. The results of the study also showed that PM levels exceeded recommended levels stipulated by in the WHO Air Quality Guidelines.

Furthermore, most authors like Nwachukwu et al. (2012) and Ofosu et al. (2013) have also used receptor models in monitoring ambient particulate matter. For example, Ofosu et al. (2013) analysed the seasonal variations (non-Harmattan and Harmattan) of $PM_{2.5}$ and carbon levels and their sources in a suburb of Navrongo, in the northern region of Ghana using positive matrix factorization. This study results revealed that about 16% of biomass combustion was the most important source of aerosol pollution next to soil dust over Navrongo during the study period. (Oluyemi & Asubiojo, 2001), using Principal Component Analysis (PCA) models, have identified soil, marine, vehicular emission and regional sulphate as the sources of PM_{10} at three sampling points in Lagos.

2.3.2 Using Modelling to Monitoring Poor Air Quality

Many authors have used complex methods such as modelling to monitor the spatial distribution of particulates in the atmosphere. They developed models that incorporate information such as population data and topography to observed particulate matter pollution over different regions around the world. One

quintessential example is the current model developed by University of Bath and World Health Organization (WHO) known as the Data Integrating Model for Air Quality (DIMAQ). DIMAQ incorporates information such as population data, topography and land use, satellite data, and among others to estimate levels of ambient particulates around the globe with their associated measures of uncertainties ('WHO | WHO Global Urban Ambient Air Pollution Database (Update 2016)', 2017). As already mentioned, from the DIMAQ model, WHO identified Aba, Kaduna, Onitsha and Umuahia among the top 20 worst-ranked cities for air quality in the world (*WHO Releases Country Estimates on Air Pollution Exposure and Health Impact*, n.d.)

2.3.3 Monitoring Poor Air Quality Using Satellite-Derived Data

In recent years, satellite instruments such as the Advanced Very High-Resolution Radiometers (AVHRR), Sea-Viewing Wide Field-of-View Sensor (SeaWiFS) and the Moderate Resolution Imaging Spectro-radiometer (MODIS) have been used to retrieve total column aerosol optical depth and estimated indirectly the spatial distribution of particulate matter pollution across the globe. Satellites observations of particulate matter pollution provide wide-field-of-view of the concentrations of particulate matter across regions because of their larger spatial resolutions.

The Advanced Very High-Resolution Radiometer was the first satellite instrument to be used to estimate the global-mean aerosol optical depth (AOD) (Chu et al., 2002; Li et al., 2013). Many authors have used data from the AVHRR sensor to monitor particulate matter pollution. Chu et al. (2003) used the AVHRR to monitor global air pollution over land. The study showed that the increasing rate of particulate matter concentrations in most countries was due to urbanization and industrialization. (GBD 2015 Risk Factors Collaborators et al., 2016) also studied the burden of diseases globally using the AVHRR. The study observed that from 1990 to 2015, DALYs declined for micronutrient deficiencies, childhood

undernutrition, unsafe sanitation and water, and household air pollution; reductions in risk-deleted DALY rates rather than reductions in exposure drove these declines.

Some authors such as Colarco et al. (2004) and Heilman et al. (2014) have been able to use the Sea-Viewing Wide Field-of-View Sensor (SeaWiFS) to observe the transportation of particulate matter from wildfires sources. In 2010, Witte et al. (2011) observed the impact of wildfires on particulate matter concentrations over western Russia and parts of Eastern Europe using Sea-Viewing Wide Field-of-View Sensor (SeaWiFS). Chem et al. (2018) also observed the escalated levels of particulate matter concentrations over most West African countries including Ghana, Togo, Benin and Nigeria using SeaWiFS.

The Visible Infrared Imaging Radiometer Suite (VIIRS) has been used to retrieve total column aerosol optical depth and estimated indirectly the spatial distribution of particulate matter pollution across the globe. Wang et al. (2016) analysed the potential application of the Visible Infrared Imaging Radiometer Suite (VIIRS) Day / Night Band for monitoring night-time surface particulate matter air quality from August to October 2012 in Atlanta (Georgia, US). The study showed that DNB at night is sensitive to the change of aerosols and much less sensitive to the change of water vapor in the atmosphere illuminated by common outdoor light bulbs at the surface. M. Wang et al. (2015) also used the Visible Infrared Imaging Radiometer Suite (VIIRS) on the S-NPP - Suomi National Polar- orbiting Partnership satellite to monitor the performance of VIIRS reflective solar bands for ocean colour data processing. Furthermore, Cao & Bai (2014) did a quantitative analysis of VIIRS DNB nightlight point source for light power estimation and stability monitoring over China. The study revealed that the VIIRS DNB nightlight bands enabled accurate measurements of low light radiances which resulted in enhanced quantitative applications at night.

Authors such as Schaap et al. (2009) and Emeis & Karlsruhe (2004), Welton et al. (2016) and Brito et al. (2014) have used the Light Detection and Ranging (LIDAR), to monitor the spatial distribution of particulate matter in their respective regions of interest around the world. Emeis & Karlsruhe (2004) conducted a research in Germany using Light Detection and Ranging (LIDAR) mounted on aircraft to monitor the spatial distribution of particulate matter. The study observed that particulate matter pollution is rising in most urban areas in Germany. Welton et al. (2016) also conducted a study in Canary Island of Tenerife using Light Detection and Ranging (LIDAR) based on land to monitor the concentrations of aerosols. The study showed that particulate matter concentration in Tenerife is influenced by Saharan desert dust storms. (Brito et al., 2014) observed particulate matter concentrations over Rondonia and Porto Velho by using Light Detection and Ranging (LIDAR) mounted on aircraft. Nemuc et al. (2007) also observed particulate matter pollution in Magurele-Bucharest, Romania using LIDAR. The study observed the seasonal variations of particulate matter resulting from different aerosol sources such as biomass burning and mineral dust.

Some authors also have employed LIDAR to capture the vertical distribution of aerosol at specific location. For example, Schaap et al. (2009) observed that locally derived AOD to particulate matter less than 2.5 microns relationships cannot be extended easily to other regions because of variation in meteorology and aerosol composition. Unique, local, time-dependent AOD–$PM_{2.5}$ relationships are necessary to infer global estimates of particulate matter less than 2.5 microns.

The Moderate Resolution Imaging Spectro-radiometer (MODIS) on board the Terra and Aqua satellites has been used extensively to retrieve total column aerosol optical depth and to estimate indirectly the spatial distribution of particulate matter pollution across the globe. Aqua and Terra satellites are part of NASA's primary EOS - Earth Observing System. On December 18th, 1999, the NASA Terra satellite was

launched while on May 4th, 2002, Aqua was also launched. In addition to MODIS, both satellites carry other instruments for applications like water and land-cover analysis. Further, each satellite has a different local overpass time. For example, in sub-Saharan African regions, Terra satellite overpass time is10:30 AM while Aqua is 1:30 PM in opposite directions.

Difference authors have used AOD derived from the MODIS sensor to monitor the concentration of PM in different parts of the world. For example, Donkelaar et al. (2010) estimated global ground-level particulate levels using aerosol optical depth from the MODIS sensor. They concluded that Satellite derived total column AOD provides estimates of global long-term average particulate matter ($PM_{2.5}$) concentrations. Welton et al. (2016) also assessed particulate matter air quality over different locations across the global urban areas spread over 26 locations in Sydney, Delhi, Hong Kong, New York City and Switzerland using the Moderate Resolution Imaging Spectro-radiometer (MODIS) sensor. The study revealed increasing trends of particulate matter concentrations over Delhi, Hong Kong and Sydney respectively, during the study period. Mao et al. (2014b) conducted a global study on AOD retrieval by using data from the MODIS sensor to observe the wide range of effects of particulates on solar energy, sulphur and nitrogen cycles as well as climate. The study revealed low levels of AOD in 2010 while high levels occurred in 2007.

2.3.3.1 End-User Algorithms for Satellite-Derived Data

Many End-User Algorithms have been developed for satellite sensors such as MODIS, SeaWiFS and AVHRR, to retrieve total column aerosol optical depth and to estimate indirectly, particulate matter concentrations over land and ocean. End-user algorithms used by passive satellite remote sensing sensor do not make direct measurement of aerosol optical depth but retrieve aerosol optical depth based on assumptions, by depending on meteorological parameters such as temperature, humidity, surface

brightness, surface darkness and amount of sunlight. Therefore, there are uncertainties in the aerosol optical depth-retrieval-values which vary from region to region across the globe depending on the climatic conditions.

One of such End-User Algorithm is the Deep Blue algorithm which is used to calculate aerosol optical depth (AOD) and Angstrom Exponent (α or AE) over land (Misra et al., 2015). Deep Blue utilizes the 412 nm band to capture aerosols at bright surfaces (Gupta et al., 2016). The deep blue algorithm has been used to retrieve total column aerosol optical depth from the aerosol products of MODIS because of its efficiency in bright surfaces. Sayer et al., (2015) validated the Deep Blue (DB) algorithm from the MODIS Collection 6 (C6) aerosol products from the Terra satellite with Aerosol Robotic Network (AERONET) data. The study discovered that the C6 DB Terra AOD quality was stable throughout the mission to date.

Relative to the Deep Blue algorithm is the Dark Target algorithm which retrieves aerosol optical depth over dark vegetative surfaces on land and ocean. Authors such as Gupta et al. (2016) have used the Dark Target algorithm to addressed the inaccuracies produced by remote sensing sensors. For example, Gupta et al. (2016) conducted a study to address the inaccuracies produced by the MODIS aerosol optical depth (AOD) retrievals over urban areas and suggested improvements by modifying the surface reflectance scheme in the algorithm. The study observed that the number of AOD retrievals over urban areas, falling within expected error (EE %) has increased by 20 % and the strong positive bias against ground-based sun photometry has been eliminated.

Furthermore, the Combined DT and DB algorithm of MODIS 10 km aerosol products as discussed by Sayer et al. (2014) and Gupta et al. (2016) respectively has been developed to retrieve total column aerosol optical depth over bright and dark vegetative surfaces respectively.

Sayer et al. (2014) used MODIS collection 6 (C6) aerosol products to compare the algorithms, namely, deep blue (DB), dark target (DT) and Combined deep blue/dark target from Aqua satellite to understand the performance of the MODIS sensor algorithms. In their study, they discovered that in many regions the DB, DT, and Combined DB and DT algorithms are all suitable for quantitative applications.

2.3.3.2 Validation of Satellite Total Column Data

Validation of satellite derived aerosol optical depth against ground measurement is paramount in satellite remote sensing for air quality. This is because satellite sensors do not make direct measurement of aerosol optical depth (AOD) but retrieve aerosol optical depth using end-user algorithms. Therefore, there are uncertainties in the aerosol optical depth-retrieval-values which need to be validated with ground-based air quality monitoring instruments such as sun photometers.

The National Aeronautical and Space Administration (NASA) run a network of ground-based sun photometers around the world called Aerosol Robotic Network (AERONET). There are about 400 active Aerosol Robotic Network sites around the world making measurement every 15 minutes during the daytime. These measurements of aerosol optical depth are considered ground-truth to the mapped AOD from satellite sensors. They are also used to get other useful information about atmospheric aerosols such as their shape, size distribution, their scattering or absorption properties including scattering albedo and reflective indexes. These measurements also help to improve satellite end-user algorithms in regions where the algorithm performances are not up to the mark.

AERONET is very useful in the validating satellite derived dataset (Gupta et al., 2016). For example, Sulprizio (2015) mapped particulate matter concentration from MODIS satellite data over Vietnam. The results from their findings were validated using four AERONET stations located in Vietnam. The study observed that most of the MODIS total column aerosol optical depth retrievals overestimated the

concentrations of particulate matter over many regions in Vietnam. In another study by Jin et al. (2005), the diurnal, weekly, seasonal, and inter-annual variations of urban aerosols were examined. With an emphasis on summer months, comparison was made between the Moderate Resolution Imaging Spectro-radiometer (MODIS) observations, ground Aerosol Robotic Network (AERONET) observations and U.S. EPA $PM_{2.5}$ low-cost sensor data over a period of four years. The study observed that the MODIS aerosol optical depth derived data compared well with the AERONET and U.S EPA $PM_{2.5}$ low-cost air quality dataset.

Microtops which are handheld and user-friendly portable sun photometers can also be used to validate satellite derived aerosol optical depth values. The data obtained from Microtops contribute to the Maritime Aerosol Network (MAN) over Oceanic regions which are also part of Aerosol Robotic Network (AERONET). For example, Cisek et al. (2017) used Microtops to observe that an increase of AOD along the measurement profile towards the open sea was due to local breeze circulations of particulate matter. In a comparative study using data obtained from Microtops and satellite data derived from MODIS sensor, Zawadzka et al. (2014) showed that Microtops sun photometers are reliable instruments for field campaigns in the Coastal Areas of the Baltic Sea.

Comparative studies with Microtops are not limited to oceanic regions. Lee et al., (2015) developed a new method for retrieving Aerosol Size Distribution (ASD) from spectral aerosol optical thickness (AOT) measured by Microtops sun photometer in Hong Kong. The results of the Aerosol Size Distribution (ASD) retrievals showed reasonable agreements with AERONET inversion products.

2.5 Monitoring Poor Air Quality in Ghana

Poor air quality monitoring using in-situ point instruments is monitored in few metropolises by the GEPA - Ghana Environmental Protection Agency and individual researchers.

The Ghana Environmental Protection Agency currently manages and monitor air quality network mainly the Greater Accra Region. The monitoring network is made up of 14 stations with 10 located along the roadside while the remaining 4 stations at various industrial sites in the Greater Accra Region, Ghana.

Particulate matter pollution over Ghana has also been monitored by many researchers. Rooney et al. (2012) used ground-based air quality monitoring instruments and receptor models located in the northern and southern parts of Ghana. Receptor models are important tools used for source identification and apportionment of particulate matter (Ede & Edokpa, 2017; Nwachukwu et al., 2012; Ofosu et al., 2013; World Bank, 2015). The models use the physical and chemical characteristics of air pollutants collected at the receptor locations. Examples of receptor models that have been used mainly to monitor particulate matter pollution in Ghana are Principal Component Analysis (PCA) and Positive Matrix Factorization (PMF). The main advantage of receptor model is to develop a mitigating strategy for ambient particulate.

In the southern part of Ghana, authors such as Ofosu et al. (2012), Dionisio et al. (2010) and Rooney et al. (2012) have used Positive Matrix Factorization (PMF) and ground-based air quality monitoring instruments to monitor particulate matter concentrations. Ofosu et al. (2012) analysed space-time patterns of $PM_{2.5}$ and carbon levels and their sources over Ashaiman, a suburb in the Greater Accra Region of Ghana using positive matrix factorization. The result of the study revealed that about 16% of biomass combustion was the most important source of $PM_{2.5}$ pollution following soil dust over Ashaiman during the study period.

Dionisio et al. (2010) evaluated the spatiotemporal variability of ambient air pollution in four selected neighbourhoods in Accra, Ghana, using integrated and continuous rooftop monitors. The study revealed that Particulate Matter (PM) was higher than the WHO Air Quality Guidelines. Also, Rooney et al. (2012) observed the Spatial and temporal patterns of particulate matter sources and pollution in four communities in Accra, Ghana. The socio-economic status of the neighbourhood can also influence the concentration of particulate matter in the neighbourhood. Arku et al. (2008b; 2008a) investigated the spatiotemporal patterns of $PM_{2.5}$ and sources of this pollutant in four neighbourhoods in the Greater Accra Metropolitan Area (GAMA), Ghana. The results of the study showed that the density of wood stoves, fish smoking, and trash burning along the mobile monitoring path as well as road capacity and surface were associated with higher $PM_{2.5}$. In the GAMA, biomass burning from wood and fish smoking were the major sources of pollution during the study period.

Zhou et al. (2011) collected and analysed geo-referenced data on household and community particulate matter (PM) pollution, socioeconomic status (SES), fuel use for domestic and small scale commercial cooking, housing characteristics, and distance to major roads. The study observed high levels of particulates in areas where biomass is used for cooking while lower levels was observed in high residential neighbourhoods. The study further revealed that lack of regular physical access to clean fuels is an obstacle to fuel switching in low-income neighbourhoods and should be addressed through equitable energy infrastructure.

CHAPTER THREE

RESEARCH METHODOLOGY AND DATA PROCESSING

3.1 Description of Study Area

Ghana is located along the Gulf of Guinea and the Atlantic Ocean in the sub region of West Africa. With a total land mass of about 238,535 square kilometers, Ghana is bounded between latitude 3.750277^0N and 11.750277^0N and longitude 2.416944^0E and 3.900277^0W. The country is bordered by the Ivory Coast in the west, Burkina Faso in the north and Togo in the east as shown in figure 3.1. In the south, Ghana it is bordered by the Gulf of Guinea and the Atlantic Ocean. Its notional centre, (0°, 0°) is located in the Atlantic Ocean approximately 614 km off the south-east coast on the Gulf of Guinea. Grasslands mixed with south coastal shrub lands and forests dominate Ghana, with forest extending northward from the south-west coast of Ghana on the Gulf of Guinea in the Atlantic Ocean 320 km and eastward for a maximum of about 270 km.

Ghana is made of 16 regions including Greater Accra Region, Central Region, Western North Region, Western Region, Eastern Region, Ashanti Region, Volta Region, Bono Region, Bono East Region, Brong Ahafo Region, Savanna Region, Oti Region, North East Region, Northern Region, Upper East and Upper West Region. The projected population of Ghana in 2021 is 30,832,019 (https://census 2021.statsghana.gov.gh/).

The study focused mainly in the Greater Accra Region (5.8143° N, 0.0747° E) with a land surface area of about 3,245 km^2 (www.ghanahealthservice.org). In 2021, the population in the Greater region was estimated to be 5,455,692 which constitute about 17.7% ahead of the Ashanti region (https://census 2021.statsghana.gov.gh/). The Greater Accra region being the capital of Ghana, is mostly urbanised and

thus, serve as a hub for huge industrial and economic activities (World Health Organization & Mudu, 2021) . The region has two distinguished dry seasons – July to August as minor dry season and December to February as major dry season.

The study utilised 5 Ghana Environmental Protection Agency air quality ground-based sensors distributed in the Greater Accra Metropolitan Area (GAMA) as can be seen in figure 3.2.

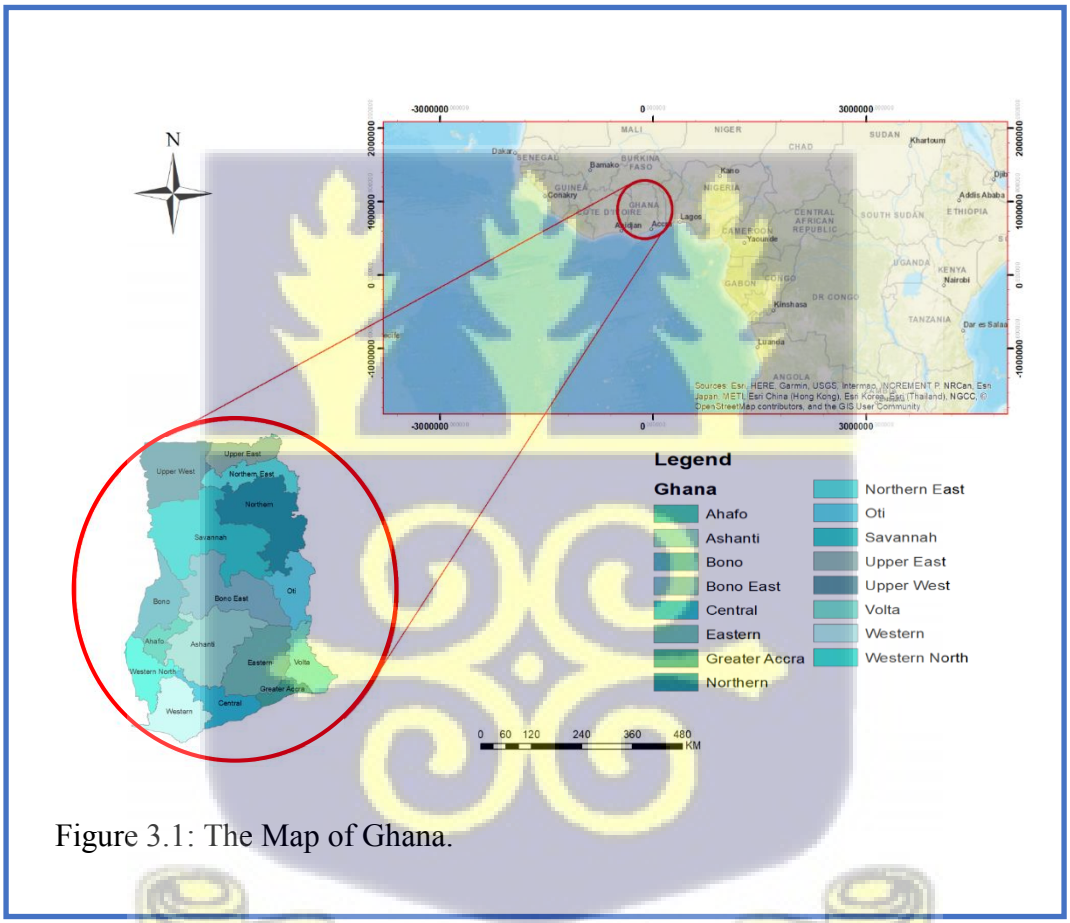

Figure 3.1: The Map of Ghana.

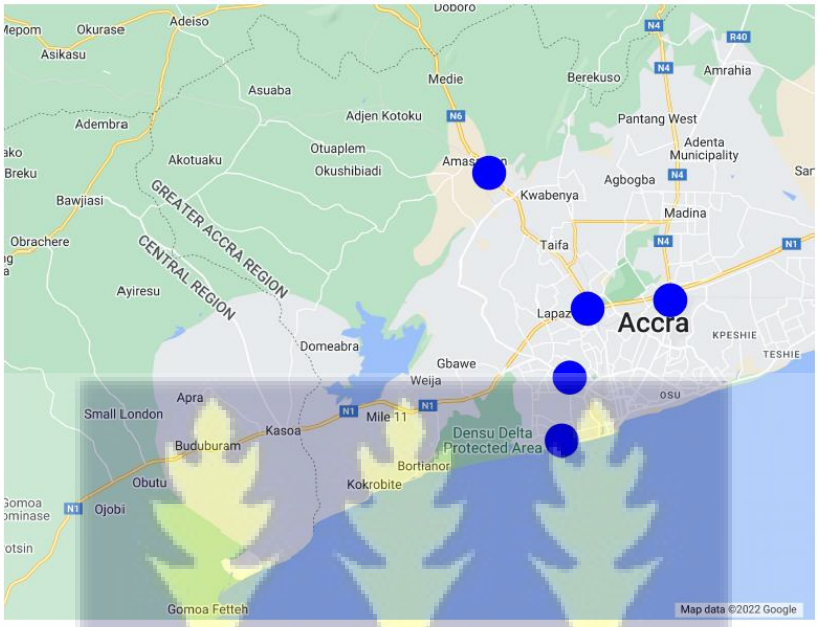

Figure 3.2: Map of the 5 EPA Air Quality Stations in Greater Accra region

3.2 Dataset for the Study

The dataset used for this study was derived from the Moderate Resolution Imaging Spectro-Radiometer (MODIS) and Ozone Monitoring Instrument (OMI). MODIS is (on board of both Terra and Aqua satellites) and OMI (on board of Aura satellite) and are part of the sensors in the NASA Earth Observing System (EOS). Aerosol Optical Depth (AOD) was retrieved at gridded $(111 \times 111)\, km^2$ spatial resolution (1Degree) from the MODIS Terra (imaging in the morning) and Aqua ((imaging in the afternoon) satellites. This study utilized MODIS Terra and Aqua level 3 daily aerosol product combined

dark target and deep blue algorithm. Total column nitrogen dioxide and ozone data were retrieved at level 3 gridded $(25 \times 25)\ km^2$ spatial resolution from OMI sensor on board of Aura satellite using the Differential Optical Absorption Spectroscopy (DOAS) algorithm. Detail information about OMI total column retrieval data for both ozone and nitrogen dioxide can be found in (Levelt et al., 2006, 2018).

The estimated uncertainty of the MODIS AOD combined dark target and deep blue algorithm was reported by Chu et al. (2003) to be 0.05 and 0.15 (deep blue algorithm) over land against 0.03 and 0.05 (dark target algorithm) over ocean.

3.2.1 Dataset Retrieval Site

The Moderate Resolution Imaging Spectro-Radiometer (MODIS) and Ozone Monitoring Instrument (OMI) sensors on board of Terra Aqua and AURA satellites respectively, were used to retrieve multiple aerosol, nitrogen dioxide and ozone dataset to study atmospheric pollutants levels. For this study, gridded MODIS (1º x1º) on board Terra (10:00 UTC) and Aqua (13:00 UTC) satellites and OMI (0.25º x 0.25º) level 3 daily datasets were downloaded from Goddard Earth Sciences Data and Information Services Center (GIOVANNI) provided by the National Aeronautical and Space Administration (NASA) https://giovanni.gsfc.nasa.gov/giovanni/ (Figure3.3).

3.4 Data Analytical Tools

3.4.1 Spyder (Python 3.7)

The Spyder software is an efficient scientific environment which is written in Python and designed by and for scientists, engineers and data analysts including remote sensing scientist (*Spyder · PyPI*, n.d.).

For this study, Spyder was installed through Anaconda which incorporate Python 3.7 open source programming language. Anaconda is a free and open source distribution of the Python and R programming

languages for data science and machine learning related applications, that aims to simplify package management and deployment (Datasets, 2018).

Python script (Figure 3.4) was written to perform different analysis on MODIS Level 3 netcdf total column retrieval dataset. These analyses included:

- Using the geopy module to subset the Area of Interest (AOI) from the global dataset. After sub-setting the AOI (Ghana) using a grid sizes of (1^o x1^o) and (0.25^o x 0.25^o), each of the five EPA stations was further sub-setted using grid sizes of $(25 \times 25)\ km^2$ and $(50 \times 50)\ km^2$ respectively.
- Performing data cleaning of the dataset for the Area of Interest using the Pandas and Numpy modules. For example quartile and inter-quartile ranges approach were employed to find outliers and eliminated from both Clarity and satellite derived dataset. Noises in the dataset were also minimized employing daily, weekly and monthly resampling methods.
- Using the Xarray module to map the total column particulate, NO_2 and O_3 pollutants from MODIS and OMI respectively over Ghana. For example, monthly maps for both OMI and MODIS dataset were plotted for the study period, utilizing Xarray and combination with Matplotlib and GeoPandas, which are compatible with Xarray (Schaap et al., 2009).
- The Statsmodels was used to perform validation (between total column MODIS and ground datasets) and time series trend analysis of 10 years total column MODIS and OMI dataset using non-parametric sequential Mann-Kendall test. To get the trend dataset, the total column dataset (2012-2021) was decomposed so as to select the de-seasonalized dataset from the seasonal and residual parts. The non-parametric sequential Mann-Kendall test has been explained extensively by Shikwambana et al. (2020) and Matandirotya (2021). Furthermore, coefficient of determination

(R^2), in the Python Statsmodel was used to measure the level of agreement (correlation) between the ground –based and satellite derived AOD dataset during the study period.

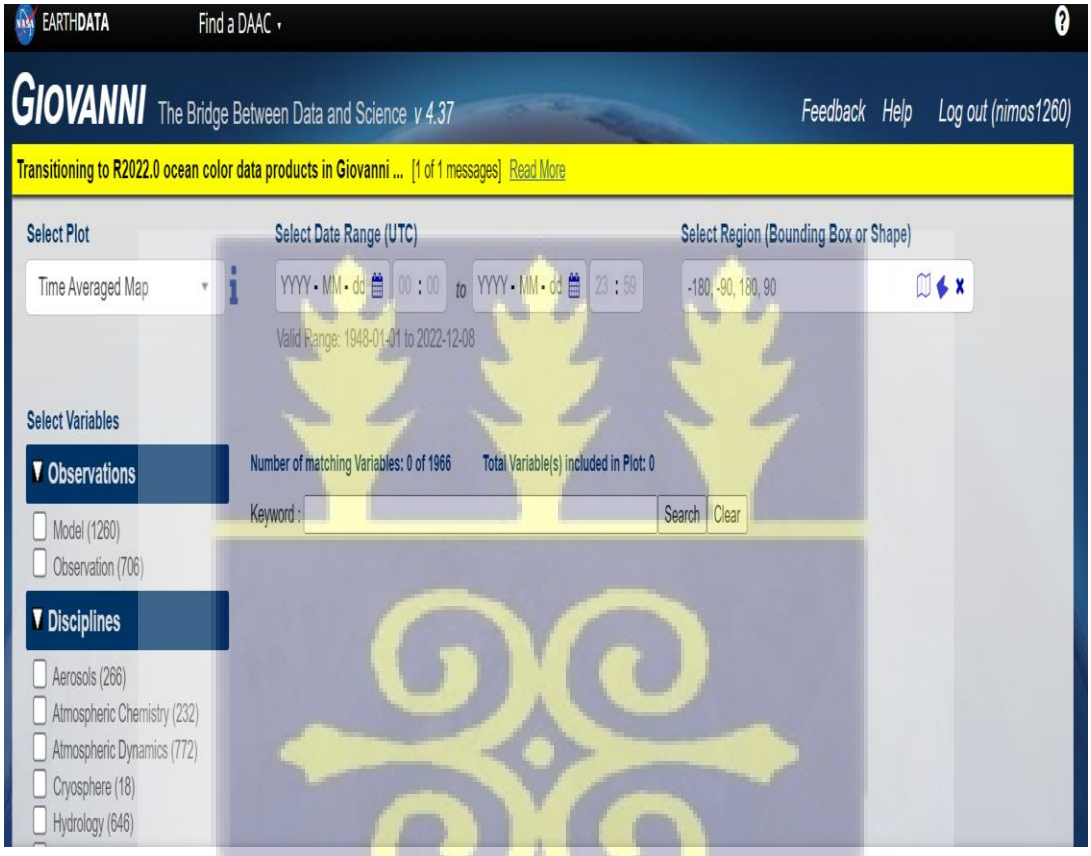

Figure 3.3: A Snapshot of GIOVANNI for Downloading MODIS and OMI daily level 3 Dataset

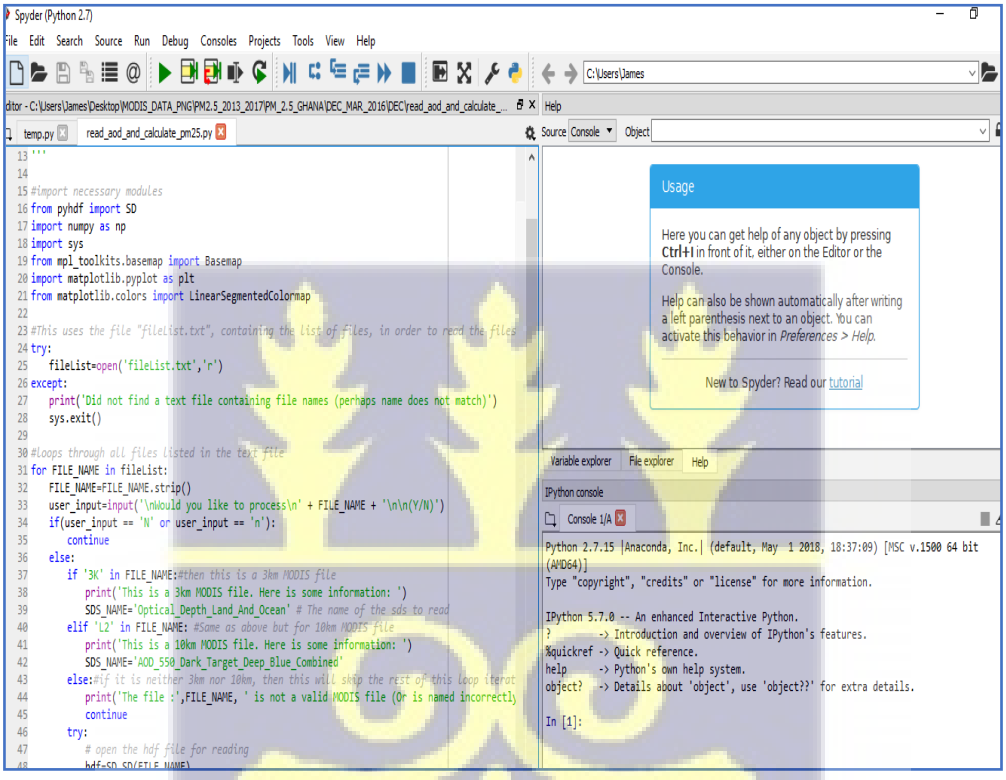

Figure 3.4: A Snapshot of the Spyder Software interface in the Anaconda environment.

CHAPTER FOUR

RESULTS AND DISCUSSION

The results obtained when MODIS and OMI total column particulates, NO_2 and O_3 retrieved values were used to observe the spatio-temporal variation of particulates NO_2 and O_3 pollution over Ghana are presented in this chapter. Furthermore, results from the validation of the total column particulates with ground monitoring $PM_{2.5}$ sensors over 5 EPA stations in the Greater Accra region is presented. Results from the long-term time series analysis using 10 years total column particulates, NO_2 and O_3 dataset from the non-parametric sequential Mann-Kendall test is also presented. The results acquired from satellite derived products, were compared to research findings from various authors who utilized conventional methods to monitor particulate matter pollution over Ghana and the Greater Accra region. The sections are arrange with reference to the specific objectives of the study.

4.1 Spatial Distribution of Total Column Particulates, Nitrogen Dioxide and Ozone over Ghana

The outcome of the first objective on mapping monthly spatial distribution of total column particulates (AOD), NO_2 and O_3 over Ghana is discussed in this section. Figure 4.1 to 4.12 shows the map of the monthly spatial distribution of total column particulates (AOD) from MODIS Terra and Aqua satellites; OMI total column NO_2 and O_3 over Ghana from 2019 to 2021.

4.1.1 Monthly Distribution of Modis AOD over Ghana

Figures 4.1 to 4.6 show both MODIS Terra and Aqua AOD maps during the study period. AOD values ranged between 0.0 and 0.6 with the highest AOD values occurring over the middle part of Ghana. Spatial distribution of AOD was consistently high for both Terra and Aqua satellites in the middle part of Ghana (excluding October to December) throughout the study period. High AODs may be attributed to

anthropogenic emissions - predominantly agricultural activities in these regions as was observed by Fosu-Amankwah et al. (2021) over Ghana from 2005 to 2018. Furthermore, consistent high AODs may be attributed to the capabilities of the dark target and deep blue algorithm which does better in vegetative regions (Huete et al., 2010). Also, for both Aqua and Terra satellites, high AODs can be observed in the southern part of Ghana including the Greater Accra region particularly from July to August during the study period. The high AODs recorded in these months may be due to local emissions - worsened by high economic activities and the minor Harmattan season experienced in the southern part of Ghana.

From October to February during the study period, some Metropolis in the northern part such as Upper East, Upper West and Northern Regions, experienced high AOD concentrations. This observation is in consonance with the study by Ofosu et al. (2013), who observed seasonal variations of aerosols over the northern part of Ghana and concluded that anthropogenic activities especially biomass burning in the northern part of Ghana contributed to the high concentrations of aerosol in this regions. Other sources of aerosols in the northern part of Ghana, as identified by Ofosu et al. (2012) included dust storms originating from the Saharan desert.

No data was observed especially in the southern and northern parts of Ghana during the study period. This surveillance may be due to cloud cover or lack of retrieval by the deep blue and dark target algorithm. The algorithm lacks the capacity to detects aerosols in water-dominated areas like the Volta Lake and Lake Bosomtwe (Gupta et al., 2016). Hence, lack of data in other regions that are not water-dominated areas may be ascribed to cloud cover.

The uneven distribution in the values of the concentrations of AOD over the southern and northern parts of Ghana is an indication of the existence of different sources of aerosol in the regions. Ofosu et al. (2012) observed dust storm from the Saharan desert over the northern part of Ghana while Dionisio et al. (2010)

and Rooney et al. (2012) recorded in their studies predominant biomass burning in the southern part of Ghana. These previous studies and the results of this investigation indicated the existence of internal sources of aerosols in Ghana, due to biomass burning and the transportation of dust storms into the country from an external source (the Saharan desert).

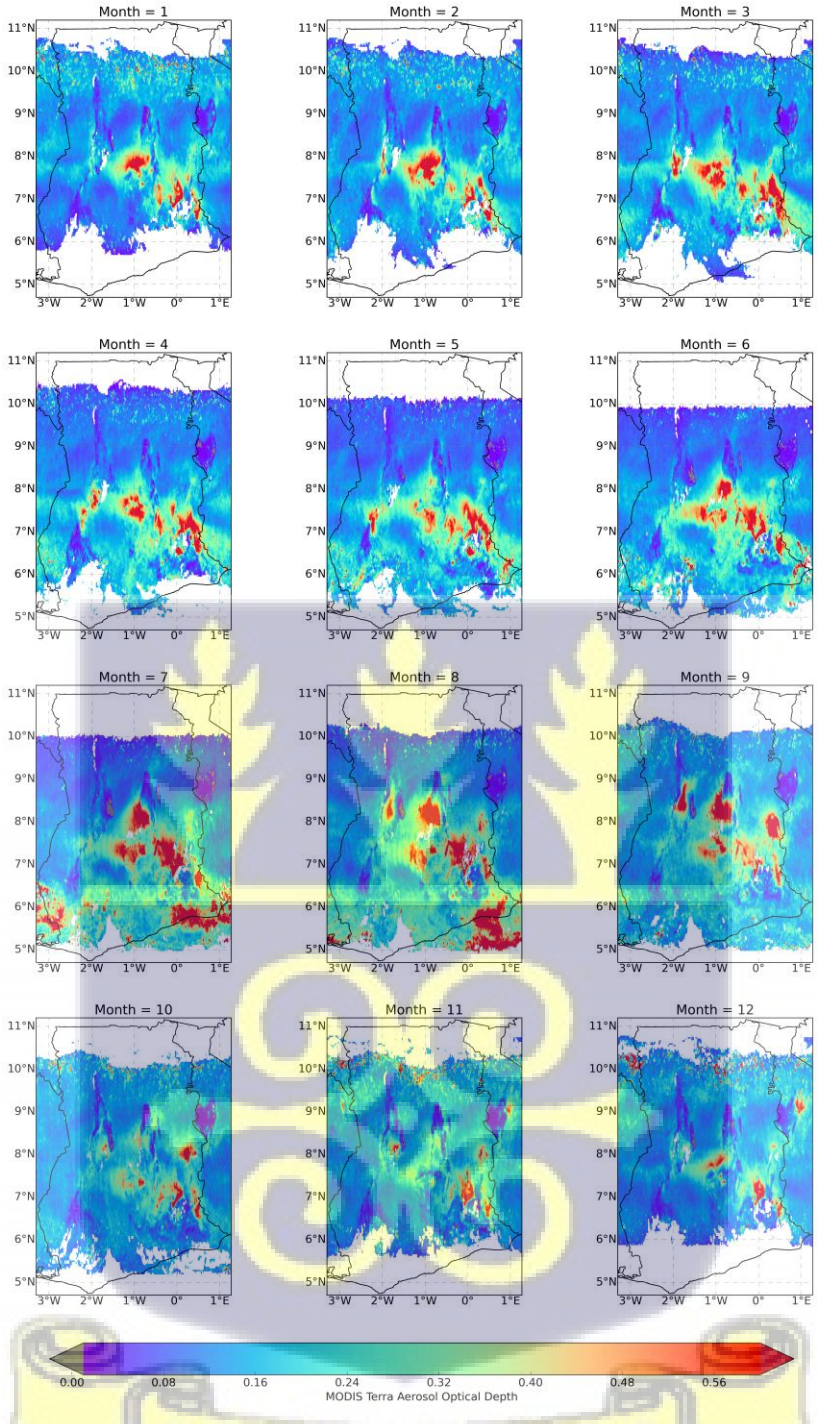

Figure 4.1: Monthly Spatial Distribution of MODIS-Derived Aerosol Optical Depth (AOD) Terra satellite over Ghana in 2019

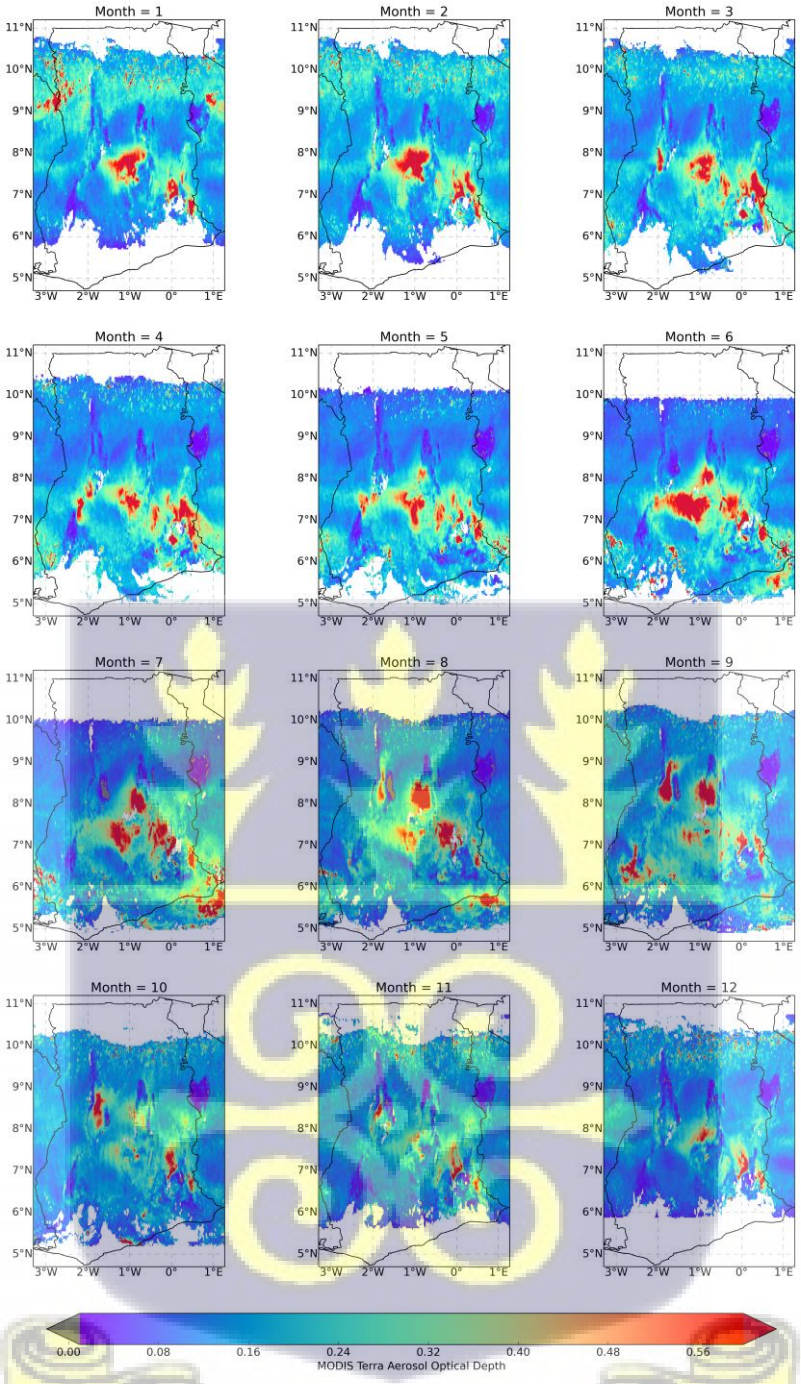

Figure 4.2: Monthly Spatial Distribution of MODIS-Derived Aerosol Optical Depth (AOD) Terra satellite over Ghana in 2020

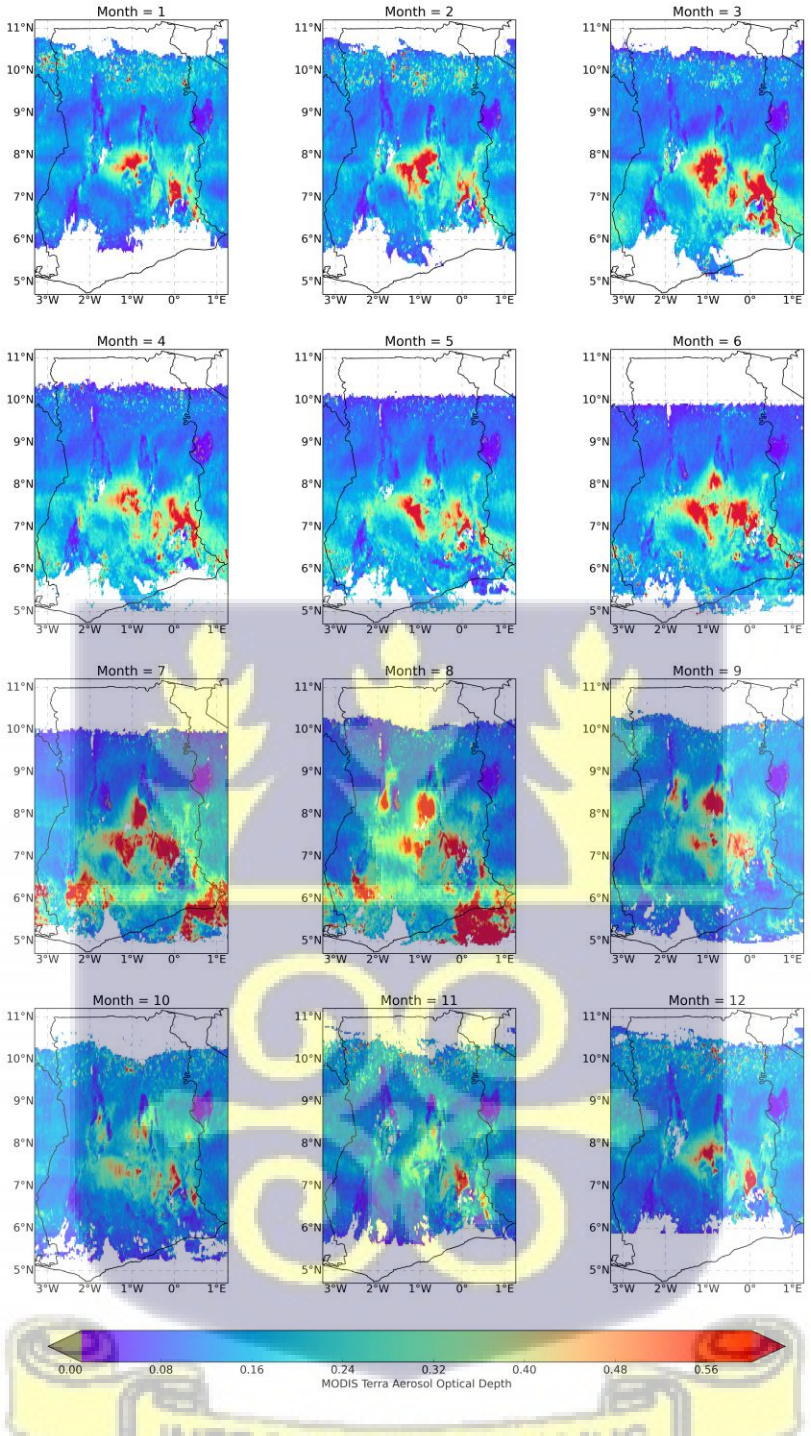

Figure 4.3: Monthly Spatial Distribution of MODIS-Derived Aerosol Optical Depth (AOD) for Terra satellite over Ghana in 2021

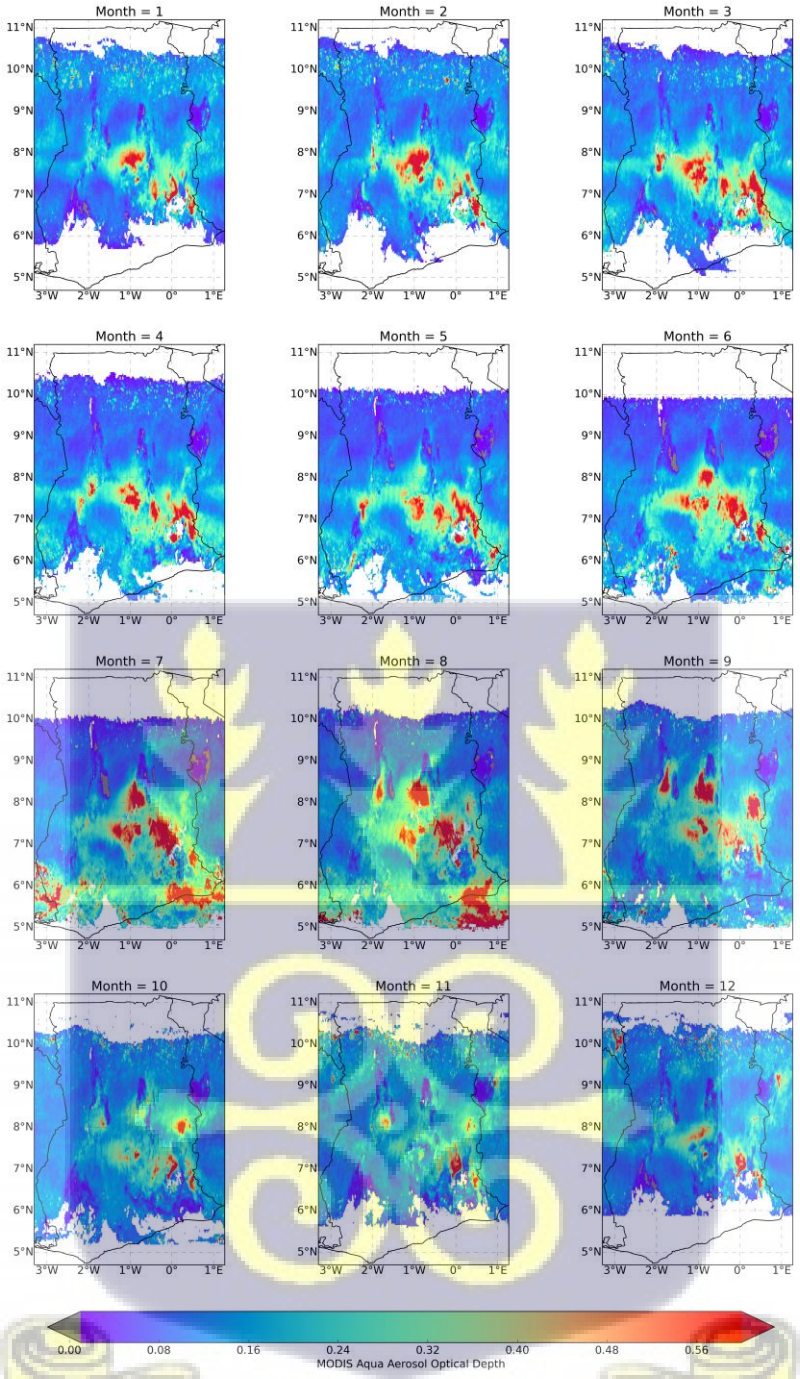

Figure 4.4: Monthly Spatial Distribution of MODIS-Derived Aerosol Optical Depth (AOD) Aqua satellite over Ghana in 2019

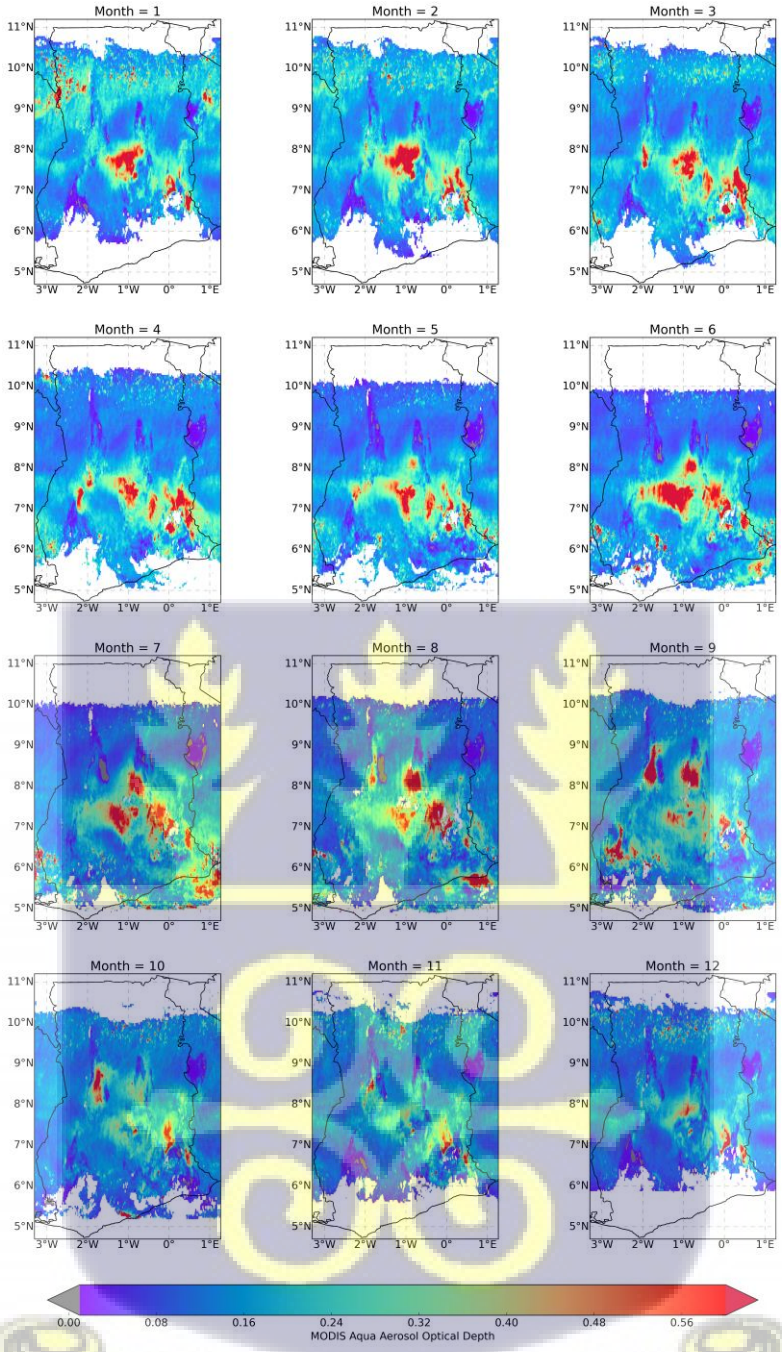

Figure 4.5: Monthly Spatial Distribution of MODIS-Derived Aerosol Optical Depth (AOD) over Aqua satellite Ghana in 2020

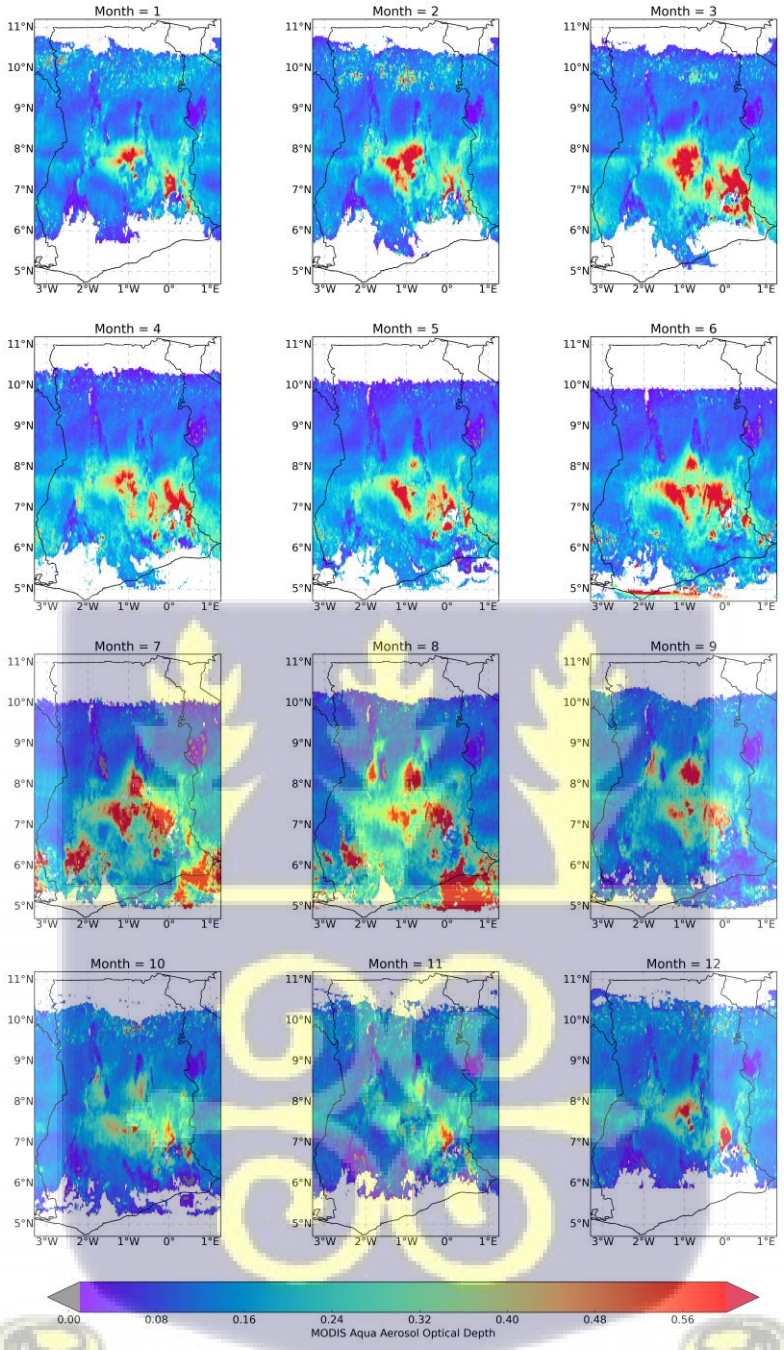

Figure 4.6: Monthly Spatial Distribution of MODIS-Derived Aerosol Optical Depth (AOD) Aqua satellite over Ghana in 2021

4.1.2 Total Column Monthly Distribution of Ozone over Ghana

Figure 4.7 to 4.9 shows monthly OMI total column ozone maps from 2019 to 2021. Total column O_3 values ranged between 120 and 400 (DU) with high O_3 levels occurring generally over the southern part of Ghana during the study period. In 2019, O_3 concentrations were intense during the month of December to March 2019 while levels were moderately lower in the other months starting from April to November. The northern part of Ghana was observed with O_3 levels higher than 120 (DU) in the month of July to November 2019. In the southern part of Ghana, the major dry season occurs in December to February while the minor dry season occurs in July to August. Furthermore, there are two major rainy seasons in the southern part of Ghana; the first rainy season occurs in April to June while the second occurs in September to November. July and October are observed as a major rainy season in the northern part of Ghana. In 2020 to 2021, spatial distribution of AOD was consistently lower in both the middle and northern parts but intense in the southern Ghana. The variations of O_3 concentrations might be due to seasonal anthropogenic emissions in both Harmattan and rainy seasons.

High concentration of O_3 levels mostly in the southern part of Ghana may be due to high pollution sources such as carbon monoxide, nitrogen oxides and volatile organic compounds from biomass burning, traffic and industrial activities. No data was observed especially in the southern and northern parts of Ghana during the study period. This surveillance may be due to cloud cover or lack of retrieval by the deep blue and dark target algorithm.

The distribution of ozone concentrations over the southern and northern parts of Ghana is an indication of the existence of different ozone precursors in the regions. Ofosu et al. (2012) observed dust storm from the Saharan desert over the northern part of Ghana while Dionisio et al. (2010) and Rooney et al. (2012) recorded in their studies predominant biomass burning in the southern part of Ghana. These previous

studies and the results of this investigation indicated the existence of internal sources of aerosols in Ghana, due to biomass burning and the transportation of dust storms into the country from an external source (the Saharan desert).

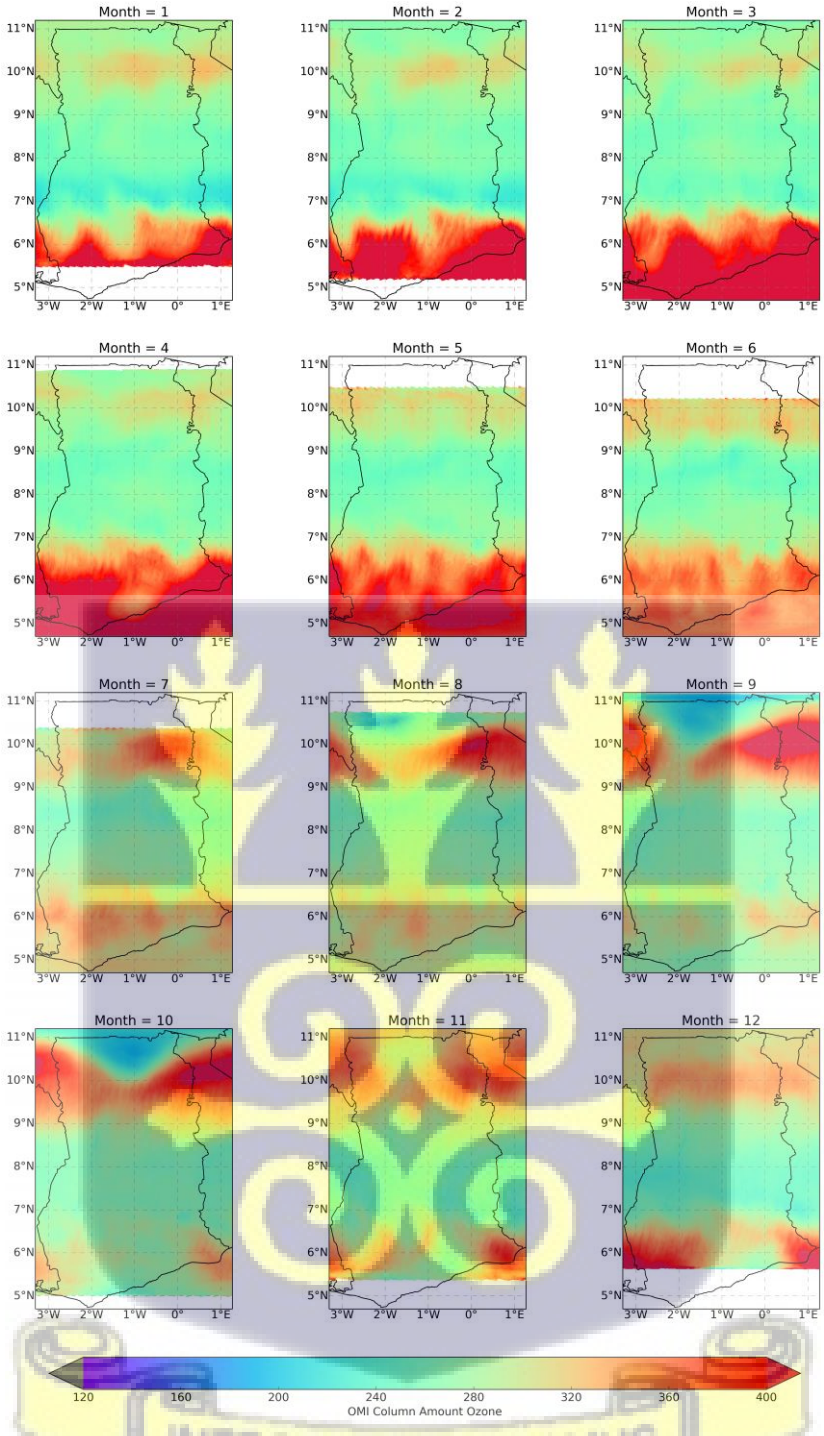

Figure 4.7: Monthly Spatial Distribution of OMI-Derived Total Column Ozone (O_3) over Ghana in 2019

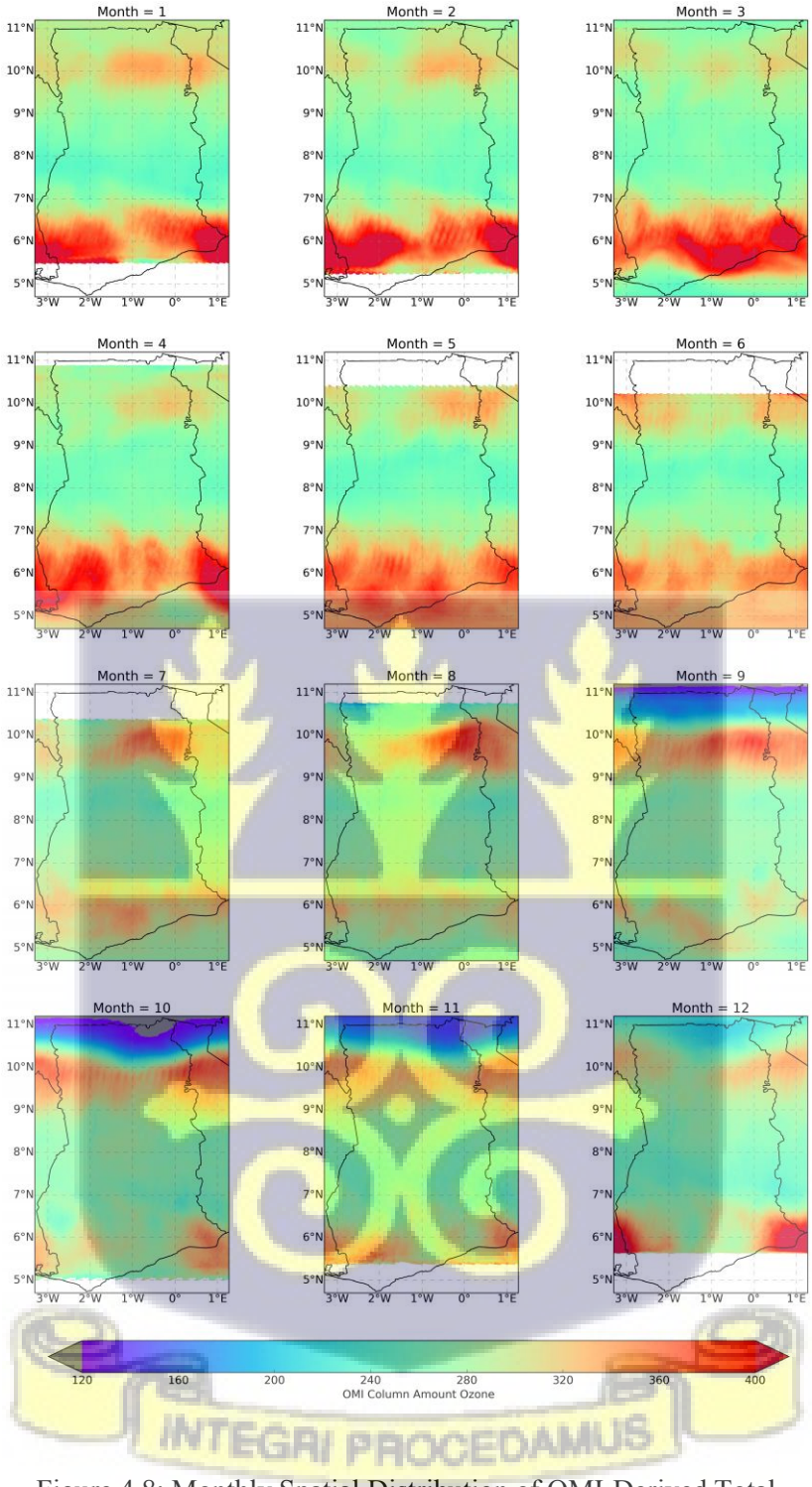

Figure 4.8: Monthly Spatial Distribution of OMI-Derived Total Column Ozone (O_3) over Ghana in 2020

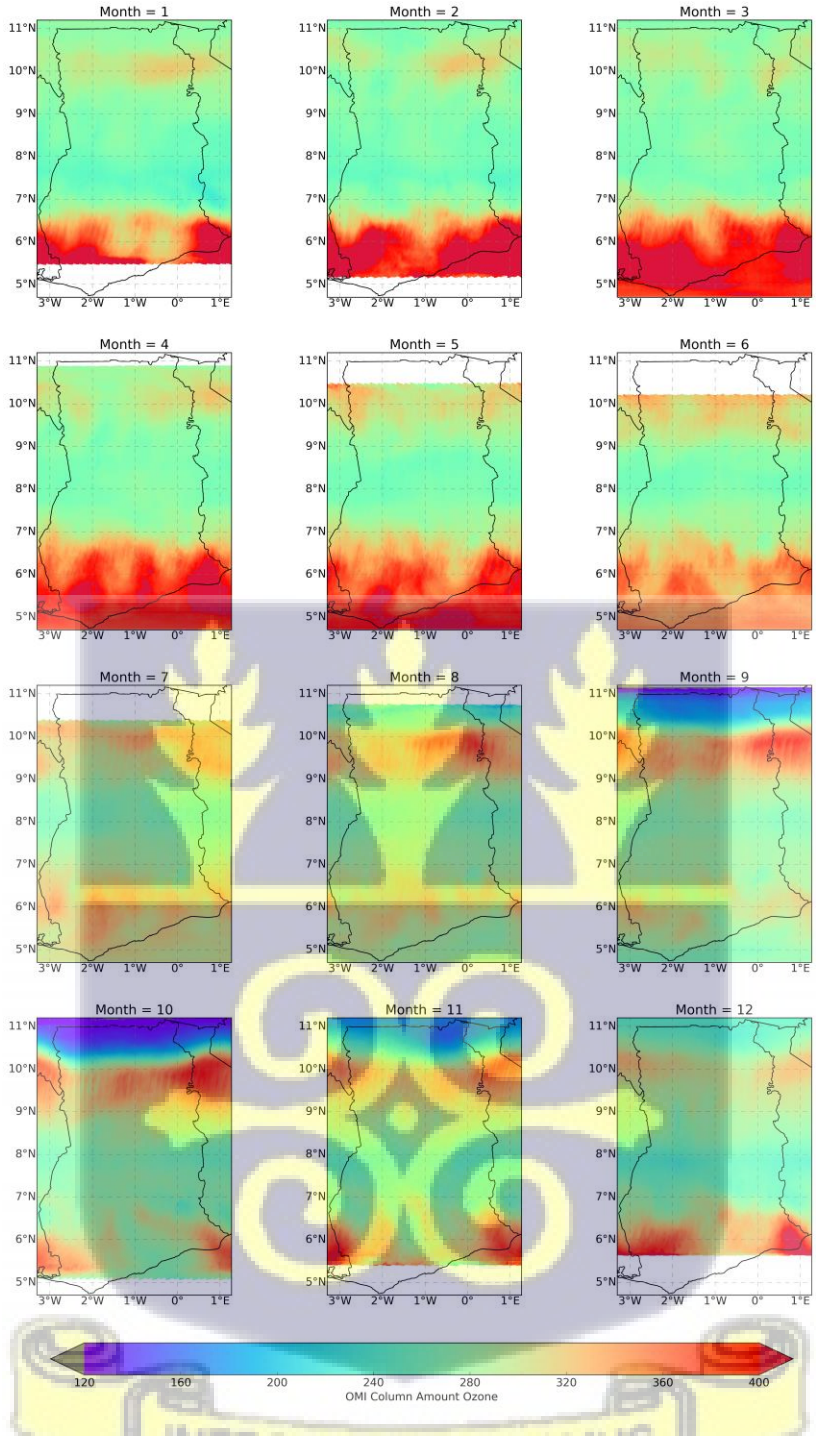

Figure 4.9: Monthly Spatial Distribution of OMI-Derived Total Column Ozone (O_3) over Ghana in 2021

4.1.3 Total Column Monthly Distribution of Nitrogen Dioxide over Ghana

Figures 4.10 to 4.12 show OMI total column NO_2 monthly maps from 2019 to 2021. NO_2 values ranged between 0.0 and 4.0 (10^{14} molecules/cm^2) with high NO_2 levels occurring in the middle and southern part of Ghana. In 2019, there was no significant high NO_2 concentration episode as was observed in O_3 levels. However, NO_2 levels were moderately high especially during the rainy season throughout the study period. The northern part of Ghana also witnessed low levels of NO_2 especially in November to March as seen in figure 4.10, 4.11 and 4.12. No data was observed in the month of November to March in some areas of southern regions whiles from April to August, some areas in the northern part experience no data during the study period. This may be due to cloud cover or lack of OMI NO_2 retrieval algorithm.

Concentration of NO_2 levels mostly in the middle part of Ghana may be due to high nitrogen oxides from biomass burning and agricultural emissions. Again, traffic and industrial emissions mostly in the urban regions may contribute to high NO_2 levels in the southern regions.

The different distribution of AOD, NO_2 and O_3 levels over Ghana is an indication of the existence of different precursors from agricultural burning, re-suspended dust and biomass burning. Also, the sub-Saharan dust storms popularly known as Harmattan winds from the Saharan desert and neighbouring countries with seasonal variations of weather variables (solar radiation, temperature, humidity), may contribute to different AOD, NO_2 and O_3 levels in Ghana.

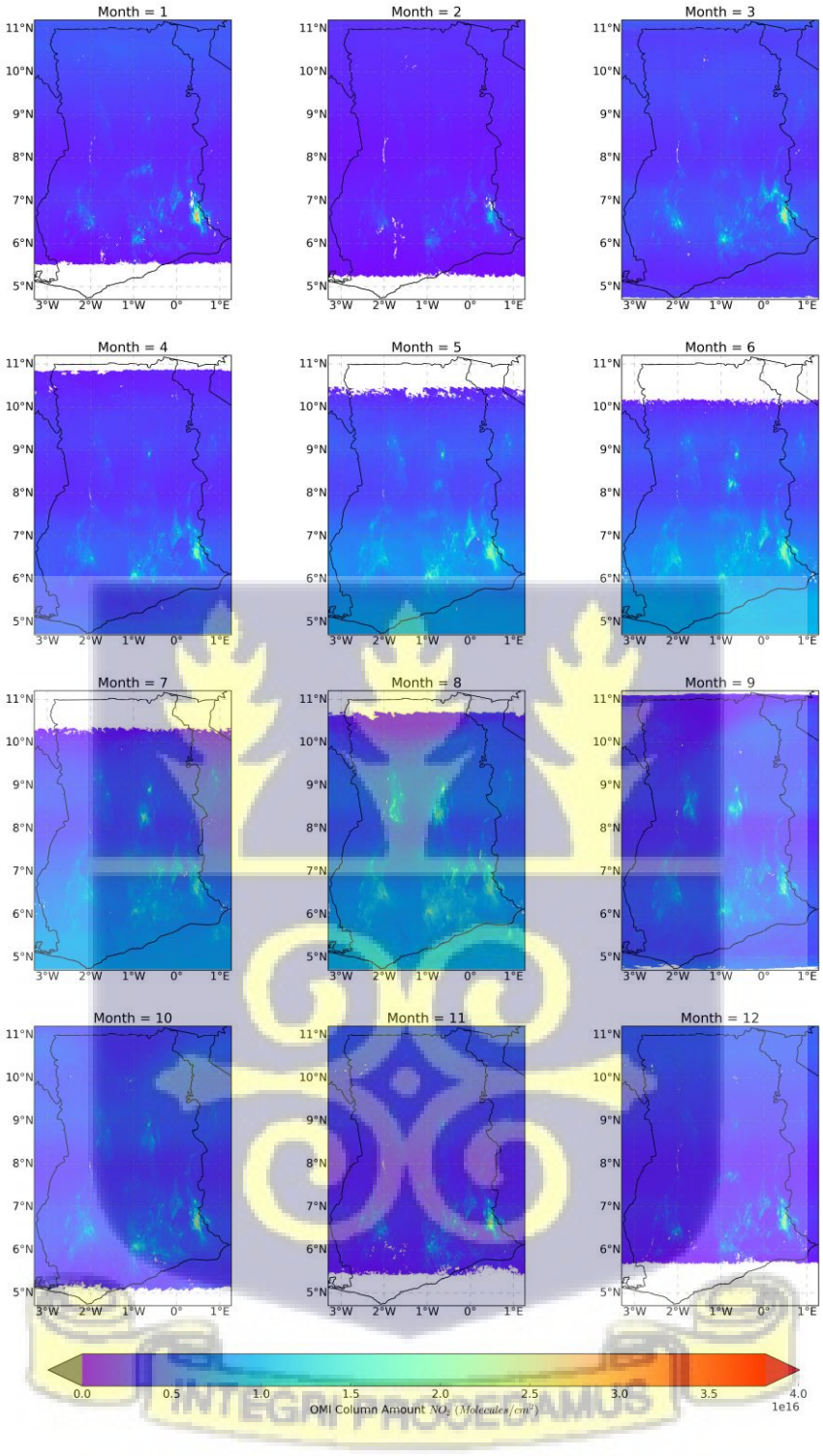

Figure 4.10: Monthly Spatial Distribution of OMI-Derived Total Column Nitrogen Dioxide (NO_2) over Ghana in 2019

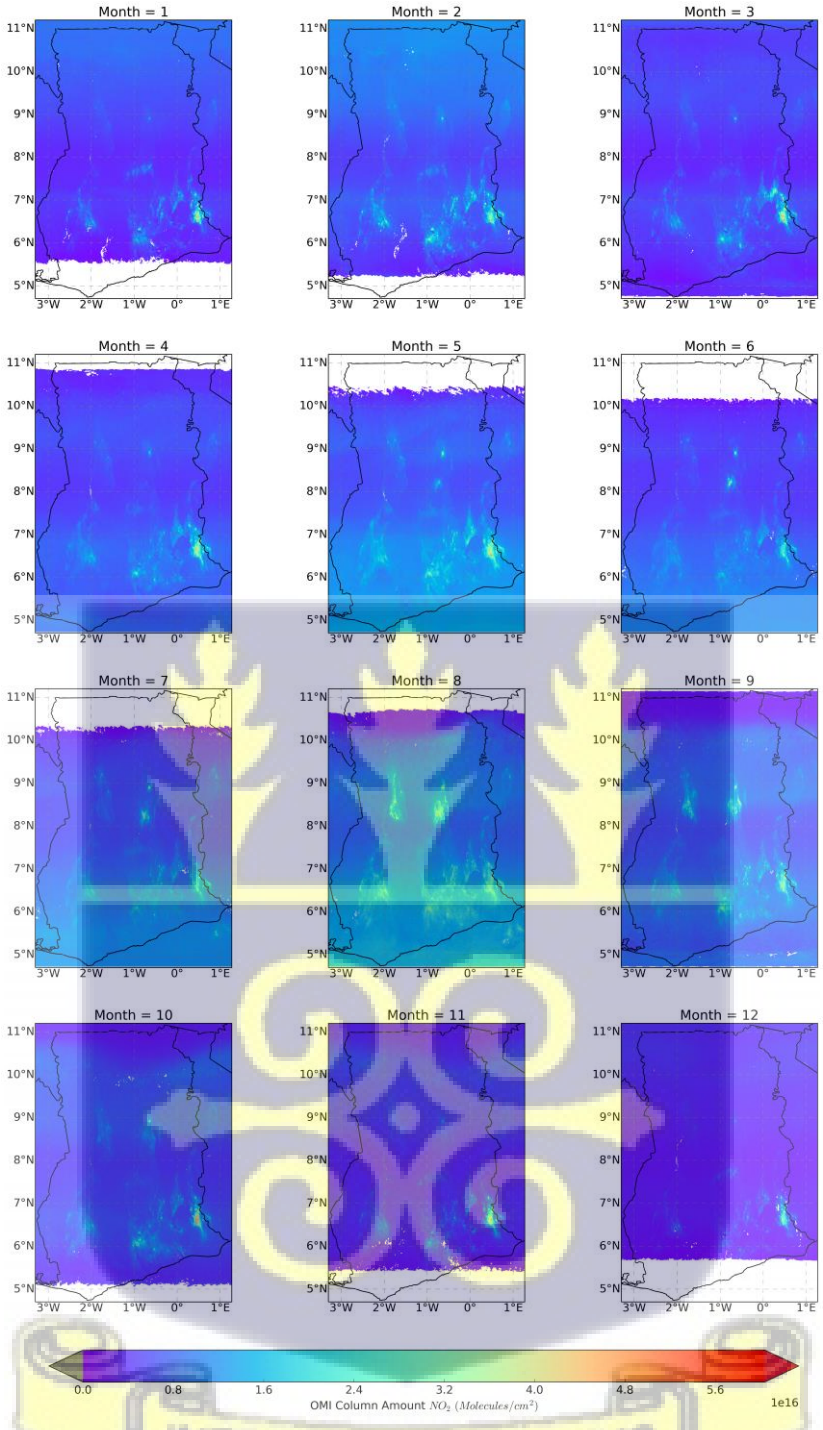

Figure 4.11: Monthly Spatial Distribution of OMI-Derived Total

Column Nitrogen Dioxide (NO_2) over Ghana in 2020

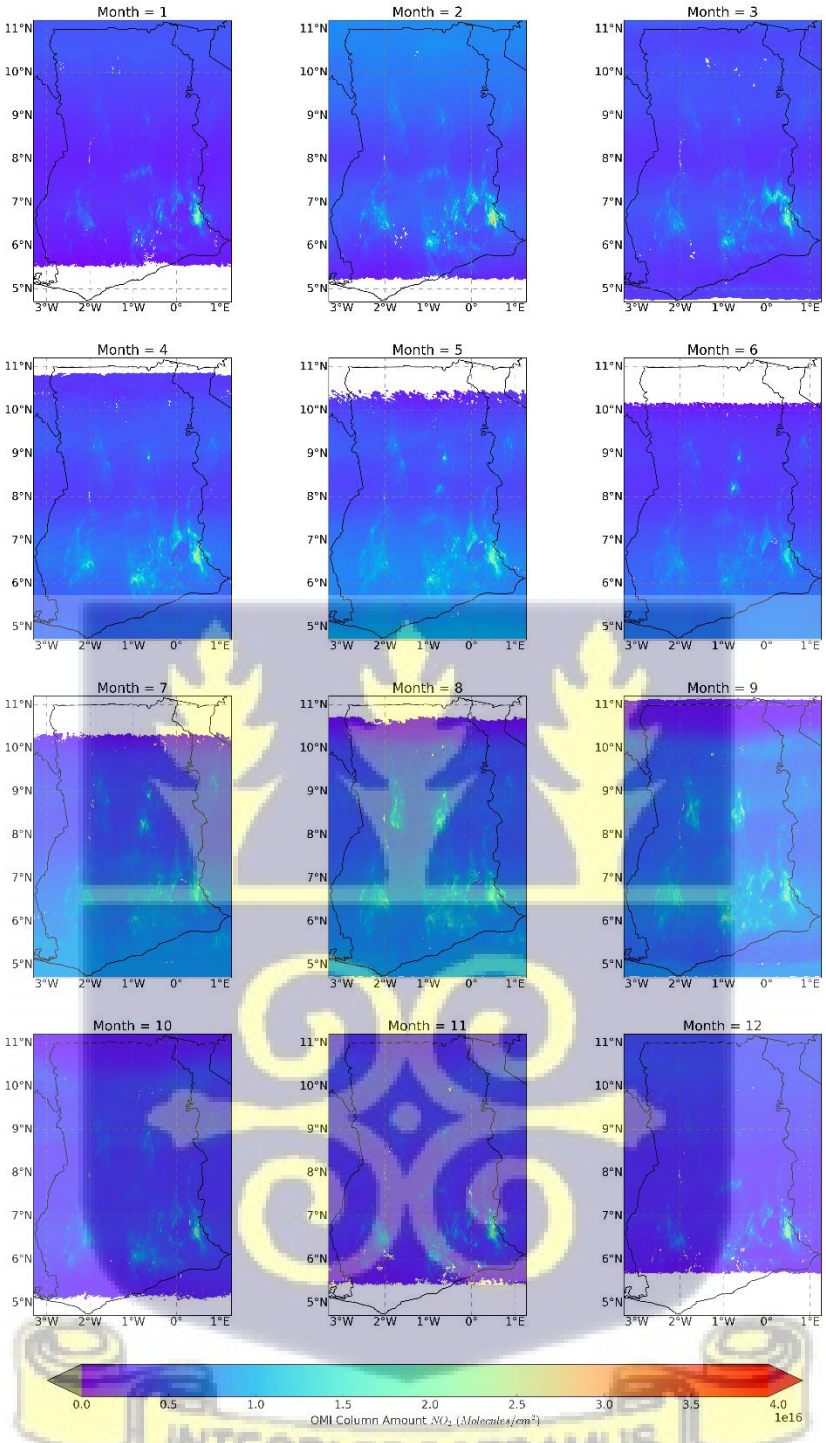

Figure 4.12: Monthly Spatial Distribution of OMI-Derived Total

Column Nitrogen Dioxide (NO_2) over Ghana in 2021

4.2 Temporal Variations, Comparison and Validation of $PM_{2.5}$ and AOD data over Greater Accra Metropolitan Area (GAMA)

This section presents the results of the second objective on the analyses of temporal variation, comparison and validation of $PM_{2.5}$ and AOD data over the 5 EPA air quality stations in the GAMA.

4.2.1 Temporal Variation of Particulate Matter Less Than 2.5 Microns over GAMA

Table 1.0 shows the summary (sample size, minimum, maximum, mean and standard deviation) of 5 Clarity Node-S sensors $PM_{2.5}$ data with 25 months sampling period from 2019 to 2021. Before field deployment, the clarity sensors were collocated with each other for about a week to ensure the credibility and consistency of the dataset. From the table, the highest $PM_{2.5}$ level occurred in Kaneshie followed by Amasaman with concentration peaking at (132 ± 15.0) $\mu g/m^3$ and (92.0 ± 13.8.0) $\mu g/m^3$ in 2019, respectively. In 2020, the highest concentration occurred in Amasaman followed by Achimota with levels (128.0 ± 19.6) $\mu g/m^3$ and (108.0 ± 15.7) $\mu g/m^3$. Overall, $PM_{2.5}$ levels were consistently high in Amasaman with average concentrations above 30.0 $\mu g/m^3$ than the other stations during the study period. This was confirmed by figure 4.13, 4.15 and table 3.0 over all the stations from 2019 to 2021. Further, seasonal impact of PM2.5 levels over stations were also assessed during the study period. From table 2.0, during the Harmattan season, $PM_{2.5}$ levels were above 50% of the overall average concentration in December, January and February. This was also confirmed in figure 4.14 by the Aqua and Terra AOD data as average concentrations were higher in the Harmattan months (December, January and February). In general, during the study period, at the peak of the raining season, $PM_{2.5}$ levels below 30% were above the overall average concentration of 32.8 $\mu g/m^3$. Lower percentage of $PM_{2.5}$ levels above the average concentration shows the influence of meteorological variables like relative humility and temperature on particulate matter. During the raining season, water droplets in ambient air increases, thereby causing the relative

humidity to increase. Particulate matter levels in ambient air decreases due to their heavy weight and slower reaction rates (interaction with other chemicals) due to lower temperature and pressure during this period (Enitan et al., 2022; Nicholson, 2018). Lower levels of $PM_{2.5}$ in the raining season in the GAMA were confirmed by Alli et al. (2021) and Wang et al. (2022) during a city-wide campaign of air pollution monitoring in the GAMA. Other months in the raining season shown PM2.5 levels above 40% of the average concentration which is due to anthropogenic activities such as agricultural waste burning which is common in the GAMA during this season (Arku et al., 2008b).

Table 1: Descriptive Statistics of Daily Clarity Node-S $PM_{2.5}$ Data over 5 EPA Stations in the GAMA

	2019					2020					2021				
EPA Stations	**n**	**Min**	**Max**	**Mean**	**Std**	**n**	**Min**	**Max**	**Mean**	**Std**	**n**	**Min**	**Max**	**Mean**	**Std**
Achimota	335.0	13.0	90.9	31.8	11.4	361.0	10.2	108.0	30.9	15.7	nan	nan	nan	nan	nan
Amasaman	335.0	12.0	92.0	36.5	13.8	366.0	11.2	128.6	37.8	19.6	31.0	36.5	83.2	51.6	11.7
Jamestown	330.0	10.2	77.2	29.8	10.7	366.0	7.6	91.0	32.0	12.7	31.0	30.5	52.2	37.7	5.8
Kaneshie	322.0	7.9	132.6	35.3	15.0	333.0	8.2	79.4	31.6	10.7	29.0	32.9	56.6	39.6	6.2
Tetteh Quarshie	335.0	14.4	88.1	32.8	9.4	362.0	11.0	104.3	30.3	12.8	31.0	26.7	52.0	36.9	5.5

Table 2: Monthly Description of Percentage Averages against Overall Monthly Average of 32.8 $\mu g/m^3$ of Clarity Node-S $PM_{2.5}$ Data over 5 EPA Stations

Months	Below Monthly Mean	Above Monthly Mean	Total Days
February	36.21%	63.79%	58
March	77.78%	22.22%	63
April	83.61%	16.39%	61
May	77.78%	22.22%	63
June	49.18%	50.82%	61
July	52.38%	47.62%	63
August	57.14%	42.86%	63
September	83.61%	16.39%	61
October	82.54%	17.46%	63
November	50.82%	49.18%	61
December	23.81%	76.19%	63
January	11.54%	88.46%	52

Table 3: Monthly Description of Percentage Averages against Overall Monthly Average of 32.8 $\mu g/m^3$ of Clarity Node-S $PM_{2.5}$ Data across the 5 EPA Stations

EPA Stations	Below Monthly Mean	Above Monthly Mean	Total Days
Amasaman	46.58%	53.28%	732
Achimota	66.52%	33.48%	696
Kaneshie	58.04%	41.96%	684
Tetteh Quarshie	62.91%	36.95%	728
Jamestown	61.9%	38.1%	727

4.2.2 Comparison and Validation of MODIS Aerosol Depth Data with Particulate Matter Less Than 2.5 Microns over GAMA

Again, comparison and validation of Modis AOD at $(50 \times 50)\ km^2$ grid scale with Clarity Node-S $PM_{2.5}$ data shows the same monthly variations (figure 4.13, 4.14 and 4.15, 4.16 and 4.20) during the rainy and Harmattan periods. To validate the AOD data, daily Clarity Node-S $PM_{2.5}$ data across the stations were matched with daily Modis AOD at (50 x 50) and $(111 \times 111)\ km^2$ grid from 2019 to 2021 (25 months), respectively. The matched data was used for the analysis. Results from figures 4.19 and 4.19 show good coefficients with R^2 values (0.72, 0.72, 0.67, 0.58 and 0.57) in Amasaman, Jamestown, Tetteh Quarshie, Kaneshie and Achimota, respectively at $(50 \times 50)\ km^2$ grid scale. At $(111 \times 111)\ km^2$ grid scale, R^2 values were (0.67, 0.73, 0.69, 0.60 and 0.60) in Amasaman, Jamestown, Tetteh Quarshie, Kaneshie and Achimota, generally higher than the $(50 \times 50)\ km^2$ grid scale during the study period.

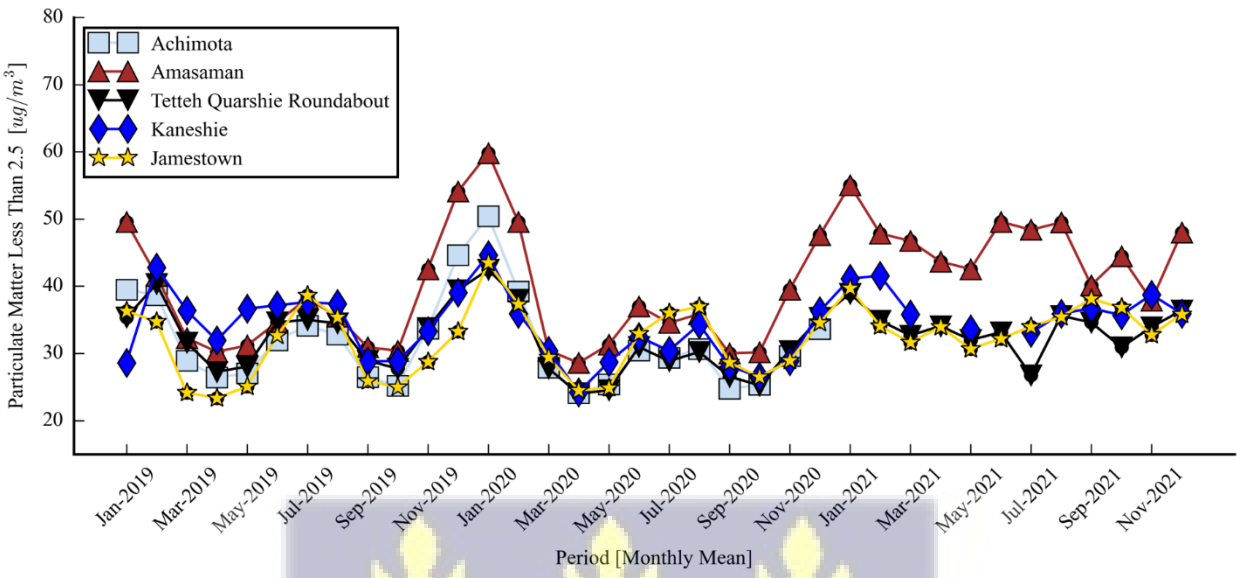

Figure 4.13: Monthly variations of $PM_{2.5}$ levels from 2019 to 2021 across 5 EPA stations in the GAMA.

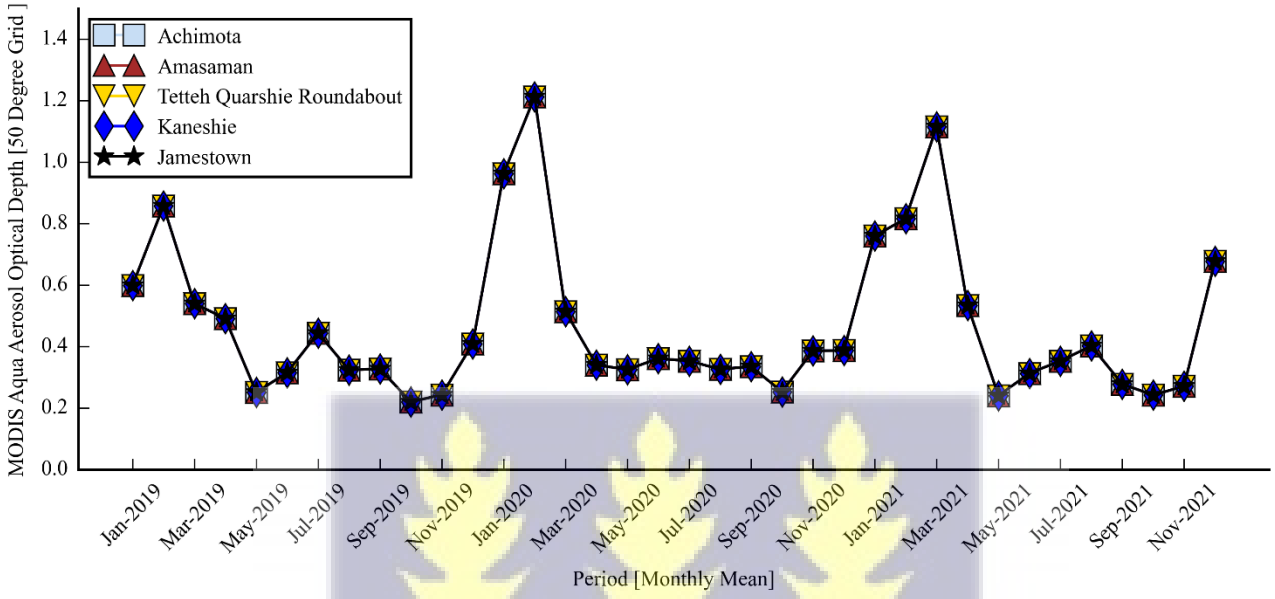

Figure 4.14: Monthly variations of MODIS Aqua AOD from 2019 to 2021 across 5 EPA stations in the GAMA.

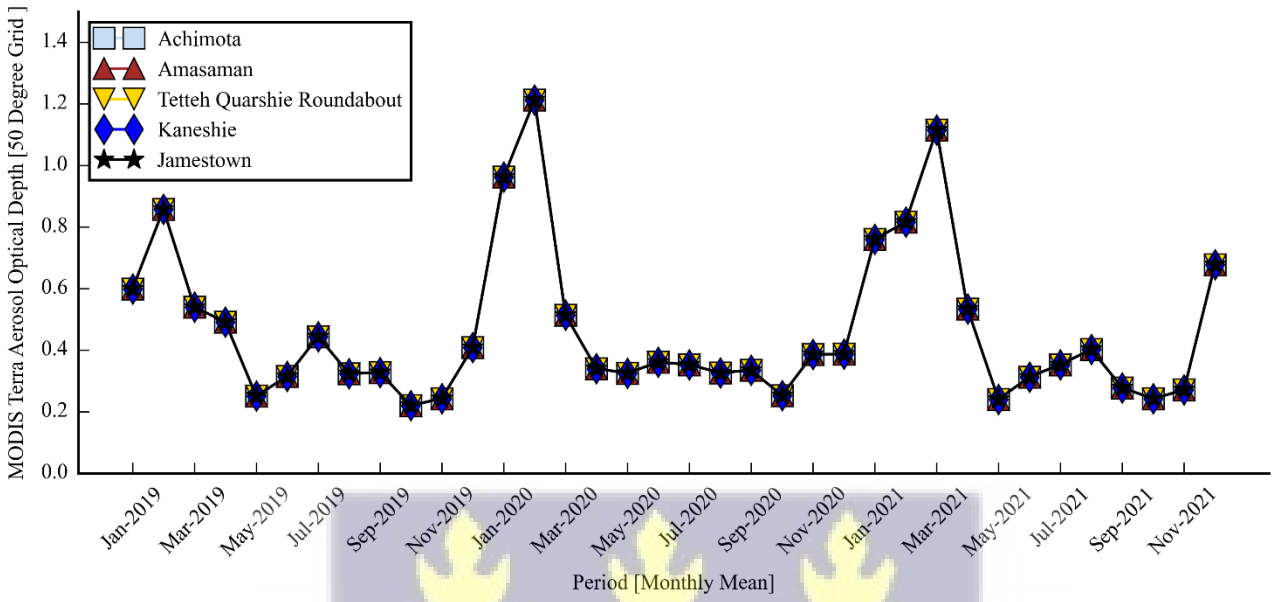

Figure 4.15: Monthly variations of MODIS Terra AOD from 2019 to 2021 across 5 EPA stations in the GAMA.

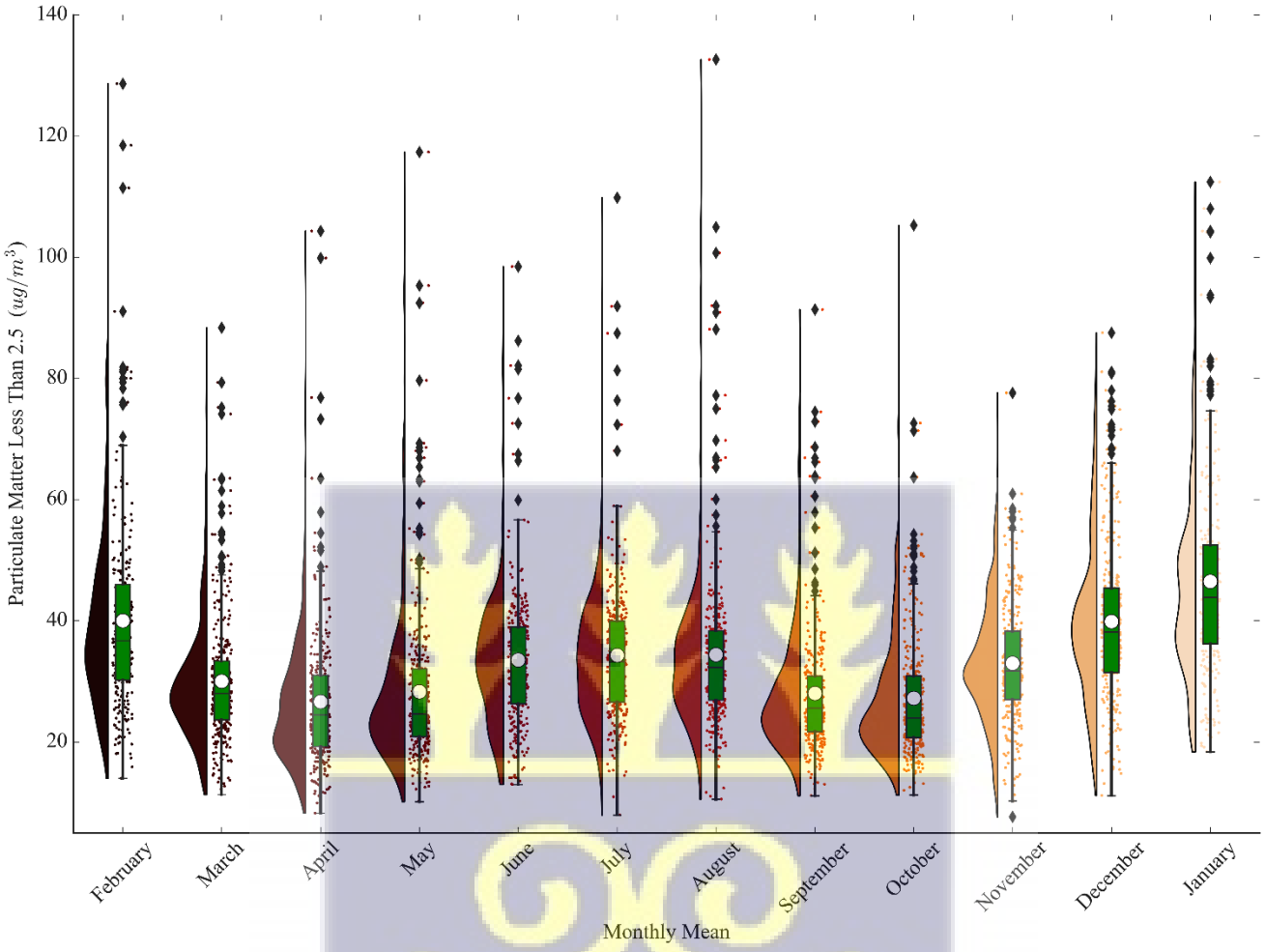

Figure 4.16: Raincloud, Stream and Boxplots of monthly average $PM_{2.5}$ over the 5 EPA stations. The raincloud and stream plots shows the distribution of the dataset. Boxplots show the first quartile to the third quartile with dark line and white dots representing the median and average respectively.

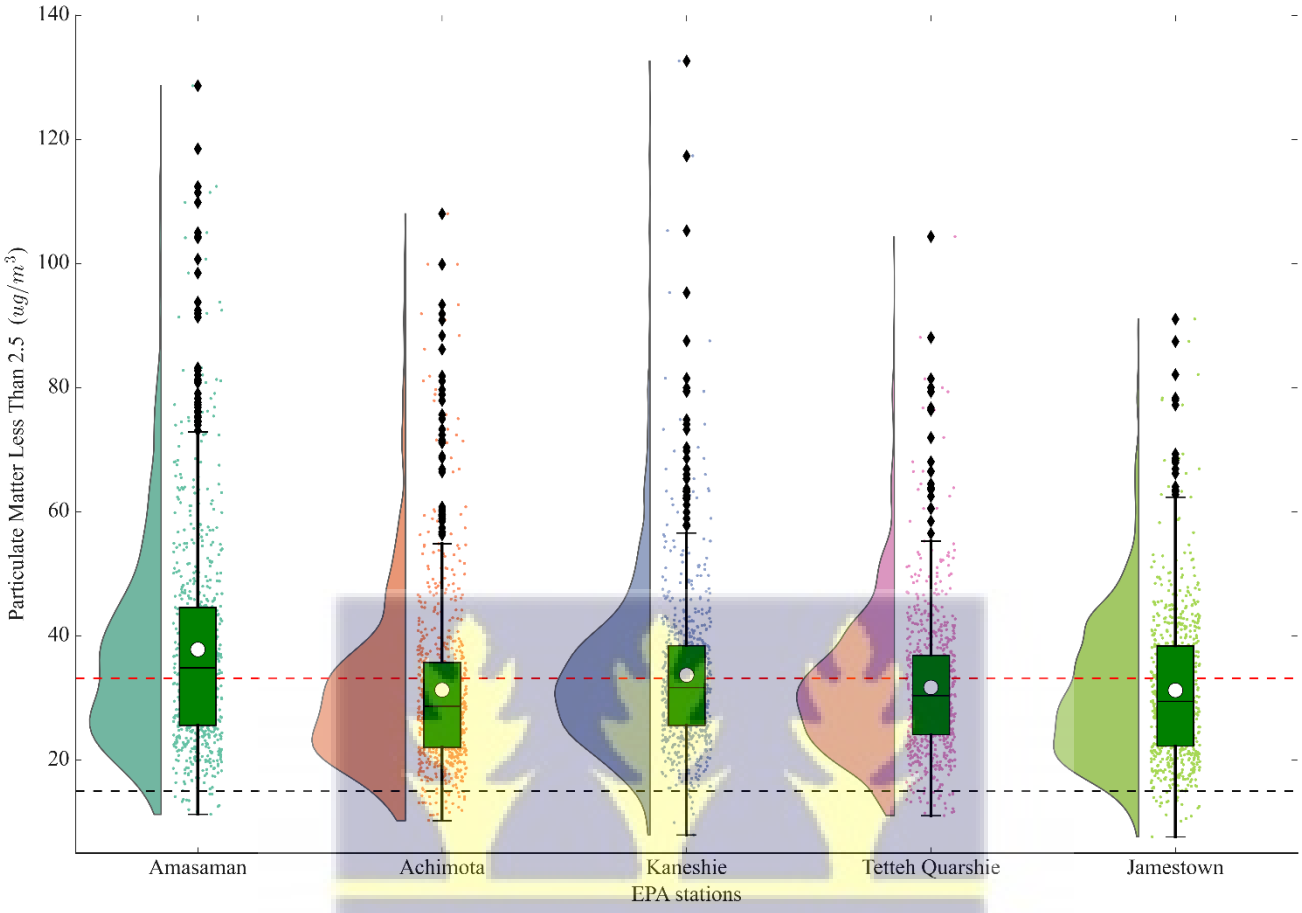

Figure 4.17: Raincloud, Stream and Boxplots of daily average $PM_{2.5}$ over the 5 EPA stations. The raincloud and stream plots show the distribution of the dataset. The black and red dotted lines represent overall mean (32.8 μgm^{-3}) and (15.0 μgm^{-3}) of WHO air quality guideline. Boxplots represent the first quartile to the third quartile with a dark line and white dots representing the median and average respectively.

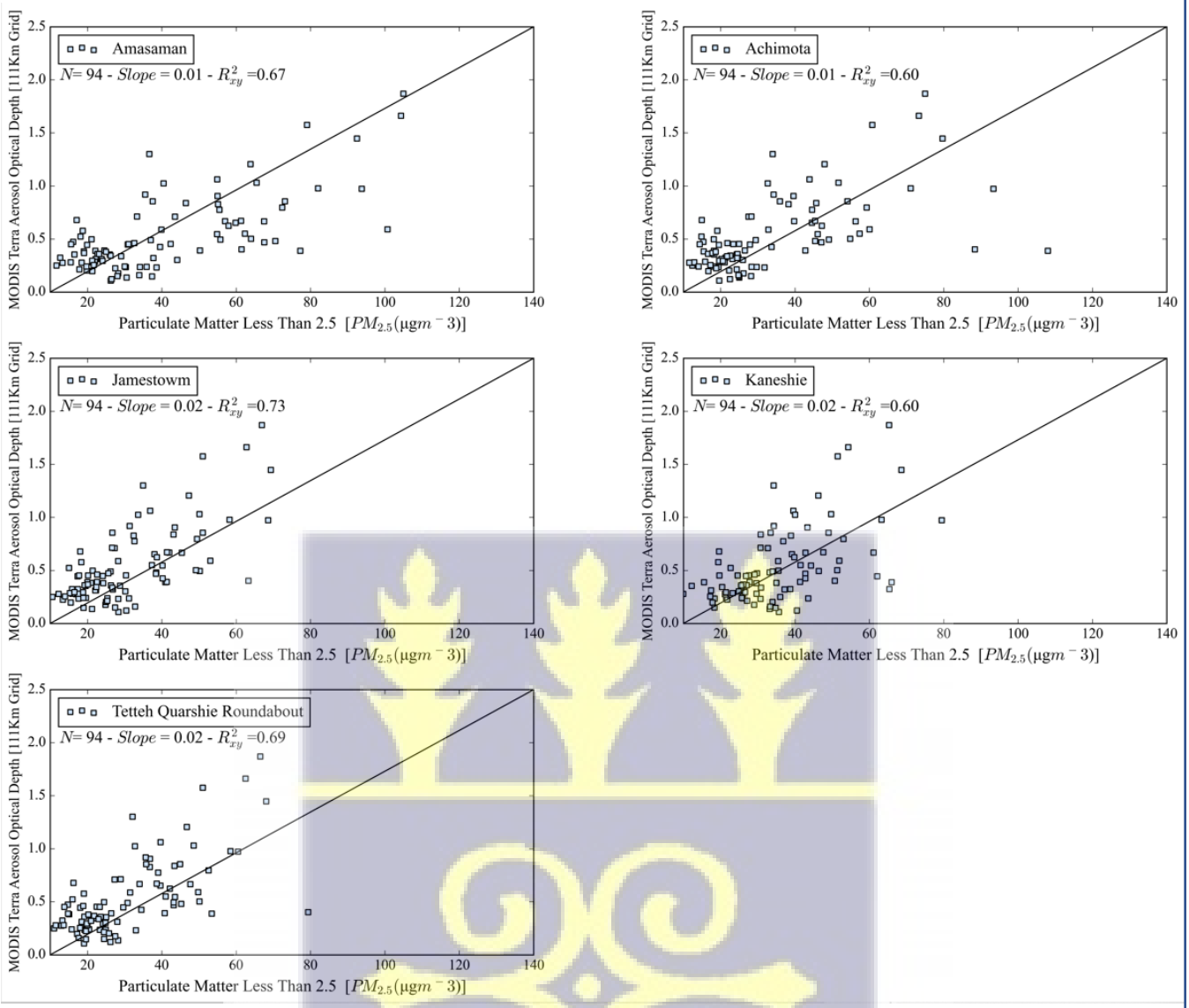

Figure 4.18: Correlation Plots between Clarity Node-S $PM_{2.5}$ and MODIS Terra Data at $(111 \times 111)\ km^2$ Grid Scale

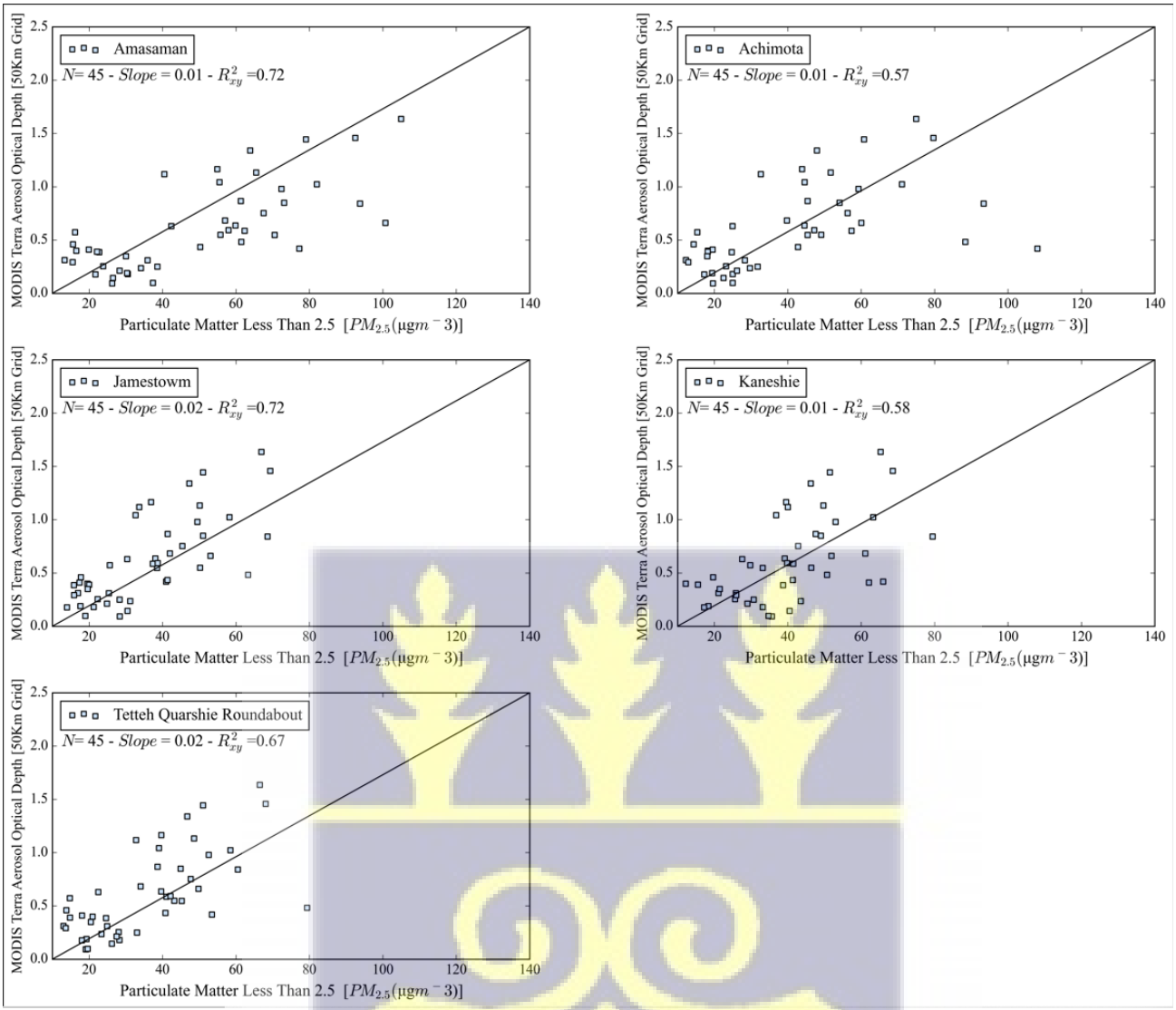

Figure 4.19: Figure 4.16: Correlation Plots between Clarity Node-S $PM_{2.5}$ and MODIS Terra Data at $(50 \times 50)\ km^2$ Grid Scale

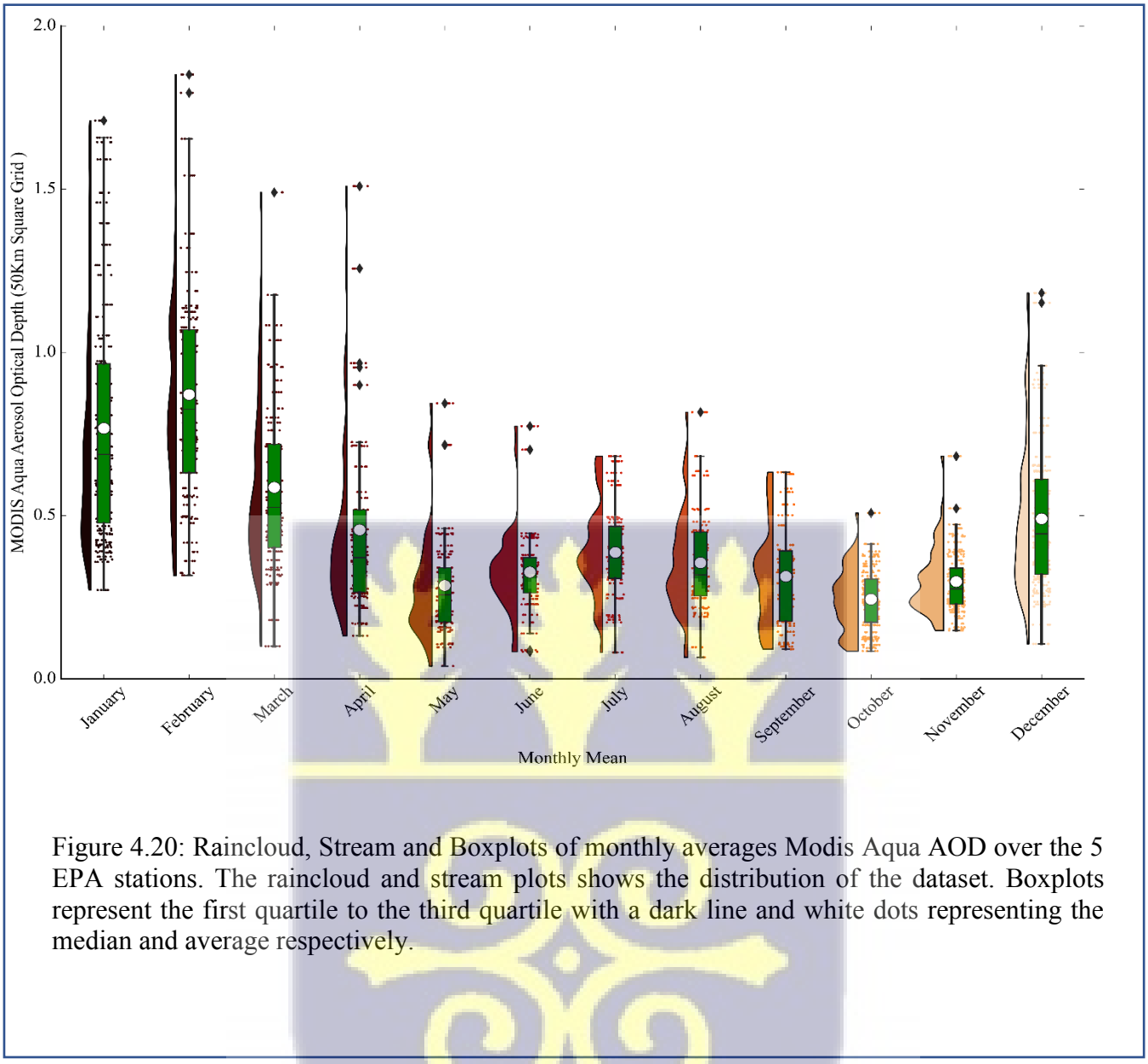

Figure 4.20: Raincloud, Stream and Boxplots of monthly averages Modis Aqua AOD over the 5 EPA stations. The raincloud and stream plots shows the distribution of the dataset. Boxplots represent the first quartile to the third quartile with a dark line and white dots representing the median and average respectively.

Table 4: Summary Descriptive Statistics of Monthly Modis Aqua AOD over Ghana

	2019				2020				2021			
Months	**Min**	**Max**	**Mean**	**Std**	**Min**	**Max**	**Mean**	**Std**	**Min**	**Max**	**Mean**	**Std**
April	0.2	1.5	0.5	0.4	0.1	0.5	0.3	0.1	0.2	1.3	0.5	0.3
August	0.2	0.5	0.3	0.1	0.1	0.5	0.3	0.1	0.1	0.8	0.4	0.2
December	0.2	0.8	0.4	0.1	0.1	0.8	0.4	0.2	0.3	1.2	0.7	0.3
February	0.4	1.8	0.9	0.4	0.4	1.9	0.9	0.3	0.3	1.5	0.8	0.3
January	0.4	0.9	0.6	0.2	0.4	1.7	1.0	0.4	0.3	1.6	0.7	0.4
July	0.3	0.7	0.4	0.1	0.2	0.7	0.4	0.1	0.1	0.7	0.4	0.2
June	0.1	0.7	0.3	0.1	0.1	0.8	0.4	0.2	0.2	0.4	0.3	0.1
March	0.3	0.9	0.5	0.2	0.1	1.1	0.5	0.3	0.4	1.5	0.8	0.3
May	0.1	0.7	0.3	0.2	0.1	0.8	0.3	0.2	0.0	0.4	0.2	0.1
November	0.1	0.4	0.2	0.1	0.2	0.7	0.4	0.1	0.2	0.4	0.3	0.0
October	0.1	0.4	0.2	0.1	0.1	0.5	0.3	0.1	0.1	0.4	0.2	0.1
September	0.1	0.6	0.3	0.1	0.2	0.6	0.3	0.1	0.1	0.6	0.3	0.2

Table 5: Summary Descriptive Statistics of Monthly Modis Terra AOD over Ghana

	2019				2020				2021			
	Min	**Max**	**Mean**	**Std**	**Min**	**Max**	**Mean**	**Std**	**Min**	**Max**	**Mean**	**Std**
April	0.2	1.0	0.5	0.2	0.2	1.4	0.5	0.3	0.2	0.9	0.4	0.2
August	0.2	0.6	0.4	0.1	0.1	0.8	0.4	0.2	0.2	0.8	0.4	0.1
December	0.1	0.7	0.3	0.1	0.1	0.5	0.3	0.1	0.2	0.9	0.5	0.2
February	0.2	1.2	0.6	0.3	0.3	1.6	0.8	0.3	0.2	1.4	0.7	0.3
January	0.2	0.6	0.4	0.1	0.2	1.3	0.8	0.3	0.2	1.1	0.5	0.2
July	0.3	0.7	0.4	0.1	0.2	0.6	0.4	0.1	0.2	0.9	0.4	0.1
June	0.2	0.6	0.3	0.1	0.2	0.8	0.4	0.1	0.2	0.7	0.3	0.1
March	0.3	0.9	0.5	0.2	0.1	1.0	0.5	0.2	0.3	1.5	0.7	0.3
May	0.1	0.5	0.3	0.1	0.2	0.7	0.3	0.1	0.1	0.7	0.3	0.1
November	0.1	0.4	0.2	0.1	0.2	0.7	0.3	0.1	0.1	0.4	0.2	0.1
October	0.2	0.4	0.3	0.1	0.2	0.7	0.3	0.1	0.2	0.5	0.3	0.1
September	0.2	0.8	0.4	0.2	0.3	0.6	0.4	0.1	0.2	0.6	0.4	0.1

Table 6: Summary of Percentage Averages against Overall Monthly Average AOD of 0.48 across the 5 EPA Stations

Month	AOD Below Monthly Mean	AOD Above Monthly Mean	Total Days
January	25.0%	75.0%	68
February	8.93%	91.07%	56
March	41.18%	58.82%	51
April	73.91%	26.09%	46
May	93.02%	6.98%	43
June	95.0%	5.0%	40
July	76.19%	23.81%	42
August	80.0%	20.0%	40
September	84.21%	15.79%	38
October	98.18%	1.82%	55
November	95.0%	5.0%	60
December	56.72%	43.28%	67

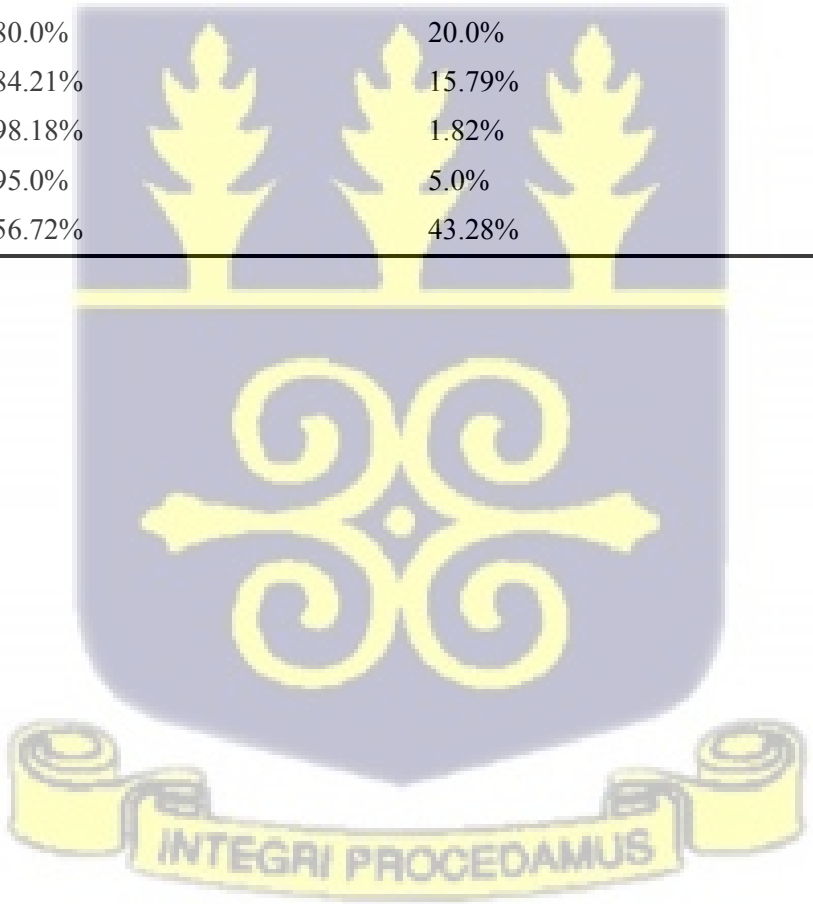

4.3 Long-Term trends of Total Column Particulates, NO_2 and O_3 over GAMA

This section presents the results of the third objective on the analyses of long-term trends over the 5 stations on $(25 \times 25)\ km^2$ grid for OMI NO_2, O_3 and $(50 \times 50)\ km^2$ grid for MODIS Terra AOD from 2012 to 2021 using the Mann-Kendall sequential test. The assessment was conducted to ascertain the impact of population growth coupled with increasing traffic, biomass burning and climate change on air quality for a period of 10 years in the GAMA.

Tables 7, 8 and 9 show the summary statistics from the Mann-Kendall test. Overall, there was an increasing trend in NO_2 (with $p < 0.05$) over 4 stations (Jamestown, Achimota, Tetteh Quarshie and Kaneshie), no trend in O_3 (with $p > 0.05$) and a decreasing trend in AOD (with $p < 0.01$) over all the stations. Further, correlation coefficients between total column NO_2 and O_3 were ($R^2 = 0.83 \pm 0.030$, $p < 0.01$), AOD and O_3 ($R^2 = 0.43 \pm 0.003$, $p < 0.01$) and NO_2 and AOD ($R^2 = 0.21 \pm 0.010$, $p > 0.01$). High correlation coefficient was observed between total column NO_2 and O_3. Low correlation coefficients between AOD, NO_2 and O_3 may reveal different emission sources from open burning, street cooking, traffic and industrial activities in the GAMA. AOD and NO_2 levels were generally high during the dry season (figure 4.21 and 4.22) while high concentrations of O_3 were observed in the wet season (figure 4.19 and 4.20) across the stations. A decreasing trend in particulate levels shows that sources of poor air quality may be shifting from the usual biomass burning to new forms including traffic emissions as observed by Wang et al., (2022) in the GAMA. However, an increasing trend of NO_2 levels in the GAMA may be due to high NOx and volatile organic compounds (VOCs) levels as a result of traffic emissions. Also, the intercontinental convergence zone (ITCZ) as due to south-westerly trade winds and African easterly winds which responds to temperature gradients may influence high pollutant levels in the GAMA (Sauvage & Thouret, 2005; Sharps et al., 2021; Shikwambana et al., 2020).

.

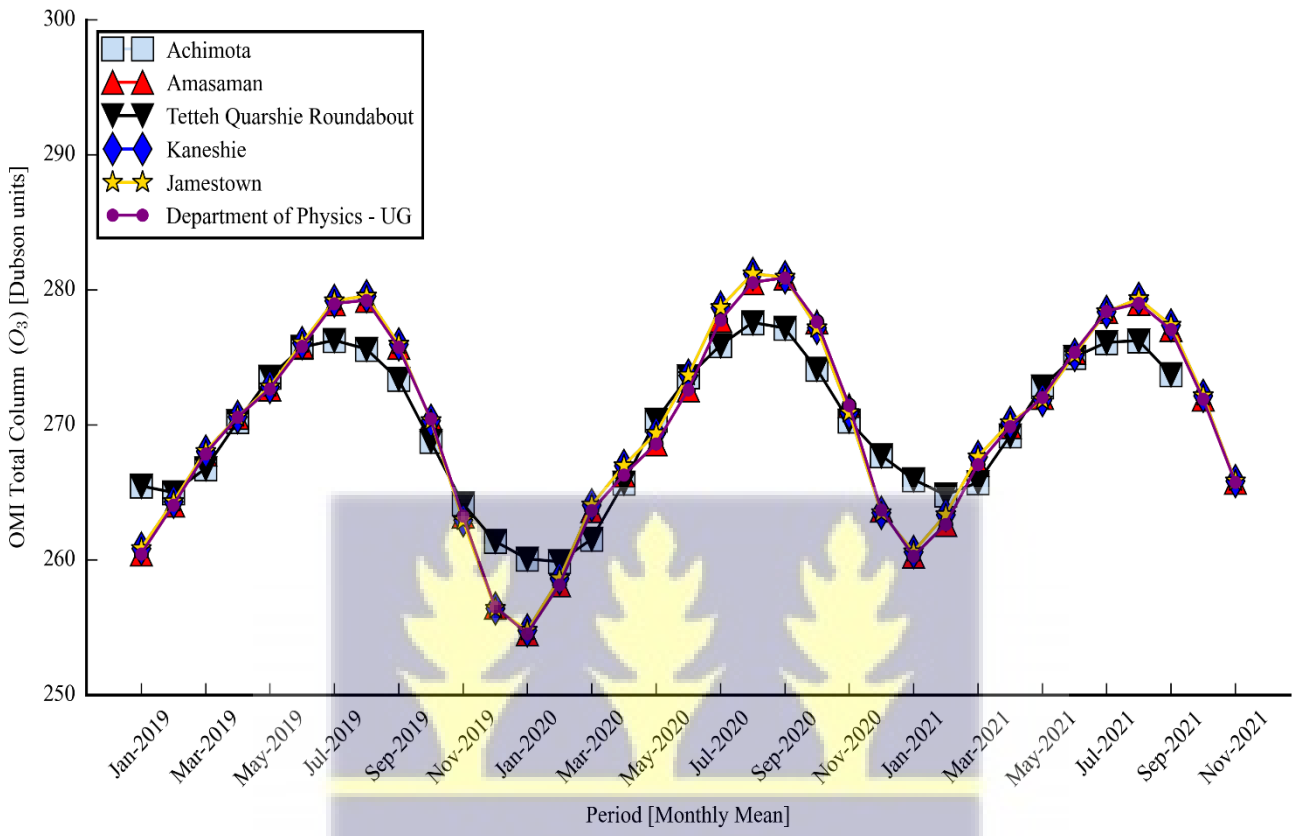

Figure 4.21: Monthly variations of total column OMI O_3 levels from 2019 to 2021 across 5 EPA stations in the GAMA.

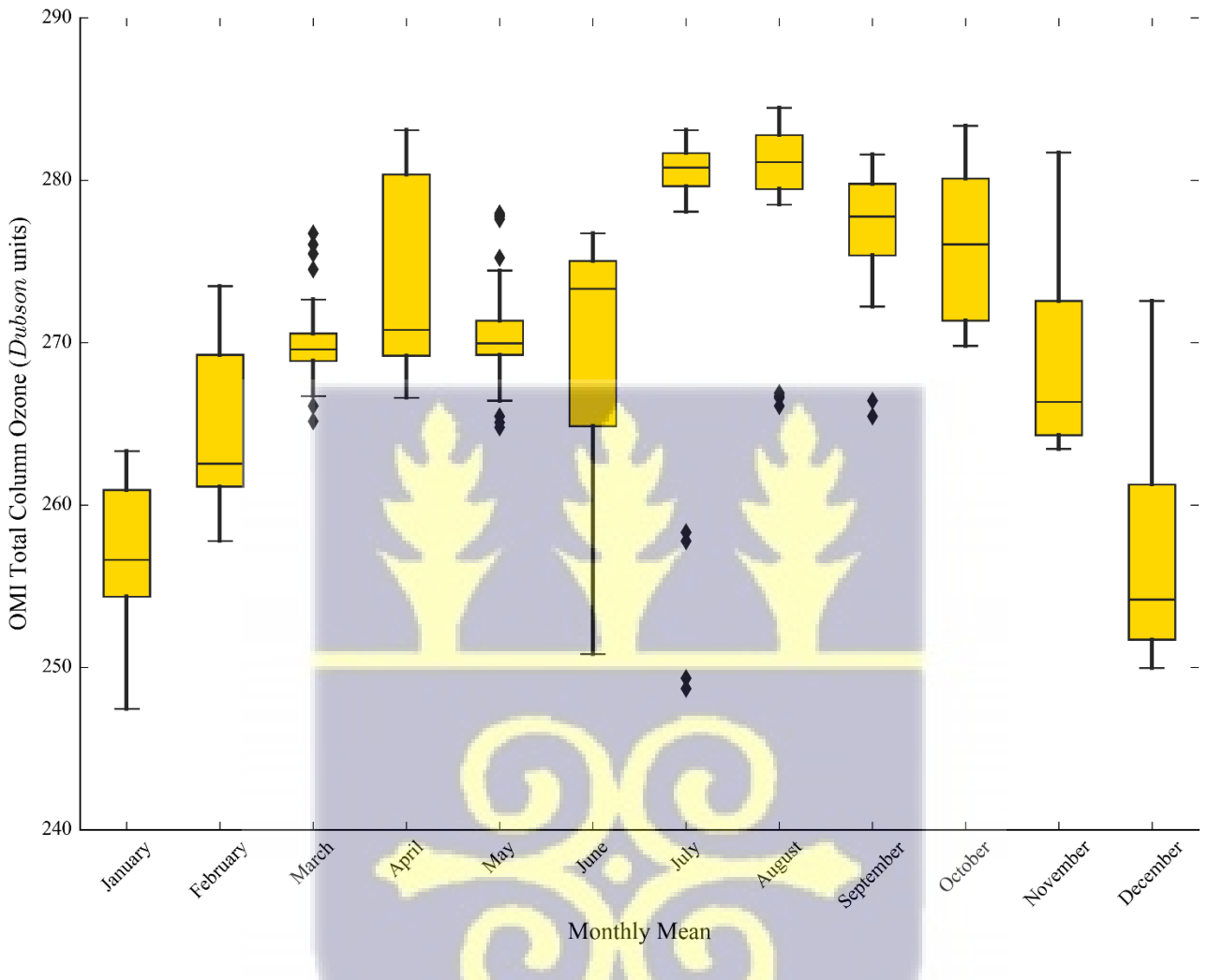

Figure 4.22: Boxplots of monthly averages total column OMI O_3 over the 5 EPA stations. The boxplots represent the first quartile to the third quartile with a black line showing the median.

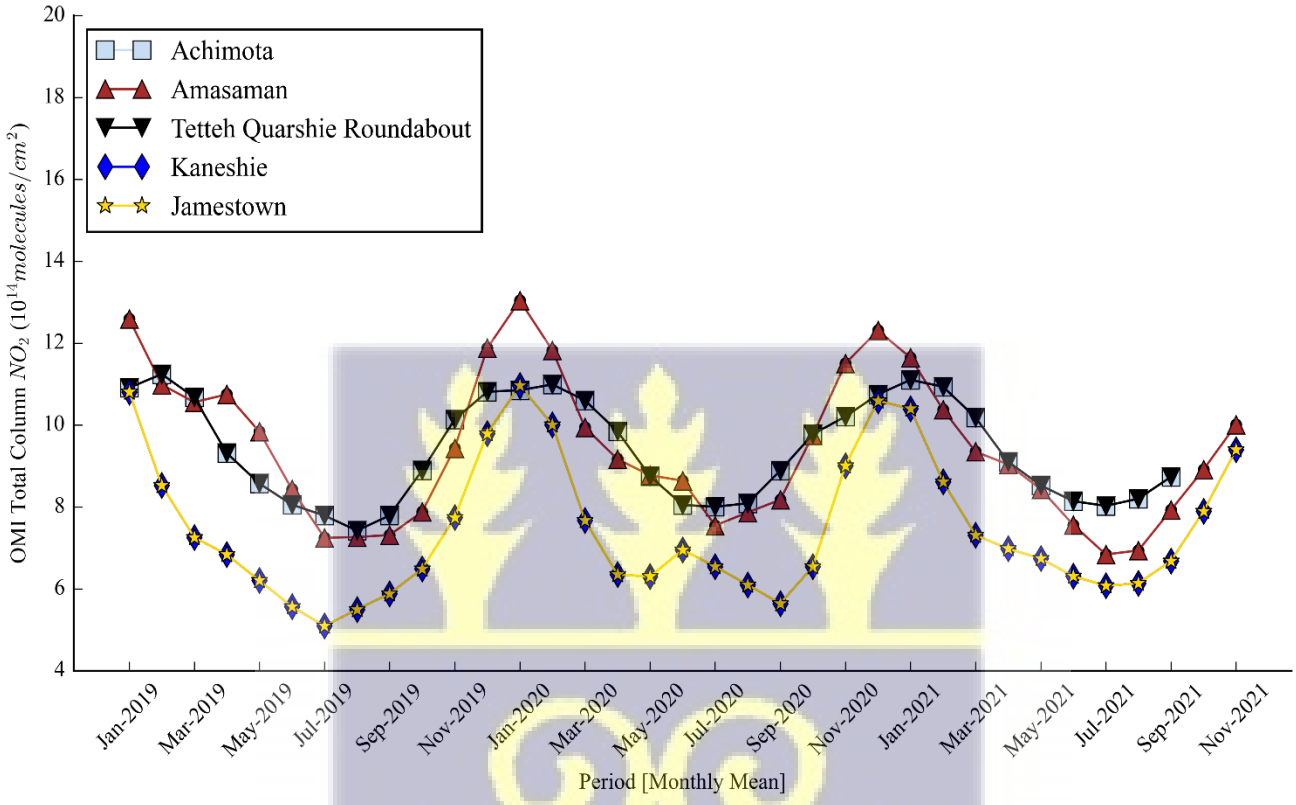

Figure 4.23: Monthly variations of total column OMI NO_2 levels from 2019 to 2021 across 5 EPA stations in the GAMA.

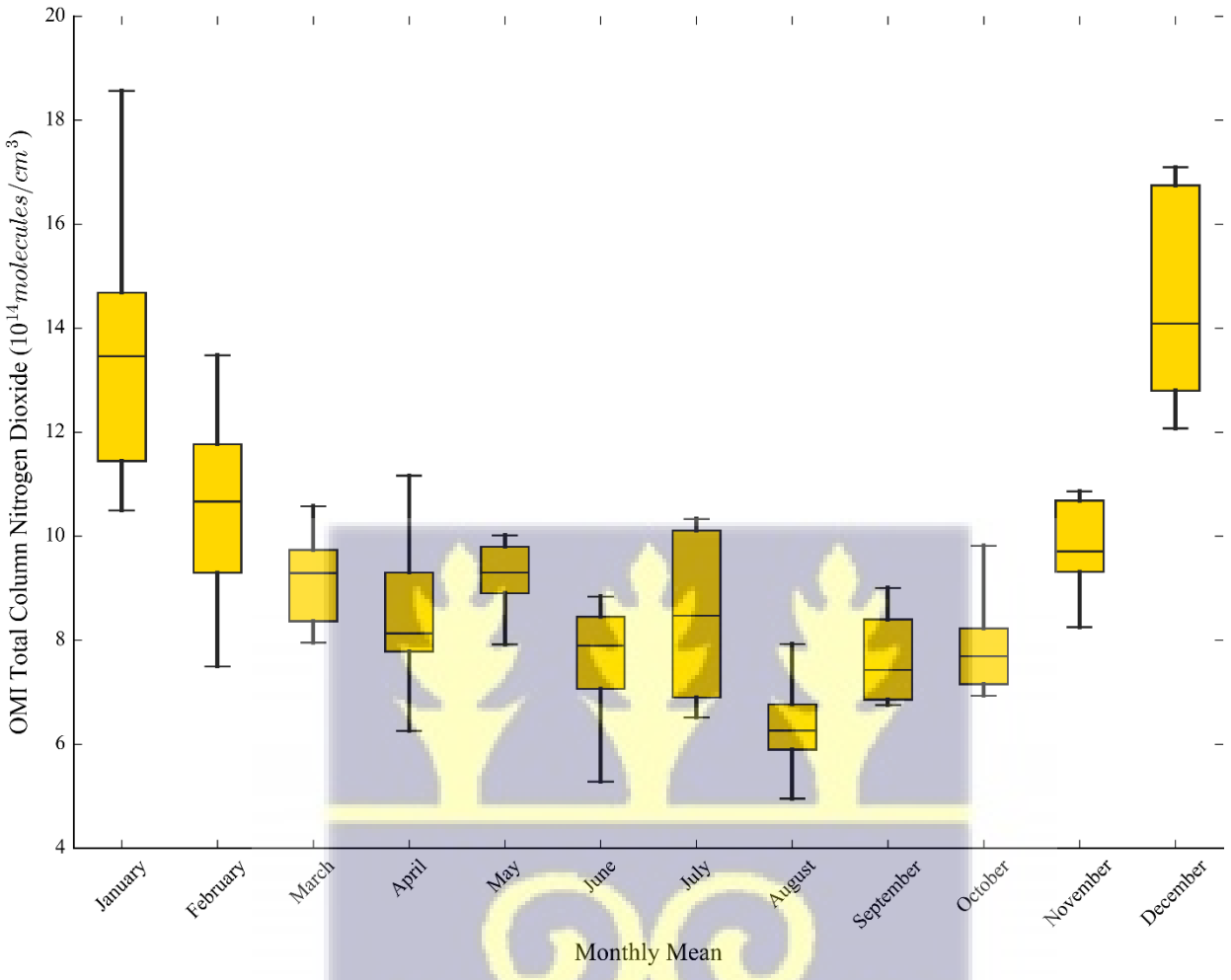

Figure 4.24: Boxplots of monthly average total column OMI NO_2 over the 5 EPA stations. The boxplots represent the first quartile to the third quartile with a black line showing the median.

Table 7: A summary of the Mann-Kendall test for the de-seasonalized Terra AOD time series at 95% confidence interval

Modis Terra	Amasaman	Jamestown	Tetteh Quarshie	Kaneshie	Achimota
p-value	0.000	0.000	0.000	0.000	0.000
Z-score	-7.526	-7.526	-7.526	-7.526	-7.526
S	-1324763.000	-1324763.000	-1324763.000	-1324763.000	-1324763.000
Tau	-0.062	-0.062	-0.062	-0.062	-0.062
Slope	0.000	0.000	0.000	0.000	0.000
Intercept	0.498	0.498	0.498	0.498	0.498

Table 8: A summary of the Mann-Kendall test for the de-seasonalized NO_2 time series at 95% confidence interval

OMI NO_2	Amasaman	Jamestown	Tetteh Quarshie	Kaneshie	Achimota
p-value	0.173	0.019	0.004	0.019	0.004
Z-score	1.364	2.351	2.853	2.351	2.853
S	4610.000	7948.000	3286.000	7948.000	3286.000
Tau	0.042	0.072	0.127	0.073	0.127
Slope	0.000700	0.000	0.000	0.000	0.000
Intercept	0.875600	0.660	0.862	0.660	0.862

Table 9: A summary of the Mann-Kendall test for the de-seasonalized O_3 time series at 95% confidence interval

OMI O_3	Amasaman	Jamestown	Tetteh Quarshie	Kaneshie	Achimota
p-value	0.072	0.061	0.452	0.061	0.452
Z-score	1.797	1.877	0.751	1.877	0.751
S	6074.000	6346.000	866.000	6346.000	866.000
Tau	0.056	0.058	0.034	0.058	0.033
Slope	0.006	0.006	0.005	0.006	0.005
Intercept	267.381	267.656	268.802	267.656	268.802

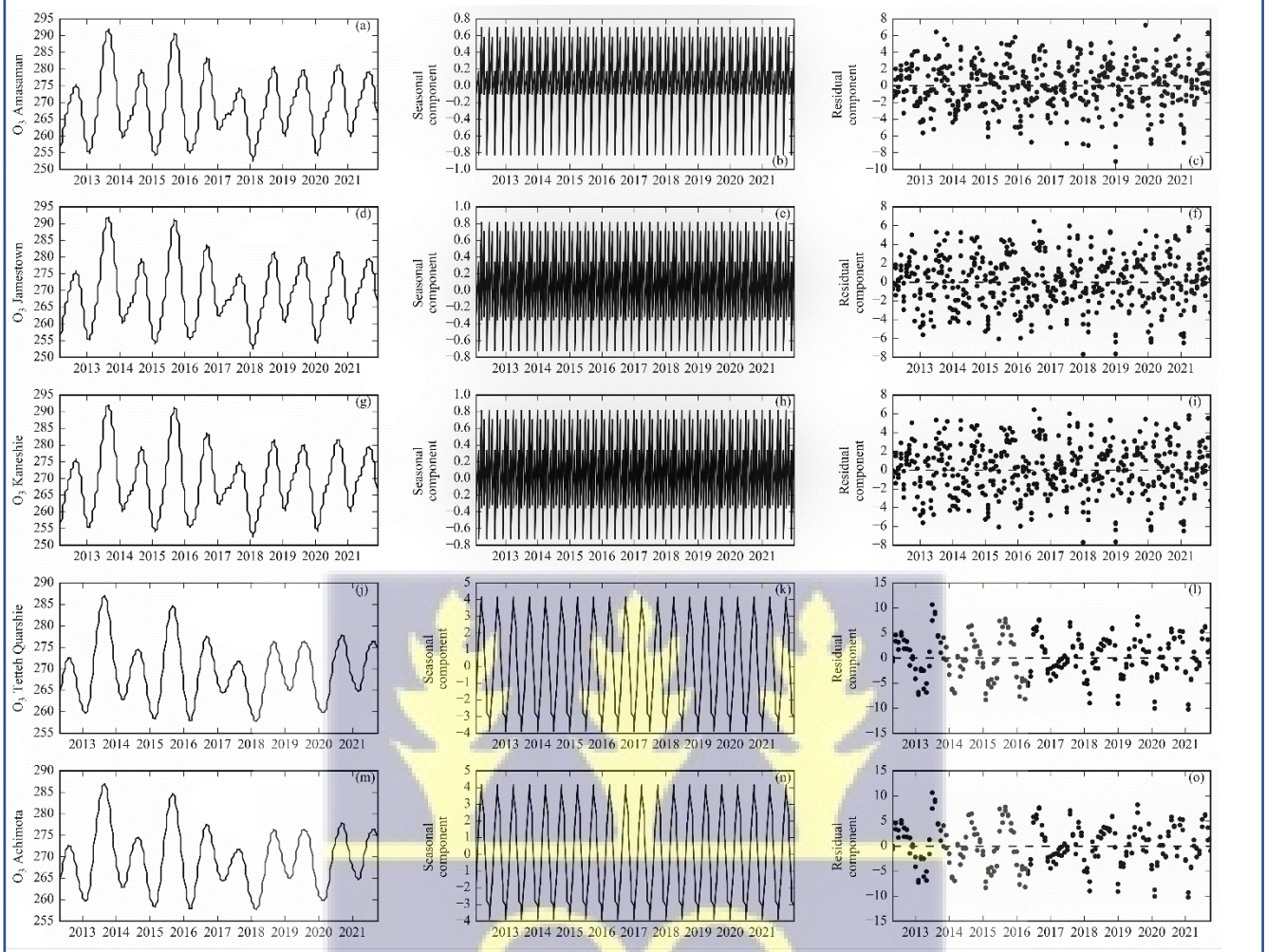

Figure 4.25: Decomposed long-term time series of O_3 (DU). Figures labelled (a, d, g, j and m) are the de-seasonalized components, (b, e, h, k, n) are the seasonal components and (c, f, i, l, o) are the residual components

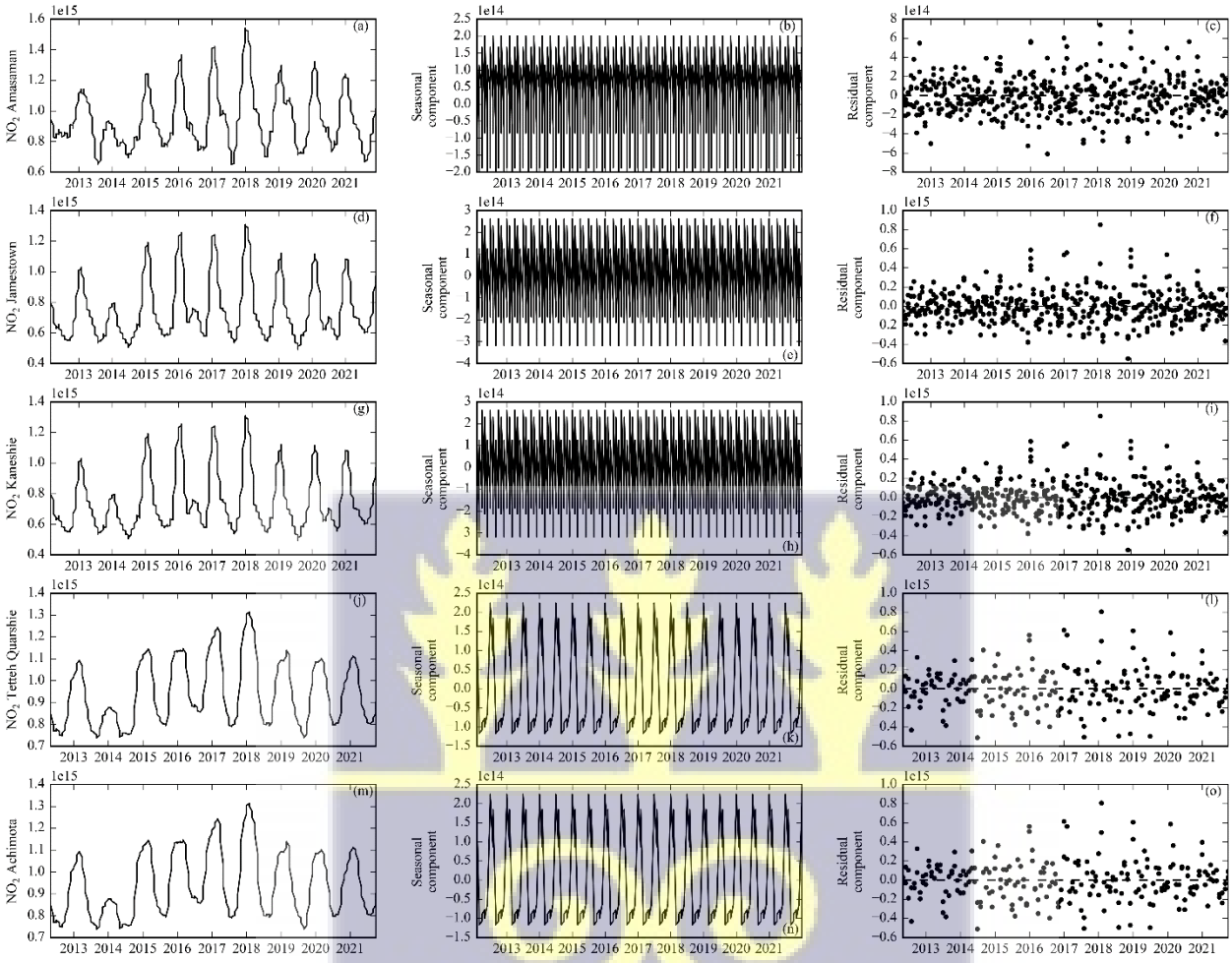

Figure 4.26: Decomposed long-term time series of NO_2 (x10^{14} molecules/cm^2). Figures labelled (a, d, g, j and m) are the de-seasonalized components, (b, e, h, k, n) are the seasonal components and (c, f, i, l, o) are the residual components

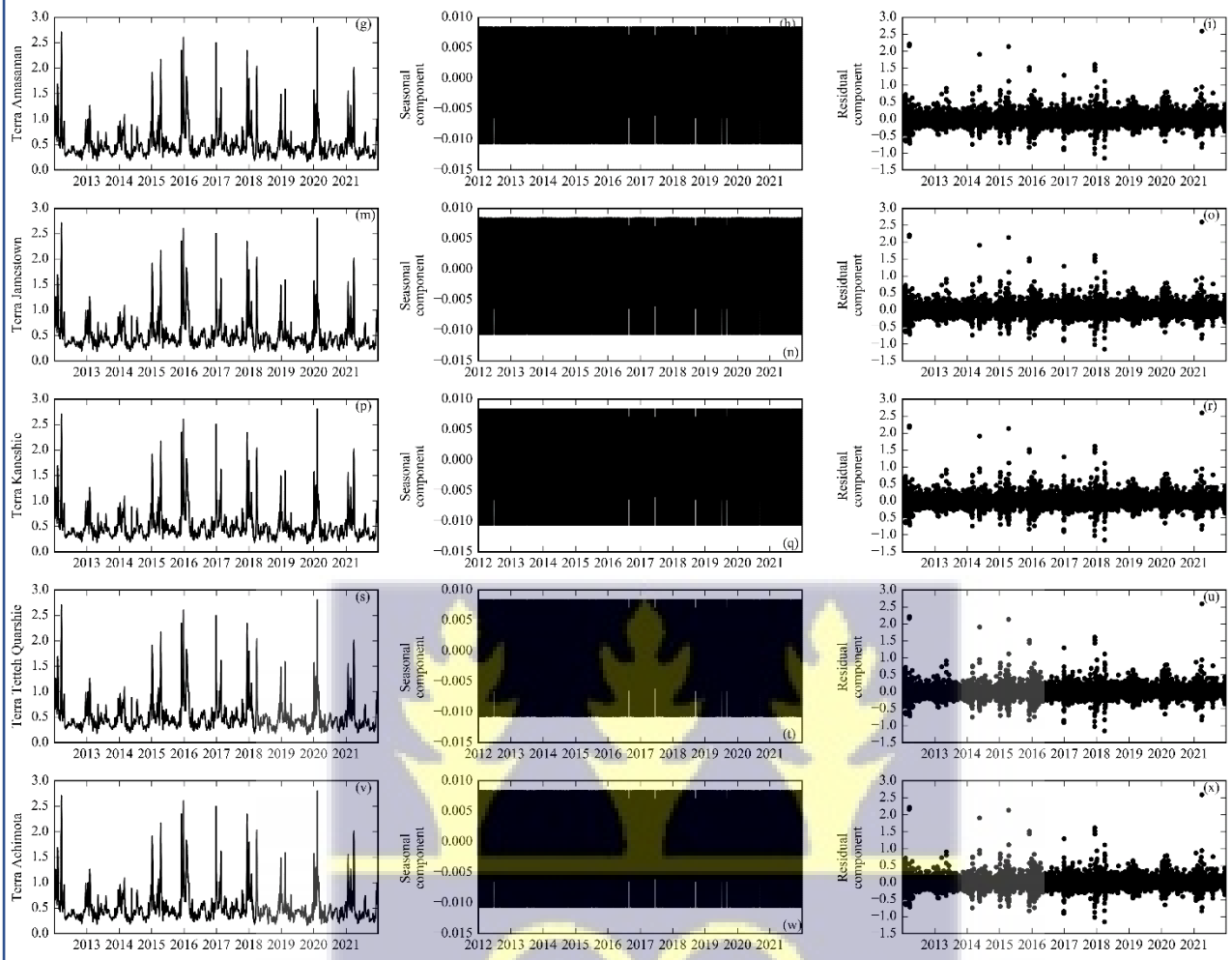

Figure 4.27: Decomposed long-term time series of AOD. Figures labelled (g, m, p, s and v) are the de-seasonalized components, (h, n, q, t, w) are the seasonal components and (i, o, r, u, x) are the residual components.

CHAPTER FIVE

CONCLUSION AND RECOMMENDATIONS

5.1 CONCLUSION

Poor air quality has been identified as a major cause of deaths from heart disease and stroke, lung cancer, chronic lung disease as well as respiratory infections around the globe. Every year, poor air quality is responsible for about 7 million deaths globally as estimated by the WHO (World Health Organization and Mudu, 2021). In sub- Saharan Africa with increasing population growth and urban emissions, the situation is no different since poor air quality is increasing at an alarming rate. Therefore, regular monitoring is required to assess the levels of pollutant in both local and regional scale. However, this is scarce in low- and middle- income countries (LMICs) especially in sub-Saharan African regions; as it is expensive to acquire, install and maintain large number of high-grade air quality monitoring sensors. Thus, has limited studies to investigate associations between particulates with aerodynamic diameter less than 2.5 microns ($PM_{2.5}$) and gas pollutants like nitrogen dioxide (NO_2) and ozone (O_3) for a long period in sub-Saharan African cities. Hence, this study sorts to bridge this gap by utilizing 5 Clarity Node-S sensors $PM_{2.5}$ data, total column particulates or Aerosol Optical Depth (AOD), NO_2 and O_3 data from satellites over 5 different Ghana Environmental Protection Agency (GEPA) air quality traffic stations in the Greater Accra Metropolitan Area (GAMA). AOD, NO_2 and O_3 were retrieved from NASA Moderate Resolution Imaging Spectro-Radiometer (MODIS) Terra and Ozone Monitoring Instrument (OMI). Long-term trends over the 5 stations on $(25 \times 25)\ km^2$ grid for OMI and $(50 \times 50)\ km^2$ grid for

MODIS Terra AOD from 2012 to 2021 were assessed using Mann-Kendall sequential test while the Pearson correlation coefficient was used to find correlations between the pollutants. Further, characterization of $PM_{2.5}$, AOD, NO_2, and O_3 levels in the GAMA were also assessed. Overall, there was an increasing trend in NO_2 (with $p < 0.05$) over 4 stations, no trend in O_3 (with $p > 0.05$) and a decreasing trend in AOD (with $p < 0.01$). Coefficients of determination between $PM_{2.5}$ data and MODIS Terra AOD on $(50 \times 50)\ km^2$ grid across the stations were (R^2 = 0.72, 0.72, 0.67, 0.58 and 0.57) respectively. Coefficients of determination between total column NO_2 and O_3 were ($R^2 = 0.83 \pm 0.030$, $p < 0.01$), AOD and O_3 ($R^2 = 0.43 \pm 0.003$, $p < 0.01$) and NO_2 and AOD ($R^2 = 0.21 \pm 0.010$, $p > 0.01$). $PM_{2.5}$, AOD and NO_2 levels were generally high during the dry season while high concentrations of O_3 were observed in the wet season across the stations. $PM_{2.5}$ daily mean level of 32.8 μgm^{-3} for 25 months between 2018 and 2021 was found be to be more than twice WHO recommended daily mean level of 15 μgm^{-3}. Good correlation coefficient was observed between total column NO_2 and O_3. Low correlation coefficients between AOD, NO_2 and O_3 may reveal different emission sources from open burning, street cooking, traffic and industrial activities in the GAMA. Furthermore, data void was observed in the northern and southern part of Ghana during the study period. This can be attributed to cloud cover or lack of retrieval by the OMI and MODIS algorithm due to meteorological effects such as wind speed, rainfall, and humidity. High population growth coupled with increasing traffic, biomass burning and climate change in growing sub-Saharan African cities requires urgent policy measures and regulations as ground air quality monitoring sensors are limited.

5.2 RECOMMENDATIONS

The satellites on the geostationary orbits, such as the Indian National Satellite (INSAT), provide regional coverage every 15 minutes over India and Africa. The high temporal resolution of the data from satellites on the geostationary orbit minimizes the variability of total column concentrations over a region. Therefore, retrieving total column air quality data over sub-Saharan Africa from a satellite on the geostationary orbit will provide better results of aerosol optical depth due to their higher temporal resolutions. Again, to obtain distribution pattern of poor air quality of over Ghana, during the dry and wet seasons, it would be recommended to use high spatial resolution and more efficient algorithms such as the Multi-Angle Implementation of Atmospheric Correction (MAIAC) Algorithm (which estimates aerosol optical depth at 1 km resolution). The MAIAC Algorithm is designed to minimize the limitation of cloud cover which is mostly observed during the rainy season. Furthermore, training is needed in the field of satellite remote sensing to enable air quality research scientist in sub-Saharan Africa to learn how to access aerosol optical depth data from satellite sensors since the technical know-how in this area is lacking. Also, governmental agencies such as the EPA can utilise satellite derived AOD data to assess long-term trends of particulate matter pollution as a replacement of ground-based sensor dataset since long-term data from ground-based sensors is scarce. This will enable governmental agencies and policy makers to understand the trend of sources and causes of air pollution to a far extent, as a result, efficient policies and mitigation strategies can be developed to minimise air pollution challenges in the sub-Saharan African countries.

REFERENCES

Abam, F. (2015). *Vehicular Emissions and Air Quality Standards in Nigeria*. *April*.

Abera, A., Mattisson, K., Eriksson, A., Ahlberg, E., Sahilu, G., Mengistie, B., Bayih, A. G., Aseffaa, A., Malmqvist, E., & Isaxon, C. (2020). Air Pollution Measurements and Land-Use Regression in Urban Sub-Saharan Africa Using Low-Cost Sensors—Possibilities and Pitfalls. *Atmosphere*, *11*(12), 1357. https://doi.org/10.3390/atmos11121357

Akinyoola, J. A., Eresanya, E. O., Orimoogunje, O. O. I., & Oladosu, K. (2018). Monitoring the spatio-temporal aerosol loading over Nigeria. *Modeling Earth Systems and Environment*, 1–11. https://doi.org/10.1007/s40808-018-0485-2

Akuro Adoki. (2012). Air Quality Survey of some locations in the Niger Delta Area. *Journal of Applied Sciences and Environmental Management*, *16*(1), 125–134.

Alli, A. S., Clark, S. N., Hughes, A., Nimo, J., Bedford-Moses, J., Baah, S., Wang, J., Vallarino, J., Agyemang, E., Barratt, B., Beddows, A., Kelly, F., Owusu, G., Baumgartner, J., Brauer, M., Ezzati, M., Agyei-Mensah, S., & Arku, R. E. (2021). Spatial-temporal patterns of ambient fine particulate matter ($PM_{2.5}$) and black carbon (BC) pollution in Accra. *Environmental Research Letters*, *16*(7), 074013. https://doi.org/10.1088/1748-9326/ac074a

Alpert, P., Shvainshtein, O., & Kishcha, P. (2012). *AOD trends over megacities based on space monitoring using MODIS and MISR*. *2012*. https://doi.org/10.4236/ajcc.2012.

Arku, R. E., Vallarino, J., Dionisio, K. L., Willis, R., Choi, H., Wilson, J. G., Hemphill, C., Agyei-Mensah, S., Spengler, J. D., & Ezzati, M. (2008a). Characterizing air pollution in two low-income neighborhoods in Accra, Ghana. *Science of the Total Environment*, *402*(2–3), 217–231. https://doi.org/10.1016/j.scitotenv.2008.04.042

Arku, R. E., Vallarino, J., Dionisio, K. L., Willis, R., Choi, H., Wilson, J. G., Hemphill, C., Agyei-Mensah, S., Spengler, J. D., & Ezzati, M. (2008b). Characterizing air pollution in two low-income neighborhoods in Accra, Ghana. *Science of the Total Environment*, *402*(2–3), 217–231. https://doi.org/10.1016/J.SCITOTENV.2008.04.042

Brito, J., Rizzo, L. V, Morgan, W. T., Coe, H., Johnson, B., Haywood, J., Longo, K., Freitas, S., Andreae, M. O., & Artaxo, P. (2014). *Ground-based aerosol characterization during the South American Biomass Burning Analysis (SAMBBA) field experiment*. *3*, 12069–12083. https://doi.org/10.5194/acp-14-12069-2014

Cao, C., & Bai, Y. (2014). *Quantitative Analysis of VIIRS DNB Nightlight Point Source for Light Power Estimation and Stability Monitoring*. 11915–11935. https://doi.org/10.3390/rs61211915

Chem, A., Discuss, P., Phys, C., Flamant, C., Deroubaix, A., Chazette, P., Brito, J., & Gaetani, M. (2018). *Aerosol distribution in the northern Gulf of Guinea: Local anthropogenic sources, long-range transport and circulations the role of coastal shallow*. *April*.

Cheng, Y.-H. (2010). Influences of Traffic Emissions and Meteorological Conditions on Ambient PM10 and PM2.5 Levels at a Highway Toll Station. *Aerosol and Air Quality Research*. https://doi.org/10.4209/aaqr.2010.04.0025

Chow, J. C., Watson, J. G., Mauderly, J. L., Costa, D. L., Wyzga, R. E., Vedal, S., Hidy, G. M., Altshuler, S. L., Marrack, D., Heuss, J. M., Wolff, G. T., Arden Pope III, C., & Dockery, D. W. (2006). Health Effects of Fine Particulate Air Pollution: Lines that Connect. *Journal of the Air & Waste Management Association*, *56*(10), 1368–1380. https://doi.org/10.1080/10473289.2006.10464545

Chu, D. A., Kaufman, Y. J., Ichoku, C., Remer, L. A., Tanre, D., & Holben, B. N. (2002). *Validation of MODIS aerosol optical depth retrieval over land*. *29*(12), 4–7.

Chu, D. A., Kaufman, Y. J., Zibordi, G., Chern, J. D., Mao, J., Li, C., & Holben, B. N. (2003). *Global monitoring of air pollution over land from the Earth Observing System-Terra Moderate Resolution Imaging Spectroradiometer (MODIS)*. *108*, 1–18. https://doi.org/10.1029/2002JD003179

Cisek, M., Petelski, T., Zielinski, T., Makuch, P., Pakszys, P., Rozwadowska, A., & Markuszewski, P. (2017). Aerosol Optical Depth variations due to local breeze circulation in Kongsfjorden , Spitsbergen. *Oceanologia*, *59*(4), 422–430. https://doi.org/10.1016/j.oceano.2017.04.005

Cohen, A. J., Brauer, M., Burnett, R., Anderson, H. R., Frostad, J., Estep, K., Balakrishnan, K., Brunekreef, B., Dandona, L., Dandona, R., Feigin, V., Freedman, G., Hubbell, B., Jobling, A., Kan, H., Knibbs, L., Liu, Y., Martin, R., Morawska, L., … Forouzanfar, M. H. (2017). Estimates and 25-year trends of the global burden of disease attributable to ambient air pollution: An analysis of data from the Global Burden of Diseases Study 2015. *The Lancet*, *389*(10082), 1907–1918. https://doi.org/10.1016/S0140-6736 (17)30505-6

Colarco, P. R., Schoeberl, M. R., Doddridge, B. G., Marufu, L. T., Torres, O., & Welton, E. J. (2004). *Transport of smoke from Canadian forest fires to the surface near Washington, D. C .: Injection height , entrainment , and optical properties*. *109*, 1–12. https://doi.org/10.1029/2003JD004248

Datasets, S. (2018). *Installing Python with Anaconda*. 7–9.

Dionisio, K. L., Hughes, A. F., Vallarino, J., Carmichael, H., & Spengler, J. D. (2010). *Air Pollution in Accra Neighborhoods: Spatial, Socioeconomic, and Temporal Patterns*. *44*(7), 2270–2276.

Donkelaar, A. Van, Martin, R. V, Brauer, M., & Boys, B. L. (n.d.). *Supplemental Material Use of Satellite Observations for Long-Term Exposure Assessment of Global Concentrations of Fine Particulate Matter*. https://doi.org/10.1289/ehp.1408646

Donkelaar, A. Van, Martin, R. V, Brauer, M., Kahn, R., Levy, R., & Verduzco, C. (2010). *Global Estimates of Ambient Fine Particulate Matter Concentrations from Satellite-Based Aerosol Optical Depth: Development and Application*. *118*(6), 847–855. https://doi.org/10.1289/ehp.0901623

Eck, T. F., Holben, B. N., Reid, J. S., Dubovik, O., Smirnov, A., O'Neill, N. T., Slutsker, I., & Kinne, S. (1999). Wavelength dependence of the optical depth of biomass burning, urban, and desert dust aerosols. *Journal of Geophysical Research: Atmospheres*, *104*(D24), 31333–31349. https://doi.org/10.1029/1999JD900923

Ede, P. N., & Edokpa, D. O. (2017). Satellite Determination of Particulate Load over Port Harcourt during Black Soot Incidents. *Journal of Atmospheric Pollution, Vol. 5, 2017, Pages 55-61*, *5*(2), 55–61. https://doi.org/10.12691/JAP-5-2-3

Emeis, S., & Karlsruhe, F. (2004). *Aerosol concentration measurements with a lidar ceilometer: Results of*. *5235*, 486–496. https://doi.org/10.1117/12.511104

Emetere, M. E., & Akinyemi, M. L. (2015). *Aerosol Optical Depth Trends over Different Regions of Nigeria: Thirteen years Analysis*. *9*(9), 267–279. https://doi.org/10.5539/mas.v9n9p267

Enitan, I. T., Durowoju, O. S., Edokpayi, J. N., & Odiyo, J. O. (2022). A Review of Air Pollution Mitigation Approach Using Air Pollution Tolerance Index (APTI) and Anticipated Performance Index (API). *Atmosphere*, *13*(3), 374. https://doi.org/10.3390/atmos13030374

Environment, A., NASA, P. G., Hong, L., & Sar, K. (2015). *Satellite remote sensing of particulate matter and air quality assessment over global cities*. *November*. https://doi.org/10.1016/j.atmosenv.2006.03.016

Fairlie, T. D., Vernier, J., Natarajan, M., Deshler, T., & Gadhavi, H. (2016). *Characterizing the Asian Tropopause Aerosol Layer (ATAL) using in situ balloon measurements: The BATAL campaigns of*

2014-2016 Transport of pollution into the UTLS linked to deep convection in Summer Asian Monsoon. 1–20.

Fawole, O. G., Cai, X., Levine, J. G., Pinker, R. T., & MacKenzie, A. R. (2016). Detection of a gas flaring signature in the AERONET optical properties of aerosols at a tropical station in West Africa. *Journal of Geophysical Research*, *121*(24), 14513–14524. https://doi.org/10.1002/2016JD025584

Fisher, S., Bellinger, D. C., Cropper, M. L., Kumar, P., Binagwaho, A., Koudenoukpo, J. B., Park, Y., Taghian, G., & Landrigan, P. J. (2021). Air pollution and development in Africa: Impacts on health, the economy, and human capital. *The Lancet Planetary Health*, *5*(10), e681–e688. https://doi.org/10.1016/S2542-5196 (21)00201-1

Fosu-Amankwah, K., Bessardon, G. E. Q., Quansah, E., Amekudzi, L. K., Brooks, B. J., & Damoah, R. (2021). Assessment of aerosol burden over Ghana. *Scientific African*, *14*, e00971. https://doi.org/10.1016/j.sciaf.2021.e00971

GBD 2015 Risk Factors Collaborators, M. H., Afshin, A., Alexander, L. T., Anderson, H. R., Bhutta, Z. A., Biryukov, S., Brauer, M., Burnett, R., Cercy, K., Charlson, F. J., Cohen, A. J., Dandona, L., Estep, K., Ferrari, A. J., Frostad, J. J., Fullman, N., Gething, P. W., Godwin, W. W., Griswold, M., … Murray, C. J. L. (2016). Global, regional, and national comparative risk assessment of 79 behavioural, environmental and occupational, and metabolic risks or clusters of risks, 1990-2015: A systematic analysis for the Global Burden of Disease Study 2015. *Lancet (London, England)*, *388*(10053), 1659–1724. https://doi.org/10.1016/S0140-6736 (16)31679-8

GSS (2012). *2010 Population and housing census: Summary report of final results.* Accra: Ghana Statistical Service.

Gupta, P., & Christopher, S. A. (2009a). *Particulate matter air quality assessment using integrated surface, satellite, and meteorological products: 2. A neural network approach United States*

using Aerosol Optical Thickness (AOT) from the Moderate Resolution Imaging SpectroRadiometer. *114*, 1–14. https://doi.org/10.1029/2008JD011497

Gupta, P., & Christopher, S. A. (2009b). *Particulate matter air quality assessment using integrated surface, satellite, and meteorological products: Multiple regression approach*. *114*(May), 1–13. https://doi.org/10.1029/2008JD011496

Gupta, P., Levy, R. C., Mattoo, S., Remer, L. A., & Munchak, L. A. (2016). A surface reflectance scheme for retrieving aerosol optical depth over urban surfaces in MODIS Dark Target retrieval algorithm. *Atmospheric Measurement Techniques*, *9*(7), 3293–3308. https://doi.org/10.5194/amt-9-3293-2016

Hao, X., & Qu, J. J. (2017). *Saharan dust storm detection using moderate resolution imaging spectroradiometer thermal infrared bands*. *1*(April 2007), 1–9. https://doi.org/10.1117/1.2740039

Heilman, W. E., Liu, Y., Urbanski, S., Kovalev, V., & Mickler, R. (2014). *Forest Ecology and Management Wildland fire emissions, carbon, and climate: Plume rise, atmospheric transport, and chemistry processes*. *317*, 70–79. https://doi.org/10.1016/j.foreco.2013.02.001

Hens, L., Thinh, N. A., Hanh, T. H., Cuong, N. S., Lan, T. D., & Van, N. (n.d.). *Sea—Level rise and resilience in Vietnam and the Asia—Pacific: A synthesis*. *40*(2), 126–152. https://doi.org/10.15625/0866-7187/40/2/11107

Horwood, Chris. Phillips,Tom., Integrated Regional Information Networks., United Nations Human Settlements Programme., & Australian Agency for International Development. (2007). *Tomorrow's crises today: The humanitarian impact of urbanisation*. OCHA/IRIN.

Hu, Z. (2009). Spatial analysis of MODIS aerosol optical depth, PM2.5, and chronic coronary heart disease. *International Journal of Health Geographics*, *8*(1), 1–10. https://doi.org/10.1186/1476-072X-8-27

Huete, A., Didan, K., van Leeuwen, W., Miura, T., & Glenn, E. (2010). *MODIS Vegetation Indices* (pp. 579–602). Springer, New York, NY. https://doi.org/10.1007/978-1-4419-6749-7_26

Ikoku, A., & College, F. (2016). *Atmospheric visibility trends in the Niger Delta Region Nigeria 1981-2012*. *3*(6), 138–144.

Ite, A. E., Ogunkunle, C. O., Obadimu, C. O., Asuaiko, E. R., & Ibok, U. J. (2017). *Particulate Matter and Staff Exposure in an Air-Conditioned Office in Akwa Ibom State University – Nigeria*. *5*(1), 24–32. https://doi.org/10.12691/jap-5-1-4

Jin, M., Shepherd, J. M., & King, M. D. (2005). *Urban aerosols and their variations with clouds and rainfall: A case study for New York and Houston*. *110*, 1–12. https://doi.org/10.1029/2004JD005081

Johnson, N. M., Hoffmann, A. R., Behlen, J. C., Lau, C., Pendleton, D., Harvey, N., Shore, R., Li, Y., Chen, J., Tian, Y., & Zhang, R. (2021). Air pollution and children's health— A review of adverse effects associated with prenatal exposure from fine to ultrafine particulate matter. *Environmental Health and Preventive Medicine*, *26*(1), 72. https://doi.org/10.1186/s12199-021-00995-5

Kahn, R. A., Chen, Y., Nelson, D. L., Leung, F., Li, Q., Diner, D. J., & Logan, J. A. (2008). *Wildfire smoke injection heights: Two perspectives from space*. *35*, 4–7. https://doi.org/10.1029/2007GL032165

Kahn, R. A., & Gaitley, B. J. (2015). *Journal of Geophysical Research: Atmospheres An analysis of global aerosol type as retrieved by MISR*. https://doi.org/10.1002/2015JD023322.Received

Lee, K. H., Wong, M. S., Nichol, J., & Chan, P. W. (2015). *Retrieval of Aerosol Size Distribution from Microtops II Sunphotometer in Hong Kong*. 1712–1719. https://doi.org/10.4209/aaqr.2015.01.0048

Levelt, P. F., Joiner, J., Tamminen, J., Veefkind, J. P., Bhartia, P. K., Stein Zweers, D. C., Duncan, B. N., Streets, D. G., Eskes, H., van der A, R., McLinden, C., Fioletov, V., Carn, S., de Laat, J., DeLand, M., Marchenko, S., McPeters, R., Ziemke, J., Fu, D., … Wargan, K. (2018). The Ozone Monitoring Instrument: Overview of 14 years in space. *Atmospheric Chemistry and Physics*, *18*(8), 5699–5745. https://doi.org/10.5194/acp-18-5699-2018

Levelt, P. F., van den Oord, G. H. J., Dobber, M. R., Malkki, A., Huib Visser, Johan de Vries, Stammes, P., Lundell, J. O. V., & Saari, H. (2006). The ozone monitoring instrument. *IEEE Transactions on Geoscience and Remote Sensing*, *44*(5), 1093–1101. https://doi.org/10.1109/TGRS.2006.872333

Levy, R. C., Mattoo, S., Munchak, L. A., Remer, L. A., Sayer, A. M., Patadia, F., & Hsu, N. C. (2013). The Collection 6 MODIS aerosol products over land and ocean. *Atmospheric Measurement Techniques*, *6*(11), 2989–3034. https://doi.org/10.5194/amt-6-2989-2013

Li, Z., Tang, B., Wu, H., Ren, H., Yan, G., Wan, Z., Trigo, I. F., & Sobrino, J. A. (2013). Remote Sensing of Environment Satellite-derived land surface temperature: Current status and perspectives. *Remote Sensing of Environment*, *131*, 14–37. https://doi.org/10.1016/j.rse.2012.12.008

Lim, H. S., MatJafri, M. Z., Abdullah, K., Saleh, N. Mohd., & Wong, C. J. (2007). Extracting spatial data from satellite sensor to support air pollution determination using remote sensing technique. *2007 IEEE International Geoscience and Remote Sensing Symposium*, 4302–4306. https://doi.org/10.1109/IGARSS.2007.4423803

Lynch, S. (2018). *OpenLitterMap. Com – Open Data on Plastic Pollution with Blockchain Rewards (Littercoin)*.

Madhavan, S., Qu, J. J., & Hao, X. (2017). Saharan dust detection using multi-sensor satellite measurements. *Heliyon*, *3*(2), e00241. https://doi.org/10.1016/j.heliyon.2017.e00241

Mao, K. B., Ma, Y., Xia, L., Chen, W. Y., Shen, X. Y., He, T. J., & Xu, T. R. (2014a). *Global aerosol change in the last decade: An analysis based on MODIS data*. *94*, 680–686. https://doi.org/10.1016/j.atmosenv.2014.04.053

Mao, K. B., Ma, Y., Xia, L., Chen, W. Y., Shen, X. Y., He, T. J., & Xu, T. R. (2014b). *Global aerosol change in the last decade: An analysis based on MODIS data*. *94*, 680–686. https://doi.org/10.1016/j.atmosenv.2014.04.053

Matandirotya, Newton. R. (2021). Research trends in the field of ambient air quality monitoring and management in South Africa: A bibliometric review. *Environmental Challenges*, *5*, 100263. https://doi.org/10.1016/j.envc.2021.100263

Metropolis, P. H., Risk, D., Harcourt, P., & Harcourt, P. (2014). *Atmospheric Concentration of Particulate Pollutants and its Implications for Respiratory Health Hazard Management in*. *6*(5), 11–18.

Misra, A., Jayaraman, A., & Ganguly, D. (2015). *Validation of Version 5. 1 MODIS Aerosol Optical Depth (Deep Blue Algorithm and Dark Target Approach) over a Semi-Arid Location in Western India*. 252–262. https://doi.org/10.4209/aaqr.2014.01.0004

Nemuc, A., Vasilescu, J., Belegante, L., & Radu, C. (2007). *Optical Properties of Aerosols from Lidar Data and Other Ground-based Instruments near Bucharest*. *409*.

Nicholson, S. E. (2018). The ITCZ and the Seasonal Cycle over Equatorial Africa. *Bulletin of the American Meteorological Society*, *99*(2), 337–348. https://doi.org/10.1175/BAMS-D-16-0287.1

Nwachukwu, A. N., Chukwuocha, E. O., & Igbudu, O. (2012). A survey on the effects of air pollution on diseases of the people of Rivers State, Nigeria. *African Journal of Environmental Science and Technology*, *6*(October), 371–379. https://doi.org/10.5897/ AJEST12.024

Nwofor, O. K. (2010). *Rising Dust Aerosol Pollution at Ilorin in the Sub-sahel Inferred from 10-year Aeronet Data: Possible Links to Persisting Drought Conditions*. *2*(4), 216–225.

Ofosu, F. G., Hopke, P. K., Aboh, I. J. K., & Bamford, S. A. (2012). Atmospheric Pollution Research Characterization of fine particulate sources at Ashaiman in Greater. *Atmospheric Pollution Research*, *3*(3), 301–310. https://doi.org/10.5094/APR.2012.033

Ofosu, F. G., Hopke, P. K., Aboh, I. J. K., Bamford, S. A., Ofosu, F. G., Hopke, P. K., Aboh, I. J. K., & Bamford, S. A. (2013). *Biomass burning contribution to ambient air particulate levels at Navrongo in the Savannah zone of Ghana Biomass burning contribution to ambient air particulate levels at Navrongo in the Savannah zone of Ghana*. *2247*(May). https://doi.org/10.1080/10962247.2013.783888

Oluyemi, E. A., & Asubiojo, O. I. (2001). Ambient Air Particulate Matter in Lagos, Nigeria: A Study using Receptor Modeling with X-Ray Flourescence Analysis. *Bu Ll. Ch Em. Soc. E t h Iop.*

Onyeuwaoma, N. D., Nwofor, O. K., Chineke, T. C., Eguaroje, E. O., & Dike, V. N. (2015). Implications of MODIS impression of aerosol loading over urban and rural settlements in Nigeria: Possible links to energy consumption patterns in the country. *Atmospheric Pollution Research*, *6*(3), 484–494. https://doi.org/10.5094/APR.2015.054

Rao, S., Pachauri, S., Dentener, F., Kinney, P., Klimont, Z., Riahi, K., & Schoepp, W. (2013). Better air for better health: Forging synergies in policies for energy access, climate change and air pollution. *Global Environmental Change*, *23*(5), 1122–1130. https://doi.org/10.1016/j.gloenvcha.2013.05.003

Rooney, M. S., Arku, R. E., Dionisio, K. L., Paciorek, C., Friedman, A. B., Carmichael, H., Zhou, Z., Hughes, A. F., Vallarino, J., Agyei-Mensah, S., Spengler, J. D., & Ezzati, M. (2012). Spatial and temporal patterns of particulate matter sources and pollution in four communities in Accra, Ghana.

Science of the Total Environment, *435–436*, 107–114. https://doi.org/10.1016/j.scitotenv.2012.06.077

Rowland, G. (2011). Air Pollution in the Niger Delta Area: Scope, Challenges and Remedies. In *The Impact of Air Pollution on Health, Economy, Environment and Agricultural Sources*. InTech. https://doi.org/10.5772/16817

Sauvage, B., & Thouret, V. (2005). Tropospheric ozone over Equatorial Africa: Regional aspects from the MOZAIC data. *Atmos. Chem. Phys.*

Sayer, A. M., Hsu, N. C., Bettenhausen, C., Jeong, M., Meister, G., & Al, S. E. T. (2015). *Effect of MODIS Terra radiometric calibration improvements on Collection 6 Deep Blue aerosol products: Validation and Terra / Aqua consistency*. 157–174. https://doi.org/10.1002/2015JD023878.Received

Sayer, A. M., Munchak, L. A., Hsu, N. C., Levy, R. C., Bettenhausen, C., & Jeong, M. J. (2014). Modis collection 6 aerosol products: Comparison between aqua's e-deep blue, dark target, and "merged" data sets, and usage recommendations. *Journal of Geophysical Research*, *119*(22), 13,965-13,989. https://doi.org/10.1002/2014JD022453

Schaap, M., Apituley, A., Nederlands, K., Instituut, M., Timmermans, R., & Koelemeijer, R. (2009) *and Physics Exploring the relation between aerosol optical depth and PM 2. 5 at Cabauw, the Netherlands. November 2014*. https://doi.org/10.5194/acpd-8-17939-2008

Schroedter-Homscheidt, M., Oumbe, A., Benedetti, A., & Morcrette, J.-J. (2013). Aerosols for Concentrating Solar Electricity Production Forecasts: Requirement Quantification and ECMWF/MACC Aerosol Forecast Assessment. *Bulletin of the American Meteorological Society*, *94*(6), 903–914. https://doi.org/10.1175/BAMS-D-11-00259.1

Shaheen, A., Kidwai, A. A., Ain, N. U., Aldabash, M., & Zeeshan, A. (2017). Estimating Air Particulate Matter 10 Using Landsat Multi-Temporal Data and Analyzing its Annual Temporal Pattern over Gaza Strip, Palestine. *Journal of Asian Scientific Research*, *7*(2), 22–37. https://doi.org/10.18488/journal.2/2017.7.2/2.2.22.37

Sharps, K., Vieno, M., Beck, R., Hayes, F., & Harmens, H. (2021). Quantifying the impact of ozone on crops in Sub-Saharan Africa demonstrates regional and local hotspots of production loss. *Environmental Science and Pollution Research*, *28*(44), 62338–62352. https://doi.org/10.1007/s11356-021-14967-3

Shikwambana, L., Mhangara, P., & Mbatha, N. (2020). Trend analysis and first time observations of sulphur dioxide and nitrogen dioxide in South Africa using TROPOMI/Sentinel-5 P data. *International Journal of Applied Earth Observation and Geoinformation*, *91*, 102130. https://doi.org/10.1016/j.jag.2020.102130

Sifakis, N. (1992). *Mapping of Air Pollution Using SPOT Satellite Data T : T : 58*(10), 1433–1437.

Spyder · PyPI. (n.d.). Retrieved 26 September 2018, from https://pypi.org/project/spyder/

Stein, A. F., Draxler, R. R., Rolph, G. D., Stunder, B. J. B., Cohen, M. D., & Ngan, F. (2015). NOAA's HYSPLIT Atmospheric Transport and Dispersion Modeling System. *Bulletin of the American Meteorological Society*, *96*(12), 2059–2077. https://doi.org/10.1175/BAMS-D-14-00110.1

Strandgren, J., Mei, L., Vountas, M., Burrows, J. P., Lyapustin, A., & Wang, Y. (2014). *Study of satellite retrieved aerosol optical depth spatial resolution effect on particulate matter concentration prediction* [Preprint]. Aerosols/Remote Sensing/Troposphere/Physics (physical properties and processes). https://doi.org/10.5194/acpd-14-25869-2014

Sulprizio, M. P. (2015). *Particulate matter concentration mapping from MODIS satellite data: A Vietnamese case study Particulate matter concentration mapping from MODIS satellite data: A Vietnamese case study*.

Vermote, E., Justice, C., Claverie, M., & Franch, B. (2016). Preliminary analysis of the performance of the Landsat 8/OLI land surface reflectance product. *Remote Sensing of Environment*, *185*, 46–56. https://doi.org/10.1016/J.RSE.2016.04.008

Wang, J., Aegerter, C., & Szykman, J. J. (2016). *Potential application of VIIRS Day / Night Band for monitoring nighttime surface PM 2. 5 air quality from space*.

Wang, J., Alli, A. S., Clark, S., Hughes, A., Ezzati, M., Beddows, A., Vallarino, J., Nimo, J., Bedford-Moses, J., Baah, S., Owusu, G., Agyemang, E., Kelly, F., Barratt, B., Beevers, S., Agyei-Mensah, S., Baumgartner, J., Brauer, M., & Arku, R. E. (2022). Nitrogen oxides (NO and NO2) pollution in the Accra metropolis: Spatiotemporal patterns and the role of meteorology. *Science of the Total Environment*, *803*, 149931. https://doi.org/10.1016/j.scitotenv.2021.149931

Wang, M., Shi, W., Jiang, L., Liu, X., Son, S., & Voss, K. (2015). *Technique for monitoring performance of VIIRS reflective solar bands for ocean color data processing*. *23*(11), 13463–13475. https://doi.org/10.1364/OE.23.014446

Weber, S. A., Insaf, T. Z., Hall, E. S., Talbot, T. O., & Huff, A. K. (2016). Assessing the impact of fine particulate matter (PM2.5) on respiratory-cardiovascular chronic diseases in the New York City Metropolitan area using Hierarchical Bayesian Model estimates. *Environmental Research*, *151*, 399–409. https://doi.org/10.1016/j.envres.2016.07.012

Welton, E. J., Voss, K. J., Gordon, H. R., Maring, H., Smirnov, A., Holben, B., Schmid, B., Livingston, J. M., Philip, A., Formenti, P., Andreae, M. O., Welton, E. J., Voss, K. J., Gordon, H. R., Maring, H., Smirnov, A., Holben, B., Schmid, B., Livingston, J. M., & Durkee, P. A. (2016). *Tellus B : Chemical*

and Physical Meteorology Ground-based lidar measurements of aerosols during ACE-2: Instrument description, results, and comparisons with other ground-based and airborne measurements Ground-based lidar measurements of aerosols during. *0889*. https://doi.org/10.3402/tellusb.v52i2.17124

WHO | WHO Global Urban Ambient Air Pollution Database (update 2016). (2017). *WHO*.

WHO Air quality guidelines for particulate matter, ozone, nitrogen dioxide and sulfur dioxide. (2005).

WHO releases country estimates on air pollution exposure and health impact. (n.d.). Retrieved 13 May 2018, from http://www.who.int/en/news-room/detail/27-09-2016-who-releases-country-estimates-on-air-pollution-exposure-and-health-impact

Witte, J. C., Douglass, A. R., Silva, A., Torres, O., Levy, R., & Duncan, B. N. (2011). *And Physics NASA A-Train and Terra observations of the 2010 Russian wildfires*. 9287–9301. https://doi.org/10.5194/acp-11-9287-2011

World Bank, T. (2015). The Little Green Data Book. In *The effects of brief mindfulness intervention on acute pain experience: An examination of individual difference* (Vol. 1). https://doi.org/10.1017/CBO9781107415324.004

World Health Organization, & Mudu, P. (2021). *Ambient air pollution and health in Accra, Ghana*. World Health Organization. https://apps.who.int/iris/handle/10665/340678

World Health Organization, Santos, A. C., Nonvignon, J., Blankson, P.-K., Johnson, A., & Aikins, M. (2020). *Economic costs of air pollution in Accra, Ghana*. World Health Organization. https://apps.who.int/iris/handle/10665/339950

Yakubu, O. (2017). Particle (Soot) Pollution in Port Harcourt Rivers State, Nigeria—Double Air Pollution Burden? Understanding and Tackling Potential Environmental Public Health Impacts. *Environments*, *5*(1), 2. https://doi.org/10.3390/environments5010002

Zawadzka, O., Markowicz, K., & Petelski, T. (2014). *Acta Geophysica Studies of Aerosol Optical Depth with the Use of Microtops II Sun Photometers and MODIS Detectors in Coastal Areas of the Baltic Sea*. *April*. https://doi.org/10.2478/s11600-013-0182-5

Zhou, Z., Dionisio, K. L., Arku, R. E., Quaye, A., Hughes, A. F., Vallarino, J., Spengler, J. D., Hill, A., Agyei-Mensah, S., & Ezzati, M. (2011). Household and community poverty, biomass use, and air pollution in Accra, Ghana. *Proceedings of the National Academy of Sciences of the United States of America*, *108*(27), 11028–11033. https://doi.org/10.1073/pnas.1019183108